ARPA ORDER NO.: 189-1
7K10 Director's Technology

R-2056-ARPA
May 1977

Molecular and Metallic Hydrogen

Marvin Ross and Charles Shishkevish

A report prepared for

DEFENSE ADVANCED RESEARCH PROJECTS AGENCY

Rand
SANTA MONICA, CA. 90406

The research described in this report was sponsored by the Defense Advanced Research Projects Agency under Contract No. DAHC15-73-C-0181.

UNCLASSIFIED
SECURITY CLASSIFICATION OF THIS PAGE (When Data Entered)

REPORT DOCUMENTATION PAGE

READ INSTRUCTIONS BEFORE COMPLETING FORM

1. REPORT NUMBER: R-2056-ARPA	2. GOVT ACCESSION NO.
3. RECIPIENT'S CATALOG NUMBER	
4. TITLE (and Subtitle): Molecular and Metallic Hydrogen.	5. TYPE OF REPORT & PERIOD COVERED: Interim rept.
6. PERFORMING ORG. REPORT NUMBER	
7. AUTHOR(s): Marvin Ross and Charles Shishkevish	8. CONTRACT OR GRANT NUMBER(s): DAHC15-73-C-0181, ARPA Order-189
9. PERFORMING ORGANIZATION NAME AND ADDRESS: The Rand Corporation, 1700 Main Street, Santa Monica, Ca. 90406	10. PROGRAM ELEMENT, PROJECT, TASK AREA & WORK UNIT NUMBERS
11. CONTROLLING OFFICE NAME AND ADDRESS: Defense Advanced Research Projects Agency, Department of Defense, Arlington, Va. 22209	12. REPORT DATE: May 1977
	13. NUMBER OF PAGES: 111
14. MONITORING AGENCY NAME & ADDRESS (if different from Controlling Office)	15. SECURITY CLASS. (of this report): UNCLASSIFIED
	15a. DECLASSIFICATION/DOWNGRADING SCHEDULE

16. DISTRIBUTION STATEMENT (of this Report)

Approved for Public Release; Distribution Unlimited

17. DISTRIBUTION STATEMENT (of the abstract entered in Block 20, if different from Report)

No restrictions

18. SUPPLEMENTARY NOTES

19. KEY WORDS (Continue on reverse side if necessary and identify by block number)

Hydrogen
Physical Chemistry
Chemical Properties
Physicochemical Properties
High Pressure Physics

20. ABSTRACT (Continue on reverse side if necessary and identify by block number)

see reverse side

This report presents a comprehensive review and analysis of the published data on metallic hydrogen and a summary of the properties of molecular hydrogen that are required to determine the molecular-to-metallic hydrogen transition pressure. The best available effective interaction potential is utilized in calculating the equation of state for solid molecular hydrogen. The equation of state of metallic hydrogen is determined by four different methods and the possible range of molecular-to-metallic hydrogen is largely responsible for the wide discrepancy in calculations of the transition pressure. Metastability of metallic hydrogen is discussed and the experimental high-pressure research pertinent to the determination of molecular-to-metallic hydrogen transition pressure is reviewed. It is pointed out that the recently proposed concept of the molecular-insulating phase becoming a molecular-conducting phase due to narrowing and closing of the band gap under high pressure provides a more likely explanation for the experimentally observed decrease in the electrical resistivity of molecular hydrogen observed in both static and shock-wave experiments and attributed to the molecular-to-metallic transition of molecular hydrogen. Ref. (Author)

ARPA ORDER NO.: 189-1
7K10 Director's Technology

R-2056-ARPA
May 1977

Molecular and Metallic Hydrogen

Marvin Ross and Charles Shishkevish

A report prepared for

DEFENSE ADVANCED RESEARCH PROJECTS AGENCY

Rand
SANTA MONICA, CA. 90406

Published by The Rand Corporation

PREFACE

This report* is part of a continuing Rand study of selected areas of science and technology, a project sponsored by the Defense Advanced Research Projects Agency. It deals with metallic hydrogen--i.e., a metallic phase of hydrogen that, according to theory, should exist at extremely high pressures ($P > 1$ Mbar). The possibility exists that metallic hydrogen may be an elevated temperature superconductor, a very efficient rocket fuel, or a powerful explosive. This report deals with the theoretical calculations of the equations of state of both molecular and metallic hydrogen required for calculations of the transition pressure into the metallic phase. The range of pressures at which metallic hydrogen transition should occur is estimated. Metastability (i.e., stability of metallic hydrogen at low pressures) is discussed. The experimental data used in calculating the molecular equation of state of hydrogen are summarized and the experimental high-pressure research pertinent to molecular-to-metallic hydrogen transition is reviewed. This report is intended for investigators specializing in high-pressure research and scientists interested in molecular and metallic hydrogen.

---

*One of the coauthors of the report, Dr. M. Ross, is with the Lawrence Livermore Laboratory, University of California.

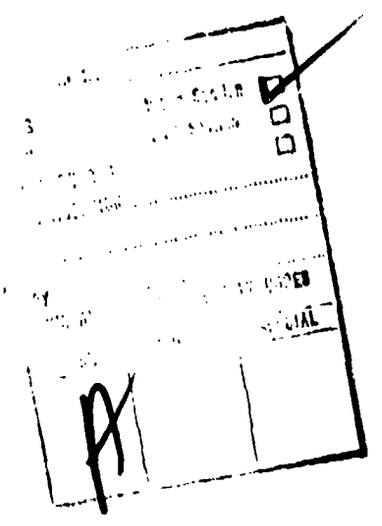

SUMMARY AND CONCLUSIONS

A. GENERAL

Hydrogen, a molecular gas under atmospheric pressure and at room temperature, becomes a fluid at a temperature of 20.4 K and solidifies at a temperature of ~14 K, becoming a low-density quantum solid having dielectric properties. Both theoretical and experimental research indicate that, at sufficiently high pressures (commonly thought to be between 1 and 4 Mbar), molecular hydrogen should undergo a phase transition into a metallic state. The new phase, metallic hydrogen, should have properties similar to those of alkali metals.

The potential usefulness of metallic hydrogen can be attributed to several factors. As a result of its high Debye temperature (~2000 to 3000 K) it may be an elevated-temperature (possible room temperature) superconductor.* The high specific impulse of metallic hydrogen (~1400 sec) compared with that of a rocket fuel, such as JP4 plus liquid oxygen (~400 sec), makes it potentially attractive as a rocket fuel. Metallic hydrogen has an energy content of 400 kJ/g mole, or 300 times greater than the best currently available aircraft fuel. This would make it attractive for aircraft propulsion. However, if the transition energy release rate is not controllable once the transition is initiated, metallic hydrogen would be an explosive rather than a fuel. If so, with energy of 50 kcal/g and a density of ~1 to 1.3 g/cm^3, it is an explosive that is approximately 35 times more powerful than TNT (E = 1.354 kcal/g). Its high density should also make metallic hydrogen useful in nuclear weapons.

Several major problems have to be resolved before it can be determined whether metallic hydrogen can be produced in the laboratory and whether it will be technologically useful. The most important problems are whether metallic hydrogen exists, whether transition into

*Unfortunately, the high Debye temperature of metallic hydrogen also indicates that it may be a quantum liquid.

the metallic state will occur at a pressure that can be reached in a static press, and whether metallic hydrogen will remain metastable.

B. THEORETICAL RESEARCH

The transition pressure--i.e., the pressure at which molecular hydrogen will undergo phase transition into its metallic phase--can be estimated theoretically from the intersection of the curve of Gibbs free energy of molecular hydrogen, plotted as a function of pressure, with a similar curve for metallic hydrogen. The point of intersection is extremely sensitive to small changes in these curves, causing a wide discrepancy in the estimates of the transition pressure. Since the variation of the Gibbs free energy with pressure is determined from the equation of state, theoretical determination of the transition pressure into metallic hydrogen requires extremely accurate knowledge of the equations of state of both molecular and metallic hydrogen. A reliable prediction of the transition pressure is extremely vital even if intended only to guide the experimentalist in his design of the optimum apparatus for this extreme pressure.

In addition to the basic question of transition pressure, the usefulness of metallic hydrogen depends on the length of time hydrogen can exist in the metallic state, i.e. its metastability. This theoretical prediction is the most elusive aspect of the overall problem.

Thus, the three major aspects of the theoretical research on metallic hydrogen involve the determination of its molecular equation of state, its metallic equation of state, and its metastability.

1. Equation of State of Molecular Hydrogen

The present status and reliability of the theoretical equation of state of molecular hydrogen is closely related to the reliability and extent of the available experimental data. While, in principle, it is possible to calculate the forces between molecules and to compute their properties, these calculations all involve some approximations whose ultimate justification is based on comparison with the experimental data. It is obviously desirable to carry out equation

of state measurements at the highest attainable pressures in order to minimize the uncertainty in the theoretical model.

The basic experimental data available at present is a low pressure ($P \leq 25$ kbar) solid isotherm and a few Hugoniot (shock compression) points for liquid molecular hydrogen at pressures ranging from 40 to 900 kbar. The lower pressure solid data, while less useful for extrapolating into the multimegabar range, is considerably more accurate than the shock data. In general, an advantage of shock wave experiments in the equation of state studies is that the high temperatures achieved during shock compression act to bring neighboring molecules much closer together than in static compression to the same density, resulting in a higher "effective" density. Thus, shock experiments are well suited for the determination of the effective pair potential at pressures near the transition of hydrogen into the metallic phase. A third class of experiments, isentropic compression, can also be used to verify the molecular equation of state. However, isentropic compression has not yet provided direct pressure measurements. Instead, pressure has been calculated using a magnetohydrodynamic code. Therefore, these data are insufficiently accurate to be useful in determining the equation of state.

Recent theoretical calculations show that the pressure of solid hydrogen to 25 kbar can be computed from a semi-theoretical pair potential of molecular hydrogen, and that the results of the calculations are in good agreement with the experimental data. In this regime of intermediate separations, the quantum mechanical methods are not convergent and a purely theoretical pair potential cannot presently be obtained. However, at higher pressures, where the methods are convergent, the molecular equation of state may well be inadequate due to the omission of many-body terms. This could explain the discrepancy between theoretical Hugoniots based on first principle pair potentials and the experimental shock compression curves for liquid hydrogen. Improved theoretical calculations of the overall pair potential would incorporate higher order interaction terms.

Ideally, one would like to make calculations for the system of molecules in a crystal, rather than calculations for pairs of molecules, which are then summed over all pairs of molecules.

Preliminary calculations of this nature have already been made, and, although they have not provided additional equation of state data, these calculations have predicted closing of the band gap. This indicates that the molecular insulating phase of hydrogen could become a molecular conductor at pressures below that of the predicted monatomic metallic transition. Should this be the case, then the experiments that were designed to identify the monatomic metallic transition from the large change in electrical resistivity would not be useful. The existence of a decreasing band gap even in the absence of the transition into a molecular conductor prior to the metallic transition would have broad implications concerning the interpretation of shock and isentropic experiments and the 0 K equation of state.

2. Equation of State of Metallic Hydrogen

Until metallic hydrogen is available in the laboratory, its equation of state must be determined theoretically. In general, calculations of the equation of state and other thermodynamic parameters of metallic hydrogen have given more consistent results than those for the molecular hydrogen. For example, the earliest calculations, using the approximate cellular method (an early version of the Wigner-Seitz method), do not differ greatly from the most recent self-consistent calculations, using the same method with an improved correlation potential energy function.

There are four general methods by which the equations of state of metals are commonly computed using current solid state theory. These are: (1) electron band methods, such as the augmented plane wave (APW); (2) free electron perturbation theory (PERT); (3) linear combination of atomic orbitals (LCAO); and (4) the Wigner-Seitz (WS) method. The most commonly used method has been the free electron perturbation theory. All calculations assume that the stable structure at 0 K is a solid; however, the possibility that it may be a quantum liquid cannot be ruled out. In view of the fact that all four methods are approximations, it is very difficult, if not impossible, to determine the absolute accuracy of the results of calculations, or even

the best method of performing these calculations. However, these methods can be compared and it can be determined how sensitive the computed metallic transition is likely to be.

In general, the equation of state of metallic hydrogen includes contributions from various interactions, as well as a contribution due to zero-point motion. The results of recent calculations of the equations of state using the above four methods were found to be in good agreement among each other and with other reliable calculations. However, it was shown that one of the contributions to the total energy, the correlation energy, is approximately four times larger than the differences between the highest and the lowest values of the total energy determined by the four models. The theory of electron correlation is a poorly understood quantum mechanical effect and the numerical results for the correlation energy of hydrogen may be in error by a factor of two or three. Thus, estimates of the transition pressure may be in error by a few Mbar. Therefore, accurate determination of the correlation energy appears to be the most important problem facing theoretical calculations of the properties of metallic hydrogen.

3. Metastability

In considering metastability, it is worthwhile to note that, relative to molecular hydrogen, the energy stored in the metallic modification is of the order of 2 Mbar/(mole/cm^3). Because of this, constant volume decomposition of metallic hydrogen would result in temperatures of several thousand degrees K and pressures over 1 Mbar. This stored energy exceeds by two orders of magnitude the energy stored in diamond relative to graphite.

Thermodynamic considerations indicate that the melting temperature of metallic hydrogen should be less than the melting temperature of molecular hydrogen and that, upon melting, metallic hydrogen should thus become a molecular liquid. However, it is unlikely that thermodynamic considerations apply to molecular hydrogen, which is a quantum solid at $T \lesssim 14$ K and a quantum liquid at $14\ \text{K} < T < 20.4$ K.

Stability of the metastable state is determined by calculating the decay rate from the less stable to the more stable form. In general, the decay rate may be slow due to the very complicated nature of the process on the molecular level. Thus, the transition from diamond to graphite (i.e., from the less stable to the more stable form) requires complicated rearrangement of the tetrahedrally coordinated carbon atoms to form a widely separated, close-packed structure. Therefore, carbon can exist in the usual stable form as graphite and, in the metastable form, as diamond. Unfortunately, the mechanism responsible for the breakdown of metallic hydrogen is very simple, requiring only that pairs of neighboring atoms link up to form molecules.

Detailed calculations of the decay rate of metallic hydrogen have not been made due to the complexity of the problem. However, approximate estimates of the time required for metallic hydrogen to decompose are of the order of fractions of a second.

The results of recent investigations indicate that maintaining metallic hydrogen for long periods of time may involve keeping it tightly enclosed in a vessel at a constant volume and under some pressure, in order to prevent evaporation and recombination. By keeping the density constant and high, one can also minimize the free energy difference between the two phases, which becomes very large when the system is allowed to expand freely at constant pressure. However, metastability remains the most crucial aspect of the problem and will no doubt have to be resolved experimentally.

C. EXPERIMENTAL RESEARCH

The experimental research on molecular hydrogen involves two distinct goals: the acquisition of experimental data to determine its equation of state and the observation of metallic hydrogen. The methods of determining the experimental and theoretical equations of state of molecular hydrogen, their reliability, and the results obtained so far were discussed in Section B. This section deals only with attempts to observe metallic hydrogen and with related experimental investigations.

Isentropic, including nearly isentropic multiple-shock compression, and static isothermal experiments are the only two methods* used today in attempting to observe metallic-phase transition of molecular hydrogen. Although not yet attempted, laser and electron-beam techniques can also be utilized to compress molecular hydrogen to the very high densities at which metallic transition occurs. However, static isothermal compression is the only method that would not result in the destruction of the sample and could produce laboratory samples of metallic hydrogen.

In the past, isentropic compression has been the only method capable of generating Mbar pressures sufficient to attain metallic-phase transition. Hawke et al. have performed isentropic compression experiments on molecular hydrogen using a rather sophisticated magnetic implosion technique. Compression of the sample of liquid molecular hydrogen was determined from the diameter of the magnetically imploded sample tube measured by means of flash x-rays. The pressure of the magnetic field acting on the sample was roughly estimated from a one-dimensional magnetohydrodynamic code. A wire placed axially in the sample made it possible to measure the electrical resistivity of the compressed sample of hydrogen. Unfortunately, Hawke et al. obtained only a single approximate volume pressure point (~2cm^3/mole at 2 to 5 Mbar). Using isentropic compression in the absence of magnetic field, Grigor'yev et al. obtained six different equations of state points at pressures estimated to be between 0.37 and 8 Mbar at calculated molar volumes between 4.5 and 1 cm^3/mole. These results show that Grigor'yev's and Hawke's experimental data can be fitted into an acceptable equation of state if one assumes a transition of molecular hydrogen into a metallic phase at a pressure of 2.8 Mbar, with a molar volume change from 1.9 to 1.6 cm^3/mole. However, as pointed out by Ross, their data can also be fitted by a straight line, thus indicating an absence of metallic transition. The resulting isentrope must be accepted as being crude and preliminary and the experimental method used will require further development.

---

*As a result of the very high temperatures generated by shock waves and the very low density of molecular hydrogen, adiabatic shock-compression (single and even double shocks) cannot produce the very high densities required for the metallic-phase transition of hydrogen.

Extremely high contact pressures of up to 4 to 5 Mbar over a very small surface area of about 10^{-2} to 10^{-3} mm^2 are claimed to have been generated by Yakovlev and his colleagues, using opposed anvils made of carbonado, a polycrystalline diamond compact. In these externally calibrated experiments the indentor, with a rounded conical tip, was used to compress a film of a cellulose nitrate varnish deposited onto a flat anvil. However, recent calculations by Ruoff and Chan show that, because of the shape of the indentor used in the experiments, the actual pressure achieved at the maximum applied load of 200 kg was about 1 Mbar. Taking into account other factors, such as plastic flow, could reduce even this estimate substantially.

A significant achievement in static high pressure research, especially from the point of view of production of metallic hydrogen, is the construction of the segmented sphere apparatus by Kawai. Unlike the opposed anvils device where only contact pressure is generated over a very small area, the segmented sphere can be used to generate high pressures in "fairly large" sample volume. First developed by Von Platten and used by him to synthesize diamond, the segmented sphere has been perfected to the point where it is claimed that pressures up to approximately 2.5 Mbar are generated in an approximately 1 mm^3 sample volume, without the onset of plastic flow. Conceivably, the use of higher strength materials, such as carbonado developed by Yakovlev or diamond compact developed by Wentorf, in the sample chamber and other inner sections of the sphere may further extend the pressures that can be generated.

The claim of pressures up to 2.5 Mbar achieved in the segmented sphere appear to be overly exaggerated. In Kawai's experiments, the pressure generated is calculated by multiplying the external hydrostatic load by the ratio of the external area of the sphere with its internal area. The calculations are based on the assumption that the pressure is transmitted with a 100 percent efficiency. In practice, as a result of friction, deformation, and a number of other factors, the actual efficiency may be only a small fraction of its ideal value.

Yakovlev's and Kawai's groups have performed a series of experiments in which even such wide-gap insulators as diamond, SiO_2, NaCl, S, MgO, water (ice), BN, and Al_2O_3 became electrical conductors at pressures estimated to exceed 1 Mbar. While the actual transition pressures are unknown, these experiments further substantiate the theoretical prediction that, at sufficiently high pressures, all insulators, including hydrogen, should become conductors. In the latest experiments by Yakovlev et al. and Kawai et al., a 6 to 8 order decrease in electrical resistivity of hydrogen was interpreted as a possible transition of molecular hydrogen into its metallic phase. The Russian experiments were performed using opposed carbonado anvils, with a thin film of solid molecular hydrogen deposited on the surface of the flat carbonado anvil cooled to 4.2 K. The Japanese used a room-temperature segmented sphere charged with hydrogen gas. Metallic hydrogen, if it actually was produced, was not metastable.

Explanations other than metallic transition can account for the experimentally observed decrease in the electrical resistivity of hydrogen claimed or implied to have occurred at pressures of less than or approximately 1 Mbar. One of the most intriguing explanations is based on the very recently proposed concept of the molecular-insulating phase becoming a molecular-conducting phase due to narrowing and possible closing of the band gap. If this transition does indeed occur, it takes place at lower pressures than the metallic-phase transition and may have been reached in both the Russian and Japanese experiments.

Since external rather than internal calibration was used, the high pressures claimed to have been generated in Yakovlev's and Kawai's experiments were met with considerable skepticism. However, Mbar pressures were also claimed to have been generated in internally calibrated experiments performed in 1975 by Mao and Bell of the Carnegie Institution. The diamond pressure cell used in the experiments consisted of two opposed anvils made of single-crystal diamonds with the work area of each anvil equal to 1.5×10^{-3} mm^2, very carefully aligned both axially and horizontally. A ruby crystal was

placed on a 0.01-inch thick sheet of steel and compressed between the anvils. The pressure was determined from the spectral shift of the R_1 ruby fluorescence line with pressure. In more recent experiments, Mao and Bell claim to have reached 1.3 Mbar on the ruby scale. The support for the diamond anvil then failed, causing the diamond to break. Thus, it appears that even higher pressures may be attained in the future.

The ruby fluorescence gauge used in determining pressures above 291 kbar is a secondary gauge and is a linear extension of the National Bureau of Standards calibration curve based on Decker's central force equation of state for sodium chloride. According to Decker's equation of state, the B1 to B2 transition in NaCl occurs at a pressure of 291 kbar. Ruoff and Chhabildas have recently shown that the central force model is invalid. According to these authors, the B1 to B2 transition in NaCl at room temperature occurs at a pressure of 261 kbar. Assuming validity of their arguments, the pressures achieved by Mao and Bell are well below 1 Mbar. Mao and Bell also disregard a possibly significant nonlinearity of the temperature dependence of the spectral shift of the R_1 ruby fluorescence line excited by the laser beam.

Vereshchagin claims that static pressures up to 3 Mbar in a volume of several cm^3 could be generated during the next few years by a Soviet group in a 50,000-ton press with the inner stage made of carbonado. Pressures limited only by the strength of the material of which inner anvils are made can also be generated in the 22-inch diameter, room-temperature segmented sphere developed by Dr. Ruoff at Cornell University.

D. POSSIBLE OPTIONS

Several options are available to speed up the search for and development of metallic hydrogen. One of these is the construction of a segmented sphere apparatus, such as the one used by Kawai. This option is being pursued by two different groups in the United States. The NASA Lewis Research Center in Cleveland has an operational 6-inch diameter, room-temperature segmented sphere apparatus. A 12-inch

diameter, cryogenic segmented sphere is in planning stages and is expected to be constructed in a few years. However, material procurement difficulties may result in cancellation of its construction. Dr. Ruoff at Cornell University is performing calibration tests on a 22-inch diameter, room-temperature segmented sphere.

There are currently two schools of thought concerning claims of Mbar pressures supposedly achieved in static high-pressure experiments. One group of high pressure specialists believes that pressures in excess of 1 Mbar have been generated in Kawai's segmented sphere and that 5 Mbar pressures claimed by Vereshchagin and pressure of 1 Mbar supposedly achieved by Mao and Bell are not too unreasonable. If one accepts the validity of these claims, multi-Mbar pressures in a volume sufficiently large to produce metallic hydrogen can be generated in the Russian 50,000-ton press presently under construction and in Ruoff's 22-inch diameter segmented sphere. However, another group of materials scientists and high pressure specialists, which includes such prominent researchers as Ruoff, Bundy, and Wentorf, is firmly convinced that static pressures above 1 Mbar cannot be achieved due to material limitations in respect to plastic flow and fracture. The difference in opinion is difficult to resolve and will probably require establishing a reliable pressure gauge to several Mbar. The availability of such a calibration curve would immensely enhance both static and dynamic experiments done at extremely high pressures.

The development of high-strength materials, such as carbonado, which can be produced in different shapes, and a search for alternate methods of producing diamond compact, which apparently is superior to carbonado but is expensive and can only be produced in a thin film of fairly simple geometry, would be another important step.

At the present time, no theoretical analysis exists to explain the extremely high pressures reached in a segmented-sphere apparatus and, thus, to explain the capability of conventional construction materials to withstand such pressures without deformation. Therefore, it would be desirable to apply the three-dimensional elastic-plastic

code, such as the one developed at the Lawrence Livermore Laboratory, to analysis of the segmented-sphere apparatus and to designing an ultimate static high pressure press.

Another option would be to concentrate the research on (1) an attempt to experimentally observe transition into metallic state, and (2) a thorough and systematic development of theory backed up by sufficient experimental data.

The experimental effort to observe metallic transition could be achieved by means of: (a) isentropic shock-wave compression, especially magnetic implosion, and the development of an alternative that uses explosives only (nonmagnetic) and, possibly, (b) laser compression. Any such experimental program should be preceded by a complete study using computer codes. The theoretical approach should deal with the following problems:

1. Analysis of metastability (including the possibility that metallic hydrogen may be a quantum liquid).
2. Improved molecular hydrogen equation of state by:
   a. calculation of the equation of state by treating the entire crystal by band theoretical methods;
   b. theoretical analysis of additional improved shock-wave experiments to determine the effective molecular potential;* and
   c. calculation of higher order terms in the potential of molecular hydrogen.
3. Improved calculation of the correlation energy for the metallic equation of state.
4. Study of the band structure in hydrogen and the possibility that the molecular solid could become conducting due to the conduction band overlap.

---

*Such experiments have just been funded and will begin in Lawrence Livermore Laboratory in FY 1977. It is expected that the accuracy of the new experimental data will be improved by a factor of three (to ± 3 percent) over the earlier data.

Calculation of the molecular equation of state should include an investigation of effects, such as dissociation of molecular hydrogen in shock waves, the effect of spherical averaging of molecules, the adequacy of liquid models, and, possibly, quantum mechanical calculations of many body effects.

ACKNOWLEDGMENTS

The authors wish to express their gratitude to Dr. P. R. Aron, Dr. A. K. McMahan of the Lawrence Livermore Laboratory, Dr. J. C. Raich of the Colorado State University, and Dr. R. H. Wentorf, Jr., of the General Electric Company for their reviews of this report and their valuable comments.

CONTENTS

PREFACE iii

SUMMARY AND CONCLUSIONS v

ACKNOWLEDGMENTS xix

Section
I. EQUATION OF STATE OF DENSE MOLECULAR HYDROGEN 1
A. General 1
B. Interaction Potential for Hydrogen Molecules 2
C. Equation of State for Solid Hydrogen 10
1. Theory of the Quantum Solid 10
2. High-Pressure Hydrogen Calculations ... 13
D. Shock-Compressed Molecular Hydrogen and Deuterium 18
1. Theory of the Dense Fluid 18
2. Hugoniot Calculations 19
3. Many-Body Intermolecular Effects 24

II. EQUATION OF STATE OF SOLID METALLIC HYDROGEN 33
A. General 33
B. Calculation Methods 34
1. Augmented Plane Wave (APW) 34
2. Linear Combination of Atomic Orbitals (LCAO) 35
3. Wigner-Seitz (WS) 36
4. Perturbation Theory (PERT) 37
5. Zero-Point Energy Calculations 37
6. Correlation Energy Calculations 38
C. Results of the Calculations 39
D. Structure of Metallic Hydrogen 45

III. TRANSITION OF MOLECULAR HYDROGEN INTO A METALLIC PHASE 48
A. General 48
B. Transition of the Insulating Molecular Phase into a Conducting Molecular Phase ... 48
C. Transition of Molecular Hydrogen into a Monatomic Metallic Phase 50

IV. STABILITY OF METALLIC HYDROGEN 57
A. General 57
B. Melting of the Crystalline Metal Phase 57
C. Metastability of the Metallic Phase 60

V. EXPERIMENTAL RESEARCH 63
A. General 63
B. Isothermal Compression 66
1. Experimental Molecular Hydrogen Equation of State Data 66
2. Experimental High-Pressure Research ... 68
3. Theoretical Considerations 79
C. Shock-Compression Experiments 84
D. Isentropic Compression 88
E. Laser Compression 93
F. Electron-Beam Compression 96
G. Recent Reported Observations of Metallic Hydrogen 97

REFERENCES 101

I. EQUATION OF STATE OF DENSE MOLECULAR HYDROGEN

A. GENERAL

As a result of the great interest in determining the metallic hydrogen transition pressure, considerable attention has been devoted to calculating the equation of state of molecular hydrogen at high pressures.

In principle, it should be possible to use the well-established methods of quantum mechanics to calculate the forces acting between hydrogen molecules and then to apply statistical mechanics to calculate the thermodynamic properties of molecular hydrogen. Thus, the problem naturally divides into two parts, neither one of which can, in practice, be solved exactly. Fortunately, the approximate determination of thermodynamic properties by means of modeling of material properties with statistical mechanics has made great strides in the past ten years and the available solutions are sufficiently accurate. However, the determination of forces between molecules is the principal obstacle and represents the chief area of current uncertainty. As an alternative to theoretical rigor, it is possible to bypass the first principles of quantum mechanical calculations and, instead, to search for an effective intermolecular potential that, when used with satisfactory statistical mechanical models, will reproduce the available experimental data. This empirical pair potential and the statistical mechanical models can then be used to determine the thermodynamic properties. A practical difficulty with this procedure is that it breaks down and fails to predict reliably when extrapolating outside the range of the data to which the potential was calibrated. An illustration of this kind of difficulty is found in earlier work on calculations of the solid isotherm of hydrogen using pair potentials that had been obtained from second virial coefficients of low-density gas. These pair potentials failed to predict the properties of the solid at pressures up to 20 kbar originally measured by Stewart in 1956 [1]. The agreement was so poor as to cast some doubt on the accuracy of the experimental data. However, the more recent work of Anderson and

Swenson [2], repeating and extending up to a pressure of 25 kbar the earlier data by Stewart, had verified its accuracy.

These persistent attempts to calculate the properties of hydrogen despite an inadequate potential (or, perhaps, because of it) resulted in very careful theoretical modeling of the quantum solid, particularly by Krumhansl and coworkers at Cornell University [3,4,5]. Consequently, this aspect of the problem was solved when better theoretical pair potential became available. At about the same time, Ross at the Lawrence Livermore Laboratory [6,7] and Etters and co-workers [8,9,10] at Colorado State University, showed that calculations using potentials that correctly describe the repulsive forces that are the important terms in the potential at high pressure would satisfactorily predict the experimental data. The work of these three groups represents the most recent and, probably, the most complete theoretical studies of the properties of dense molecular hydrogen. Consequently, this section will focus mostly on their work. These scientists hold somewhat different views as to the significance of some of the terms in their model pair potentials. However, their final results are sufficiently close to indicate that an adequate equation of state for molecular hydrogen at near metallic densities may soon become available.

B. INTERACTION POTENTIAL FOR HYDROGEN MOLECULES

The simplest procedure used to calculate the properties of a molecular solid or liquid is to assume that the total force on a molecule is obtained by adding all the forces due to neighboring molecules. The assumption of pairwise additivity means that the behavior of a molecular system is characterized by a many-body potential of the form:

$$V = \sum_{i<j} \phi_{ij} , \qquad (1)$$

where ϕ_{ij} is the molecular potential acting between pairs i and j and may be the interaction potential for an isolated system of two

molecules, or the effective potential between pairs of molecules, modified by the presence of additional neighbors. Eq. (1) is used in statistical mechanics to compute the thermodynamic properties.

Accurate calculations can be carried out for the pair potential in the limit of large intermolecular separations (R), where the interactions are due to the induced dipole-dipole, induced dipole-quadrapole, and quadrapole-quadrapole potentials. The theory of these long-range interactions for hydrogen is well understood and discussed in some detail by Margenau and Kestner [11]. In the intermediate region near the potential minimum, *ab initio* calculations are not yet satisfactory and no attempts have been made to use the available results in equation of state calculations. In this region, the *ab initio* molecular orbital calculations require extremely large basis sets of orbitals to obtain satisfactory convergence.

The calculated properties of molecular hydrogen at megabar pressures are very sensitive to the pair potential at small separations. Therefore, the region of primary importance to the determination of the very high pressure equation of state is the calculation of the steeply repulsive short-range interaction between hydrogen molecules. Fortunately, theoretical calculation of the pair potential from first principles at small intermolecular separations ($R < 5$ bohr) is much more favorable than at intermediate separations. At short intermolecular distances, the attractive terms are considerably less important and sufficiently large basis sets of orbitals can be used in calculations that converge in reasonable computing time to determine the pair potential. An exhaustive review by McMahan et al. [12] of the calculations of the short-range interaction between hydrogen molecules has shown that recent computations of the pair potential at small separations by the configuration interaction (CI) method are correct to within better than 10 percent. They have also concluded that the intermolecular pair potential for hydrogen molecules for short separations calculated by *ab initio* techniques is expected to include all contributions to the interaction energy, including attraction. In other words, there is little to be gained from further calculations of a system of two interacting hydrogen molecules at small separations.

In the case of molecular hydrogen, the pair potential is equal to the pair potential energy (E_{AB}) of two hydrogen molecules (A and B). The pair potential energy is usually calculated by taking the difference between the total ground-state energy (E_{A+B}) of the composite H_2 - H_2 system at geometries of interest and the energy E_A and E_B ($E_A = E_B$) of two infinitely separated H_2 molecules evaluated in the same approximation:

$$E_{AB} = E_{A+B} - 2E_A. \qquad (2)$$

Computation of the energy of a hydrogen molecule is straigthforward. Thus, the main problem in calculating the intermolecular pair potential of hydrogen is the computation of E_{A+B}, the ground-state energy of the H_2 - H_2 system.

The energy E_{A+B}, at small separations required to compute the properties of molecular hydrogen at megabar pressures, is usually calculated by the present state-of-the-art *ab initio* techniques. In this approach, all four hydrogen nuclei are fixed at given positions (Born-Oppenheimer approximation) and the zero-point motion of the four nuclei is neglected. The nuclear position vectors, $\bar{R}_A$, and, thus, the geometry of the system are accordingly parameters in the problem. The ground-state energy of two interacting hydrogen molecules is then the ground-state eigenvalue of the Hamiltonian:

$$H = \sum_{A<B} \frac{1}{R_{AB}} + \sum_i \left(-\frac{1}{2} \nabla_i^2 - \sum_A r_{iA} \right) + \sum_{i<j} \frac{1}{r_{ij}}, \qquad (3)$$

where the indices A and i run over the four nuclei and four electrons, respectively, $R_{AB} = |\bar{R}_A - \bar{R}_B|$, $r_{iA} = |\vec{r}_i - \vec{R}_A|$, and atomic units* are used.

Because variational methods are generally used, they provide upper bounds for the ground-state energy. These methods may be

*In the atomic units $e^2 = 1$, $\hbar = 1$, and $m_e = 1$. The unit of length is the bohr (1 bohr = 0.5292 A°) and the unit of energy is the hartree (1 hartree = 27.21 eV = $0.3158 \cdot 10^6$ K).

categorized according to the generality of the trial wave function used in the calculation. The three most frequently used methods are the Heitler-London (HL), the Hartree-Fock self-consistent field (HF), and (limited or full) configuration interaction (CI) calculations.

The full CI wave function represents the most complete basis set, including as special cases both the HF and HL, and, obviously, the limited CI wave functions, and always yields lower upper bounds on the ground-state energy than either HF or HL. The full CI calculations also include all electron correlations and, thus, both the purely repulsive energy and the dispersion (van der Waals) energy, which is not calculated in the HF method. However, the CI and HF results converge at very small separations, when the dispersion terms become negligible. At larger separations, when the dispersion energy becomes appreciable, the number of terms in a CI calculation becomes prohibitively high for computer calculations. A more detailed discussion of the molecular orbital methods is beyond the scope of this survey.

A recent *ab initio* calculation of the H_2 - H_2 intermolecular potential, illustrating the CI method and in agreement with the best available results, is that of Ree and Bender [13]. The Hamiltonian used, Eq. (3), is that for a "super-molecule" composed of four H^+ nuclei and four electrons. The wave function is expanded in a linear combination of Slater determinants. Elements in the determinants are the molecular orbitals, which are, in turn, expressed as a suitable linear combination of atomic orbitals of the hydrogen atom. The coefficients in the expansion are obtained by minimizing the energy in the Schroedinger equation. The resulting energy must approach the exact ground-state energy of a system of two hydrogen molecules, provided that a sufficiently large number of atomic orbitals and Slater determinants are used in the calculations. The computations for the ground-state energies were carried out by the CI method using the iterative natural-orbital method developed by Davidson and Bender [14]. The CI wave functions used to calculate the energies include the HF configuration plus all configurations arising from the replacement

of, at most, two molecular orbitals consisting of five (two 1s and one set of 2p [p_x, p_y, p_z]) atomic orbitals per hydrogen atom. The accuracy of the calculated results was tested using a more precise wave function constructed from more than 3000 Slater determinants and 44 molecular orbitals. Most of the calculations were made for H-H bond length (intramolecular separation) of 1.4 bohr.

The intermolecular potential energy, E_{AB}, was calculated from Eq. (2). Four geometries were considered: (1) L-geometry, where molecular axes of both hydrogen atoms lie along a straight line, R, connecting the centers of the molecules; (2) P-geometry, where molecular axes are parallel to each other and perpendicular to R; (3) T-geometry, where one axis is perpendicular to R and the other is parallel to it; and (4) X-geometry, where both axes are perpendicular to each other and to R.

Figure 1 shows the rotational barriers at intermolecular distances that two H_2 molecules must overcome to change their spatial arrangement from one form to another. It can be seen from this figure that, at R = 3 bohr, which approximately corresponds to the highest temperature ($\approx$ 7000 K) achieved in the Hugoniot experiments, the highest rotational barrier corresponding to the L$\leftrightarrow$T rotation occurs at a temperature of about 873 K. These rotational barriers are relatively small compared with the 7000 K achieved in the Hugoniot experiments. Assuming that all molecular orientations can be classified into four geometries (L,T,P,X), only 11 percent, or the smallest number of H_2 molecules, have the L-geometry. Since the states with the L-geometry are energetically least favorable, the probability of two H_2 molecules being in the L-geometry at short intermolecular distances is even smaller. At short intermolecular distances, the H-H bond length will readjust itself so as to lower the total energy. The energy-lowering by bond shrinkage is largest for the H_2 molecule having L-geometry. A 6 percent contraction of the H-H bond was calculated to result in a 5 percent lowering of the pair potential energy, E_{AB}. It can be seen from the dashed line in Fig. 1 that contraction of the H-H bond will result in a slight reduction of the L$\leftrightarrow$T rotational barrier. This leads to the conclusion that the molecules are mostly freely rotating at intermolecular distances of approximately 3 bohr.

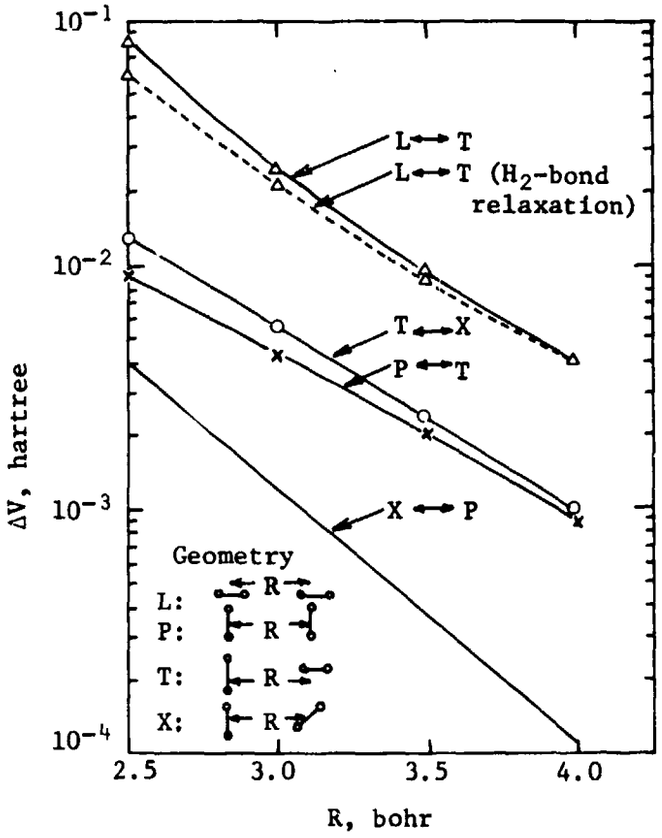

Fig. 1--Rotational barriers confronting two H_2 molecules with a fixed intermolecular separation upon changes of configuration from one of the four geometries (L,P,X,T) to another [7].

Solid lines show the results of calculations for an H-H bond length equal to 1.4 bohr, dashed line shows the results of calculations for an H-H bond length that minimizes the total energy.

Figure 2 shows the spherically averaged intermolecular potential energies as a function of the intermolecular separation R obtained from the HF and CI calculations (curves 1 and 2, respectively). It should be noted that the interaction potential energy is not very sensitive to the averaging procedure used, because the intermolecular potential energies for the T, X, and P geometries are close to each other and the L-geometry, the most repulsive, has the smallest weight (1/9). Curve 3 in Fig. 2 is a plot of the intermolecular potential energy vs the intermolecular separation determined from CI calculation, which gives the lowest energy at a given R. (Both the H-H bond length and rotations of the H_2 axes relative to R were varied to obtain the minimum energy trajectory for two hydrogen molecules.)

For convenience, at $2 < R < 5$ bohr, the spherically averaged HF and CI intermolecular pair potentials (curves 1 and 2, respectively) can be expressed in analytical form:

$$\phi(R) = 7.0\, e^{-1.65\, R} \qquad \text{(HF potential)} \quad (4)$$

and

$$\phi(R) = 7.5\, e^{-1.69\, R}. \qquad \text{(CI potential)} \quad (5)$$

It can be seen from Fig. 2 that, at small intermolecular separations (R = 2-5 bohr), CI calculations result in energies that are about 10 percent lower than energies determined from HF calculations. This is easily explained by the fact that the HF calculations do not include dispersion effects due to exclusion of the electron-electron correlation terms needed to simulate the induced dipole-dipole interaction of the van der Waals forces. These terms are included in the CI calculations at the price of very large sums of determinants. The discrepancy should increase at larger separations where HF results fall off too slowly because they do not contain attractive terms. Although the CI method is still applicable in principle for R > 5 bohr, it becomes impractical because of the large number of determinants required to accurately compute the higher order attractive terms.

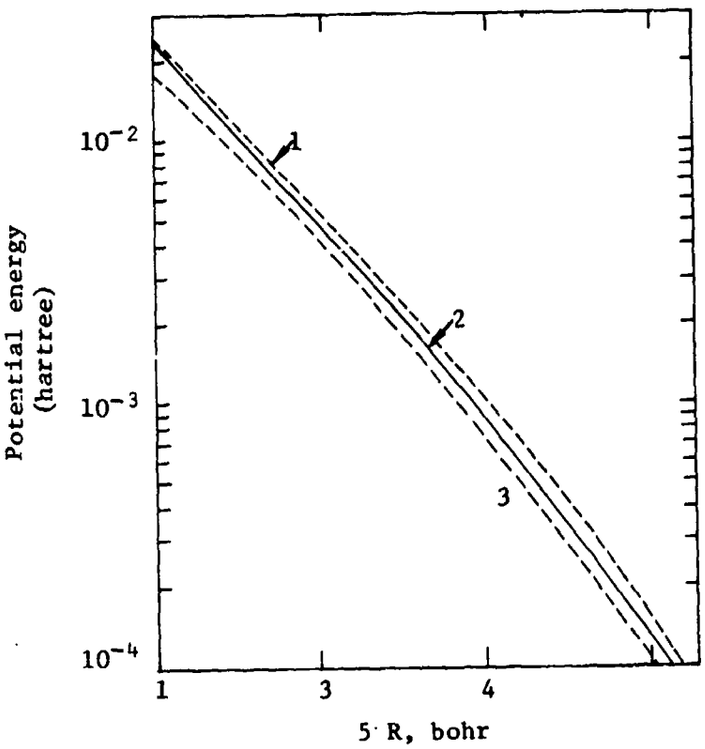

Fig. 2--Spherically averaged intermolecular potential energies (intermolecular pair potentials) of two H_2 molecules determined using *ab initio* techniques [7].

1-Hartree-Fock (HF) intermolecular pair potential, calculated self-consistently for the H-H bond length of 1.4 bohr.

2-Configuration interaction (CI) intermolecular pair potential, calculated for the H-H bond length of 1.4 bohr.

3-Configuration interaction (CI) pair potential, calculated to give the lowest energy at a given intermolecular separation.

Having determined the pair potential of two hydrogen molecules by means of quantum mechanical methods, the next step is to check the validity of these theoretical potentials by calculating the thermodynamic properties of molecular hydrogen.

C. EQUATION OF STATE FOR SOLID HYDROGEN

1. Theory of the Quantum Solid

de Boer and Blaisse [15] were among the earliest workers to point out that, in solidified hydrogen and helium, the small masses and weak interactions would lead to large de Broglie wavelengths and significant quantum effects. For these substances, the zero-point motion is sufficiently large so that neither classical nor harmonic approximation is applicable at very low pressures. The lattice properties of these substances, referred to as "quantum solids," must be calculated by quantum mechanical many-body theory.

For a system of particles interacting via two body forces, the Hamiltonian is:

$$H = -\frac{1}{2m}\sum_i \nabla_i^2 + \sum_{i<j} \phi_{ij} \ , \qquad (6)$$

where the second sum on the right-hand side is the same as that in Eq. (1). Because of the localized nature of molecules in a solid, contributions to the pressure and energy due to exchange will be extremely small. Therefore, unsymmetrized Hartree-like wave function provides a satisfactory representation of the system.

A widely used approximation for the trial wave function of this system is the correlated variational function [16]:

$$\phi = \prod_{i=1}^{N} \Psi(\bar{r}_i) \prod_{j<k}^{N} f(r_{jk}), \qquad (7)$$

where $\Psi(\bar{r}_i) = \Psi(\bar{r}_i - \bar{R}_i)$ are single particle functions localized about the equilibrium lattice sites $\bar{R}_i$, and f is a two-body correlation function used to prevent neighbors from coming unrealistically close

to each other. When dealing with the ground-state energies, an approximate choice for Ψ is the simple normalized Gaussian $\Psi = (\beta/\pi)^{3/4} \exp\left[-(\beta/2)\cdot(\bar{r}-\bar{R})^2\right]$, where β is a variational parameter. The correct two-body correlation function must, near the origin, have the form $f = \exp\left[(-1/2)(k/r)^5\right]$. Consequently, this form is generally used as the correlation function, with k treated as a variational parameter.

It should be emphasized that Eqs. (6) and (7), which represent the basic theory for calculating the equation of state of "quantum solids," are only approximations. The evaluation of the total energy and its derivatives requires the evaluation of terms such as $E = \int \Psi H \Psi d\bar{r}_1 \ldots d\bar{r}_N$, necessitating the calculation of a large number of multicentered integrals. Since an exact solution of these equations involves considerable labor, various approximate calculations have been made. In one of the earliest such computations, Bernardes [17] used a damped sine function with a variational parameter for Ψ, instead of the Gaussian. He permitted no overlap of neighboring molecular wave functions, thus defining an effective correlation function. Hurst and Levelt [18] used a quantum mechanical version the Lennard-Jones-Devonshire cell model. In this model, an atom is in the potential field of stationary neighbors and is restricted to a Wigner-Seitz sphere defined by the molar volume. The wave function, required to vanish at the cell boundary again implicitly defining f, is calculated numerically. Subsequent workers, such as Saunders [16] Nosanow and Shaw [19], and Mullin [20], explicitly included f in the correlation function. However, in order to reduce the problem to a tractable form, they neglect the three and higher centered integrals. This is done formally by the cluster expansion method, in which the ground-state energy is expanded in a series of terms of the many-centered correlations (clusters) and the series is truncated to exclude all but the two center terms. In the cluster expansion method, the energy can be written:

$$E = \frac{3N\hbar^2\beta}{4m} + \langle\phi|\phi\rangle^{-1} \sum_{\lambda<k}^{N} \int \Psi^2(r_\lambda)\Psi^2(r_k) f^2(r_{\lambda k}) \phi(r_{\lambda k}) G(r_\lambda, r_k) d\bar{r}_\lambda d\bar{r}_k, \qquad (8)$$

where $\phi(r) = V(r)-(\hbar^2/2m)\nabla^2 \ln f(r)$ and G is the series expansion. Inclusion of only two center terms is equivalent to setting G = 1. In their more recent work, Etters and Danilowicz [21] have attempted to approximate the effect of triple correlations. The most complete and, in principle, exact solutions of Eqs. (6) and (7) are obtained by the Monte Carlo (MC) method [22]. In the MC method, a few hundred particles are placed in a cell having periodic boundary conditions. The particles are moved according to certain prescribed rules and the energy and position are recorded for each move. The Markov chain made up of these steps provides the MC integration over the 3N coordinates needed to evaluate the total energy and pressure for the particular set of variational parameters. To determine the minimum energy, these calculations must be repeated for a family of such parameters. An enlightening application of this method to solid helium is given by Hansen and Levesque [23] and its application to hydrogen, by Bruce [4].

A limitation of the MC method is the restriction to a finite number of particles and the large amount of required computer time. Consequently, the MC method is not suited for a systematic study involving a large number of different pair potentials. However, since it is an exact calculation, it is well suited to undertake a systematic inspection of approximate theories using a well-defined pair potential. Such a study was undertaken and completed in 1972 by a group of workers at Cornell University under the direction of Krumhansl [3,4,5]. These workers carried out MC calculations on solid hydrogen using the Lennard-Jones and exponential-six potentials. The MC results obtained were found to be in good agreement with calculations employing a variation wave function and limited to two center clusters. These results are constantly being used in more recent tests of the approximate theories. More importantly from the point of view of this study is their discovery that a purely harmonic single-particle model, in which the characteristic Debye frequency is computed from the force constant, is a valid model for hydrogen at pressures above 1 kbar. These results apply to spherically symmetric pair potentials. This result has lead to a considerable

simplification of the theoretical procedure and the labor required for high-pressure molecular hydrogen calculations.

2. High-Pressure Hydrogen Calculations

Unfortunately, although Krumhansl and co-workers carried out a very systematic study on solid molecular hydrogen, they used an empirical potential obtained from analysis of low-density gas data, which are insufficiently sensitive to the repulsive forces that dominate the high-density solid properties. Consequently, their predicted isotherms were in poor agreement with the static data to 20 kbar by Stewart [1]. In 1970, Ross [24], aware of this shortcoming of the gas data, had used a semi-empirical exponential-six pair potential to calculate the properties of hydrogen. In this potential, the exponential parameter ($\alpha = 11.5$) was taken from the molecular orbital theory and the well depth was adjusted to agree with those typically obtained from the second virial coefficient ($\epsilon/k \sim 33$ K). This potential was then used to predict correctly the 40 kbar shock data of Van Thiel and Alder [26] as well as the static data to 20 kbar. An analysis of these and the more recent shock data, in terms of the pair potential, is presented in Section I, subsection D.

As noted earlier, the attractive terms in the pair potential of a molecular solid or liquid at very large intermolecular separations are well known and the theoretically calculated, steeply repulsive, short-range interaction terms at small separations are available. However, no truly *ab initio* method exists for the intermediate region, which includes the potential minimum. Consequently, a theoretician attempting to compute the properties of molecular hydrogen using a pair potential available in the literature faces a decision in selecting the range of intermolecular separations and, thus, the density and pressure regions for which the calculations are to be made. It will thus be illustrative to compare the approach to this problem taken by Ross [6,7] with that by Etters et al. [9,10]. Ross was primarily interested in analyzing the high-density liquid hydrogen shock wave data at pressures from 50 to 900 kbar and temperatures from 1300 to 7000 K attained at the Lawrence Livermore Laboratory. It can be

seen from the pair potential curve that, over this temperature range, the largest contributions to the pressure and energy of hydrogen will necessarily come from the intermolecular interactions at separations below 5 bohr. Thus, for the interpretation of the shock data, the available pair potential computed by the CI method for R < 5 bohr and spherically averaged over four different orientations should be correct. However, Etters et al. were primarily interested in calculating the properties of solid hydrogen at a temperature of 4 K and pressures below 25 kbar and the second virial coefficient. In this case, the correct function to choose for a pair potential is much less obvious because the significant region of intermolecular separation covered by these properties includes the intermediate region that cannot be directly computed by the current *ab initio* techniques. Etters et al. chose the results of the HF calculations, which omit the attractive contributions that are included in CI as their short-range potential. They then added the attractive multipole terms rigorously correct at large R to the short-range potential. Since the long-range attractive terms ($\sim 1/r^n$) must go to zero at small R, an exponential scaling function similar to that proposed by Trubitsyn [25] was used to reduce the attractive terms from full contributions to zero contributions in the region between R = 4.5 and 2.5 bohr. Below R = 2.5 bohr, the total potential is purely HF. All of these contributions were also spherically averaged over the available orientations. Thus, the potential obtained would span the full range of R.

The spherically averaged pair potential $U_T(r)$ derived by Etters et al. can be represented by the following expression:

$$\bar{U}_T(r) = \bar{U}_R(r) - \bar{U}_A(r) \times \left[1 + \exp[-4(r-3.5)]\right]^{-1}, \quad (9)$$

where $\bar{U}_R(r)$ is the repulsive energy averaged over four orientations and $\bar{U}_A(r)$ is the orientation-averaged attractive energy. The exponential term ensures that attraction obeys the proper limits. These authors then used the correlation cluster expansion method, Eq. (8), in which $G \neq 1$, but included the next higher order correlation. They had

previously shown that this model would provide good agreement with the MC results. The results of their pressure vs volume calculations for solid molecular hydrogen, shown in Fig. 3, are in good agreement with the data.

This and most other studies assume the potential to be spherically symmetric despite the diatomic structure of molecular hydrogen, thus neglecting the effect of anisotropy. The error introduced by neglecting anisotropy was investigated by Raich and Etters [8], who have made ground-state energy calculations for hydrogen molecules retaining the orientation dependence of the pair potential. It was found that the molecule continued to rotate freely up to a pressure of about 300 kbar. Above this pressure, the molecules no longer rotate, but vibrate about the equilibrium orientations. The authors show this loss of freedom to be sudden and accompanied by a small (5 percent) decrease in pressure and energy.

In addition to calculating solid properties, Etters et al. [9] have also shown that the same pair potential yields satisfactory results for the second virial coefficient B(T) over the temperature range of 60 to 523 K. They were also able to show that B(T), calculated from either a spherically averaged potential or a fully anisotropic representation, leads to nearly identical results, indicating that the anisotropies contribute little to B(T). Their calculations included the first two quantum corrections to the translational and rotational motions.

The work of Etters et al. appears to be the only one in which the second virial coefficient and the solid isotherm are correctly predicted to a pressure of at least 25 kbar. These workers have also attempted to compare their results with the Van Thiel and Alder [26] shock compression work. Unfortunately, they appear to have compared their low-temperature isotherm directly with the Hugoniot, thus omitting the large thermal contributions that would have approximately doubled their pressures and resulted in the predicted Hugoniot being much too stiff.

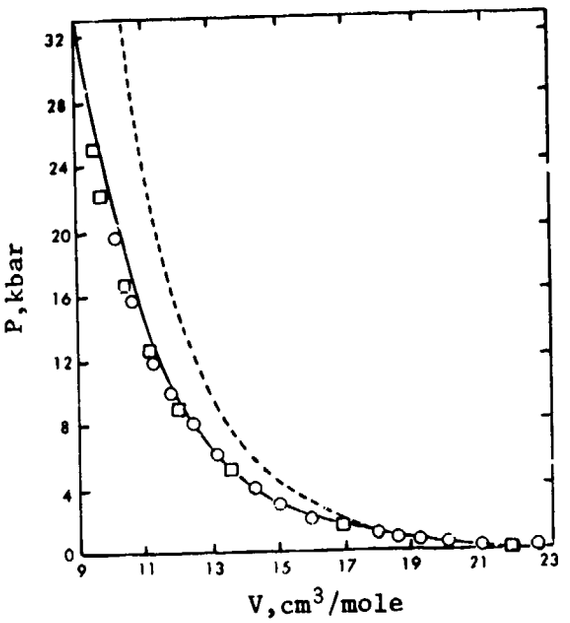

Fig. 3--The pressure vs molar volume curves at zero temperature for solid molecular hydrogen [9].

------ calculated using the 6-12 potential
——— calculated using the EERD potential
□ - experimental data obtained by Anderson & Swenson
△ - experimental data obtained by Stewart

More recently, Anderson et al. [10] used the self-consistent phonon approximation (SCPA) to calculate the pressure vs volume curve for solid molecular hydrogen at zero temperature. In these calculations, they used the pair potential proposed by Etters et al. [9] (EERD potential) and the potential determined by Ross from the shock wave and solid high-pressure data (Ross, or CI + ATT potential). The results obtained are shown in Fig. 4, where they are compared with the experimental data. The calculations appear to show that, at pressures above a few kbar, the two potentials are comparable and in good agreement for both sets of data. Calculation of the bulk modulus by Anderson et al. [10] indicates that the Ross potential may be too soft at the highest pressures. However, at lower pressures (below 2 kbar), the EERD potential predicts properties that are in better agreement with experimental data. As Anderson et al. [10] observe, "it is not

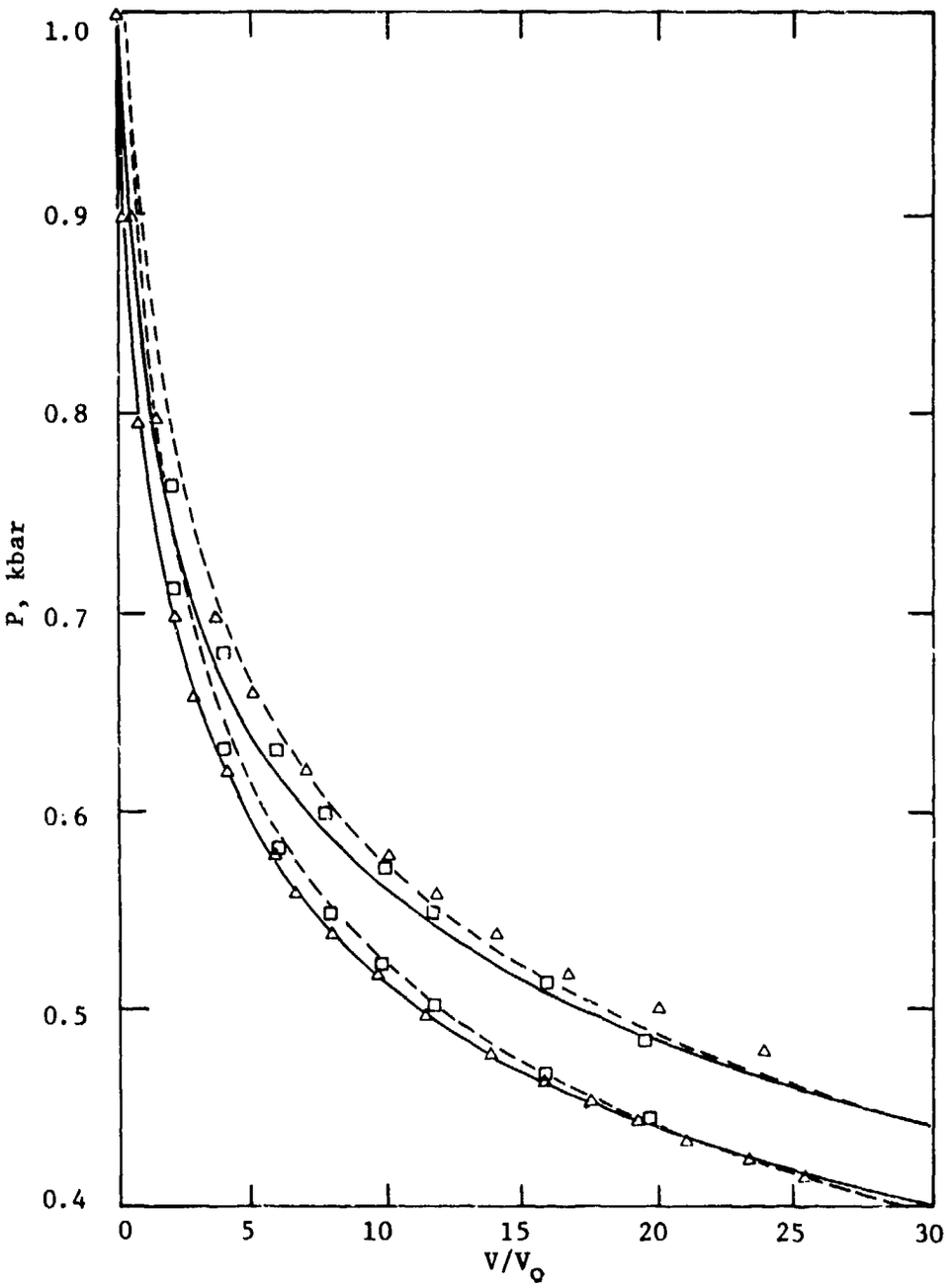

Fig. 4--The pressure vs relative volume curves at zero temperature for solid molecular hydrogen and deuterium [10].

——— calculated using the EERD potential
------ calculated using the Ross potential
△ - experimental data obtained by Anderson & Swenson
□ - experimental data obtained by Stewart

surprising since the Ross potential was in fact designed for investigation of the very high pressures of hydrogen in the neighborhood of the metal-insulator transition, and is not concerned with pressures below 2 kbar in the quantum solid region."

D. SHOCK-COMPRESSED MOLECULAR HYDROGEN AND DEUTERIUM

1. Theory of the Dense Fluid

In recent years, enormous progress has been made in the statistical mechanical theory of fluids, so that, at the present time, it is possible to accurately compute the properties of simple fluids if their pair potentials are known. This favorable state of affairs is the result of the extensive MC and molecular dynamics calculations of the properties of classical solids and fluids, carried out in the late 1950s and 1960s at Los Alamos and Livermore Laboratories. These calculations are, in fact, "computer experiments" and require large amounts of computer time.

One important result of the computer calculations was to provide the "experimental" data to build approximate models of fluids based on the hard-sphere perturbation theory originally proposed by Barker and Henderson [27,28] and improved and modified by a number of workers, including Mansoori and Canfield [29]. Ross [30] has applied a version of the latter model to compute to within ± 1 percent the fluid properties using a wide range of pair potentials, including the Lennard-Jones, exponential-six, inverse-12, inverse-9, inverse-6, and screened Coulomb potential for plasma. Ross has also used this model for calculations of liquid argon shock compressed to 900 kbar [31].

In the only two shock-wave studies of hydrogen and deuterium performed so far [26,32], they are initially in the liquid state at 20 K. Since the temperatures reached are well above the melting temperature, the final state is a compressed fluid. As a result, the shock Hugoniots were computed using hard-sphere fluid perturbation theory.

In the hard-sphere perturbation theory, it is assumed that atoms in a real liquid are arranged as in a hard-sphere liquid, and interact

via a realistic intermolecular potential. The hard-sphere pair distribution function is known analytically and the hard-sphere diameter is determined by minimizing the Helmholtz free energy given by the following expression:

$$\frac{F}{NkT} = \frac{F_0(d,V)}{NkT} + \frac{2\pi N}{V}\int_d^\infty \phi(R)g(R/d)R^2dR - \ln\left(\frac{V}{\Lambda^3 N}\right) - 1 + \frac{F_{int}}{NkT}, \quad (10)$$

where $F_0(d,V)$ is the configurational free energy of hard spheres of diameter d at a volume V and temperature T, $\phi(R)$ is the spherically-symmetric intermolecular potential, $g(R/d)$ is the hard-sphere energy of the internal degrees of freedom, $\Lambda = (h^2/2\pi mkT)^{1/2}$, and other symbols have their usual meaning. For a diatomic molecule,

$$\frac{F_{int}}{NkT} = \ln\frac{T}{2\Theta_R} + \ln\left(1 - e^{-h\nu/kT}\right) + \left(\frac{h\nu}{2} - D_o\right)\left(\frac{1-\alpha}{kT}\right) - \ln q_e - \ln q_{vr}, \quad (11)$$

where Θ_R is the rotational temperature, ν is the diatomic vibrational frequency, $D_o - h\nu/2$ is the dissociation energy, α is the degree of dissociation (number of moles dissociated), q_e is the electronic partition function, and q_{vr} is the effective contribution to the rotation-vibration partition function resulting from the coupling of these two degrees of freedom and from anharmonicity of the vibrator.

It is assumed that ν and D_o are independent of volume and that the molecules rotate freely. It can be shown that these approximations and the effect of nonsphericity are much smaller than the experimental error in determining Hugoniot points from the shock-wave data. The theoretical pair potentials are used in Eq. (10), and, therefore, the Helmholtz free energy, F, is obtained by minimizing F (i.e., from the condition $\partial F/\partial d = 0$). The thermodynamic properties are computed by taking proper derivatives of the minimized free energy.

2. Hugoniot Calculations

The theoretical Hugoniot curve is determined from the relationship:

$$E = E_o + (P + P_o)(V_o - V)/2, \quad (12)$$

where E, P, and V are the energy, pressure, and volume, respectively, of the compressed state, and the subscript o refers to the initial state. In practice, the Hugoniot is calculated by choosing a temperature; calculating the Hugoniot function HUG = $(E - E_o) - (P + P_o)x$ $(V_o-V)/2$ along an isotherm; and finding the E, P, V such that HUG = 0.

The Hugoniots curves of liquid molecular hydrogen calculated using the HF and CI intermolecular pair potentials given by Eqs. (4) and (5) are plotted in Figs. 5 and 6 (curves 1 and 2), respectively. The reflected portion of the Hugoniot was calculated using P, V, and E achieved during the first shock as the initial conditions--i.e., as P_o, V_o, and E_o for the second shock. The computed Hugoniots show that the HF and CI potentials given by Eqs. (4) and (5) are too stiff and that attractive terms must be added in order to obtain agreement with the experimental shock-wave data. The effective pair potentials obtained by adding two attractive terms (ATT) multiplied by a damping factor to Eqs. (4) and (5) are as follows:

$$\phi(R) = 7.0e^{-1.65R} - (13/R^6 + 116/R^8)e^{-400/R^6} \quad \text{(HF + ATT potential)} \quad (13)$$

and

$$\phi(R) = 7.5e^{-1.69R} - (13/R^6 + 116/R^8)e^{-400/R^6} \quad \text{(CI + ATT potential)}. \quad (14)$$

The inverse sixth-power attractive term was determined from an analysis of the experimental oscillator strengths and the inverse eighth power term, from theoretical calculations. The attractive terms are multiplied by the damping factor suggested by Trubitsyn [25] on theoretical grounds. Addition of the damping term makes the attractive terms go to zero at a short range, preventing them from becoming unrealistically large, without affecting their long-range behavior.

The HF + ATT and CI + ATT potentials given by Eqs. (13) and (14) were used to calculate the Hugoniots of liquid molecular hydrogen. The results obtained are plotted in Figs. 5 and 6 (curves 3 and 4). It can be seen from these figures that the Hugoniots determined from Eqs. (13) and (14) are in much better agreement with the experimental data than the Hugoniots determined from Eqs. (4) and (5). The CI + ATT

potential given by Eq. (14) appears to be in best agreement with the available shock compression data. Some of the Hugoniot points (P, V, T) calculated using the CI + ATT potential are given in Table 1. Static isotherms to pressures of 25 kbar, calculated by Ross using this potential, are in good agreement with experiment. This same pair potential (CI + ATT) was used independently by Anderson et al. [10], whose work was reviewed in Section II, subsection C. His calculations, shown in Fig. 4, confirmed that CI + ATT potential is in good agreement with the static work. Hugoniots calculated using Eq. (14) are also in good agreement with the shock-compression data obtained by Dick [33] on liquid hydrogen at 150 kbar.

A pair potential that is in somewhat better agreement with the 900 kbar point, but in poorer agreement with the 210 kbar points, is given by the equation

$$\phi(R) = 1.555e^{-1.495R}. \qquad (15)$$

The Hugoniots calculated from this potential are shown in Figs. 5 and 6 (curves 5). This potential may be considered a rough lower bound on the softness of the potential, while the HF + ATT potential given by Eq. (13) may be similarly considered a rough upper bound.

Table 1

HUGONIOT POINTS CALCULATED USING THE CI + ATT POTENTIAL*

Parameters	Hydrogen	Deuterium		
		First Shock	Reflected from First Shock	
V (cm^3/mole)	10.5	6.9	4.0	3.8
P (kbar)	43.8	205	810	937
T (K)	1334	4579	6464	6891
R (bohr)	5.50	4.78	3.99	3.92
d (bohr)	3.76	3.09	2.81	2.77
Nd^3 (cm^3/mole)	4.73	2.64	1.98	1.91

*Initial conditions: V_o = 28.6 cm^3/mole (H_2) and V_o = 23.79 cm^3/mole, (D_2) T = 20.7 K.

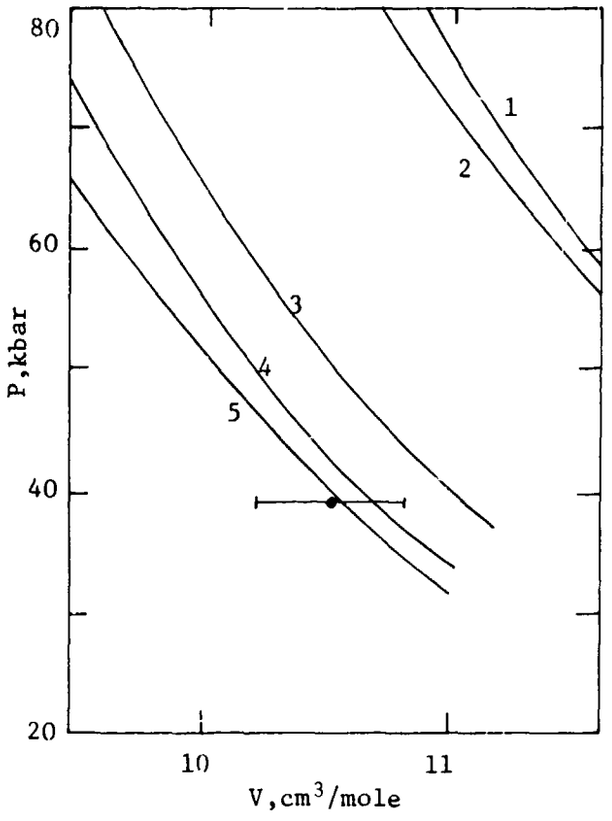

Fig. 5--Theoretical Hugoniots and the shock deuterium data of van Thiel and Alder.

1-Hugoniots calculated using pair potential given by Eq. (4) (HF potential)
2-Hugoniot calculated using pair potential given by Eq. (5) (CI potential)
3-Hugoniot calculated using pair potential given by Eq. (13) (HF + ATT potential)
4-Hugoniot calculated using pair potential given by Eq. (14) (CI + ATT potential)
5-Hugoniot calculated using pair potential given by Eq. (15)

The circles are the Hugoniot points of deuterium obtained by Van Thiel and Alder [26]. The bar indicates the uncertainty (possible error) in determining the Hugoniot points.

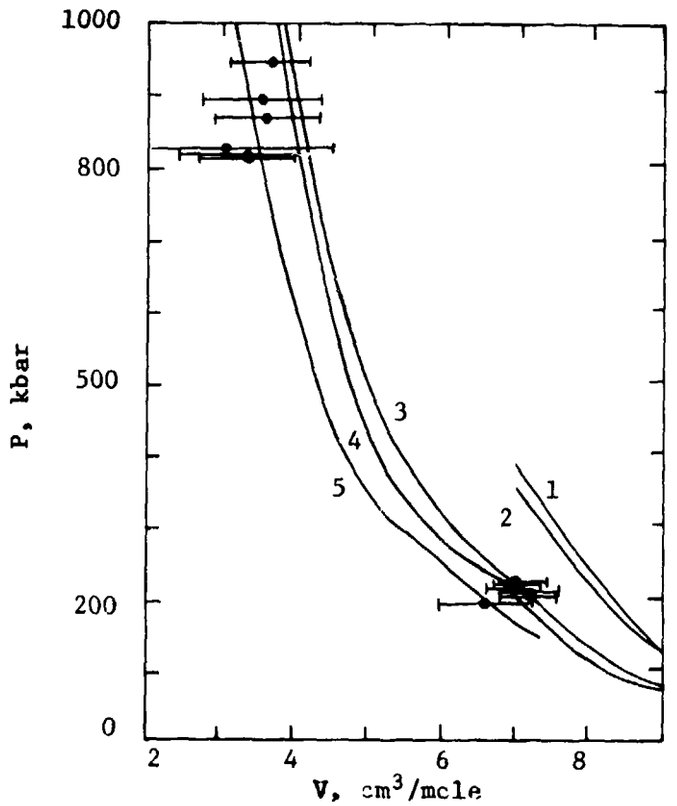

Fig. 6--Theoretical Hugoniots and the shock deuterium data of van Thiel et al.

1-Hugoniot calculated using pair potential given by Eq. (4) (HF potential)
2-Hugoniot calculated using pair potential given by Eq. (5) (CI potential)
3-Hugoniot calculated using pair potential given by Eq. (13) (HF + ATT potential)
4-Hugoniot calculated using pair potential given by Eq. (14) (CI + ATT potential)
5-Hugoniot calculated using pair potential given by Eq. (15)

The circles are the shock Hugoniot points of deuterium obtained by van Thiel et al. [32]. The bars indicate the uncertainty (possible error) in determining the Hugoniot points. Apparent kinks in curves result when the primary Hugoniots are reflected into a new path.

Table 1 summarizes the data on the effective hard-sphere diameter, d, and illustrates quite clearly how shock data provide information on the pair potential at small separations. The hard-sphere diameter, d, represents the closest approach of shock-compressed molecules to each other, and Nd^3 represents the effective volume to which the molecules are compressed due to the effect of both compression and high temperature--i.e., the effective volume on which information can be obtained on the intermolecular pair potential. From this table, it can be seen that, at a shock pressure of 900 kbar and a shock temperature of 6891 K, the volume is 3.8 cm^3/mole, the effective volume is Nd^3 = 1.91 cm^3/mole, and, thus, the ratio is $V/Nd^3 \geq 2$. This same value of the ratio is also maintained at the other three Hugoniot points given in Table 1. Since the metallic transition of hydrogen is usually predicted to occur near 2 cm^3/mole, the high temperatures achieved in shock-compression experiments make it possible to determine the intermolecular potential at about the same density as that required to reliably predict the metallic transition.

The analysis in Section I, subsection B, of theoretical calculations of the pair potential showed that at temperatures and separations along the Hugoniot, most of the molecules are freely rotating and that the bond distance and probably the vibrational frequency are not significantly affected. Calculations show that the molecular dissociation does not exceed 4 percent. Therefore, it appears that the approximations made in deriving Eqs. (4) and (5) are adequate. As noted earlier, the CI intermolecular pair potential (Eq. (5)) at intermolecular separations between 2 and 5 bohr is generally determined with an error not exceeding 10 percent. Nevertheless, considerable discrepancy exists between this potential and the CI + ATT potential of Eq. (14), which best fits the data but contains additional attractive terms.

3. Many-Body Intermolecular Effects

It was recognized that the discrepancy between the *ab initio* calculated CI pair potential and the "effective" CI + ATT potential may be due to energy lowering by many-body effects. However, no

computations of nonpairwise additive contributions to the interaction energy of a system of hydrogen molecules had ever been made. Ree and Bender [13] performed such calculations involving three molecules. In their calculations, the three-body potential energy, E_{ABC}, is obtained by taking the difference between the total ground-state energy, E_{A+B+C}, of three H_2 molecules (A, B, and C) and the sum of energies for geometries where at least one molecule is sufficiently far away from the others--i.e.:

$$E_{ABC} = E_{A+B+C} - E_{AB} - E_{AC} - E_{BC} - 3E_A, \quad (16)$$

where the H-H bond lengths are fixed at 1.4 bohr. Geometries used in the calculations (see Fig. 7) are isosceles triangles formed by the H_2-H_2 center-to-center intermolecular distances, with $R_{AB} = R_{AC}$ and R_{BC} varying from $R_{BC} = R_{AB}$ (an equilateral triangle) to $R_{BC} = 2R_{AB}$ (equidistantly located molecules along a straight line). Calculations were performed for R_{AB} = 2, 2.5, 3, and 3.5 bohr. The axes of the H-H bonds are restricted to lie perpendicular to the plane formed by the three centers of H_2 molecules.

The results of these calculations are summarized by three curves shown in Fig. 7, which is a plot of $E_{ABC}/(E_{AB} + E_{AC} + E_{BC})$ vs θ, where E_{ABC} is the three-body potential energy of three hydrogen molecules arranged in parallel geometry; $E_{AB} + E_{AC} + E_{BC}$ is the two-body potential energy of three hydrogen molecules; and θ is the angle between R_{AB} and R_{BC}. It can be seen from this figure that the three-body potential of molecular hydrogen is large and negative for the equilateral configurations, and small and positive for the linear geometries. Although only a limited number of simple configurations were considered, the results show conclusively that a large three-body effect is a general phenomenon for all highly condensed states of molecular hydrogen.

The effect of the three-body contribution to the theoretically calculated pair potentials for the hydrogen molecule is shown in Fig. 8. Curve 1 in this figure is the theoretically calculated CI pair potential given by Eq. (5). Curve 2 is the empirical CI + ATT pair

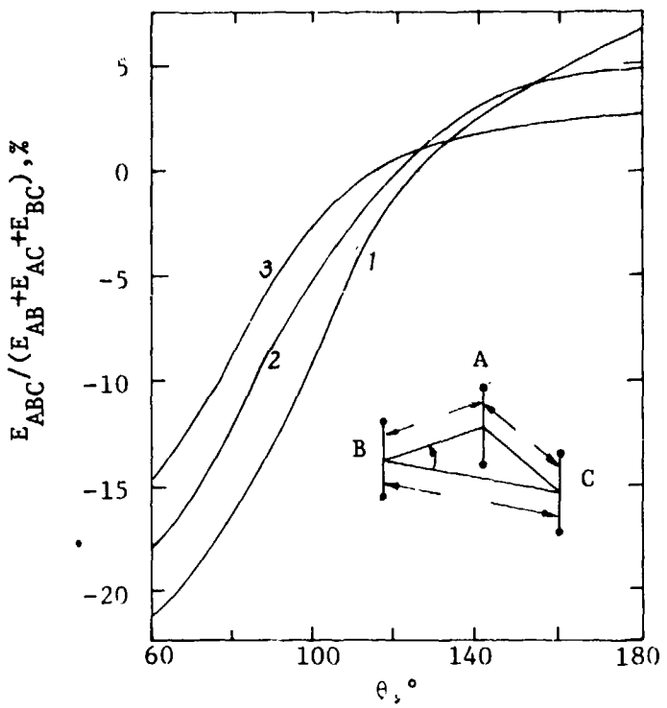

Fig. 7--A plot of the ratio (in percent) of the three-body potential energy to the two-body potential energy of three hydrogen molecules arranged in parallel geometry as a function of θ, the angle between R_{AB} and R_{BC} at fixed values of $R_{AB} = R_{BC}$. (The small figure on the right-hand side shows the configurations used in the calculations.) [13]

1-a = 2.5 bohr

2-a = 3.0 bohr

3-a = 3.5 bohr

potential given by Eq. (14), obtained by adding attractive terms to Eq. (5). The CI pair potential lies above the CI + ATT pair potential that best fits all of the available experimental data. Curve 3 is the effective pair potential with the effect of the third body taken into account, as described by Ree and Bender. It can be seen from this figure that, taking into account the effect of the third body on the pair potential results in a potential (curve 3) that is in

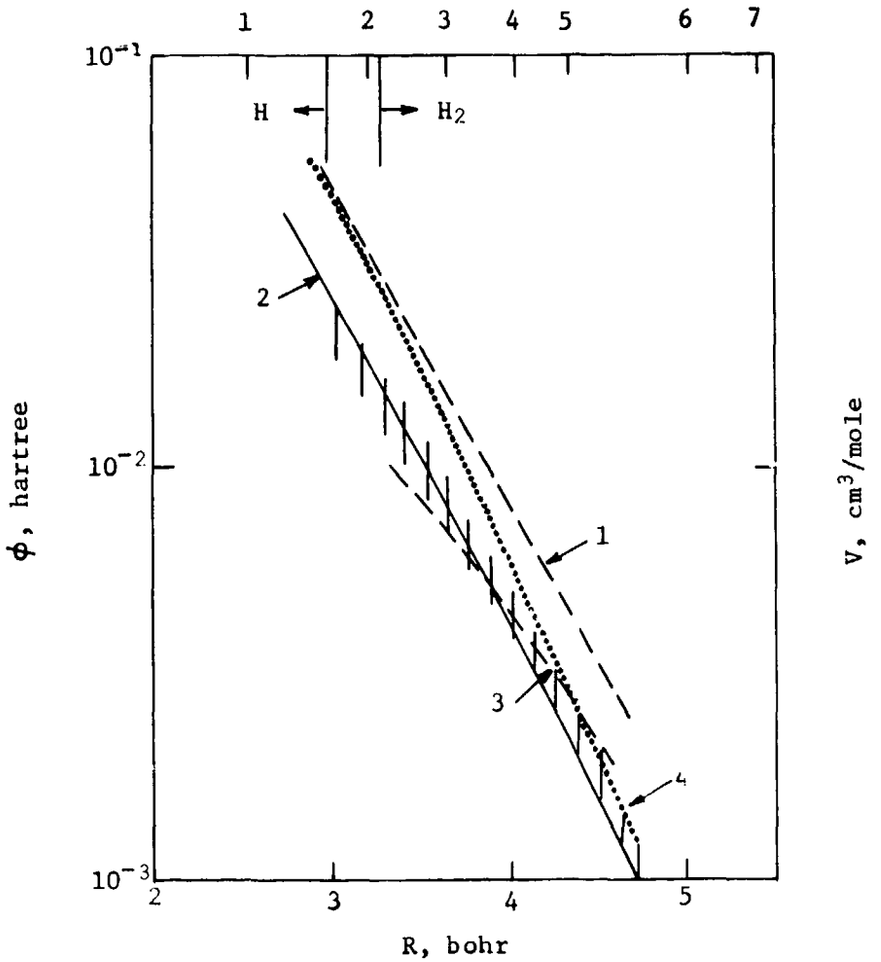

Fig. 8--A plot of theoretically calculated vs experimentally obtained molecular hydrogen pair potentials [7].

1 - theoretically calculated CI pair potential given by Eq. (5)
2 - CI + ATT pair potential given by Eq. (14)
3 - CI pair potential with the effect of the third body taken into account
4 - EERD potential [9,10]

The vertical lines indicate the range of values of the pair potential agreeing with the experimental data (Eqs. (13) through (15)).
The expected region of transition into metallic state is marked off by the arrows and letters H_2, H.

qualitative agreement with the best-fit pair potential (CI + ATT, curve 2) in the region of H_2 stability. The agreement indicates that adding the attractive terms to the pair potential of high-density molecular hydrogen, as in CI + ATT potential, is equivalent to adding the many-body effects to the CI pair potential. Also included for comparison is the EERD potential used by Etters et al. [9,10] to evaluate the solid state and gas data. This potential is in agreement with the CI + ATT potential at large intermolecular separations and, for this reason, both provide good agreement with the experimental static data. However, the EERD potential is much stiffer at small separations. It should be noted that near R = 4 bohr, the EERD potential lies considerably below the CI results (which, at this separation, should be accurate to 10 percent), indicating that the simple ad hoc addition of long-range attractive terms to a Hartree-Fock result (containing no attraction) may, in fact, overestimate the attractive energy. From a more pragmatic or operational point of view, the potentials are very similar--particularly when one considers that Etters et al. made no serious attempt to interpret shock data.

The pressure and energy of dense solid molecular hydrogen under compression were calculated in the harmonic approximation, known to be valid above 2 kbar, using the HF + ATT and CI + ATT potentials. The results obtained are used in Section III to compute the metallic transition of hydrogen. The 0 K static isotherms (excluding vibrational pressure) calculated using HF, CI, and CI + ATT potentials are plotted in Fig. 9, where they are compared with the theoretical results of Liberman [34].

The isotherm calculated using the CI + ATT potential (curve 4 in Fig. 9) is consistent with that of Liberman, who has calculated the equation of state for molecular hydrogen using the Korringer-Kohn-Rostocker (KKR) solid state band theory method, which treats each molecule as a pseudo-molecule in which the two nuclear charges were sphericalized. This converts the two-center spherical potential into a one-center spherical potential, which can be handled by Liberman's KKR band theory code for a face-centered lattice.

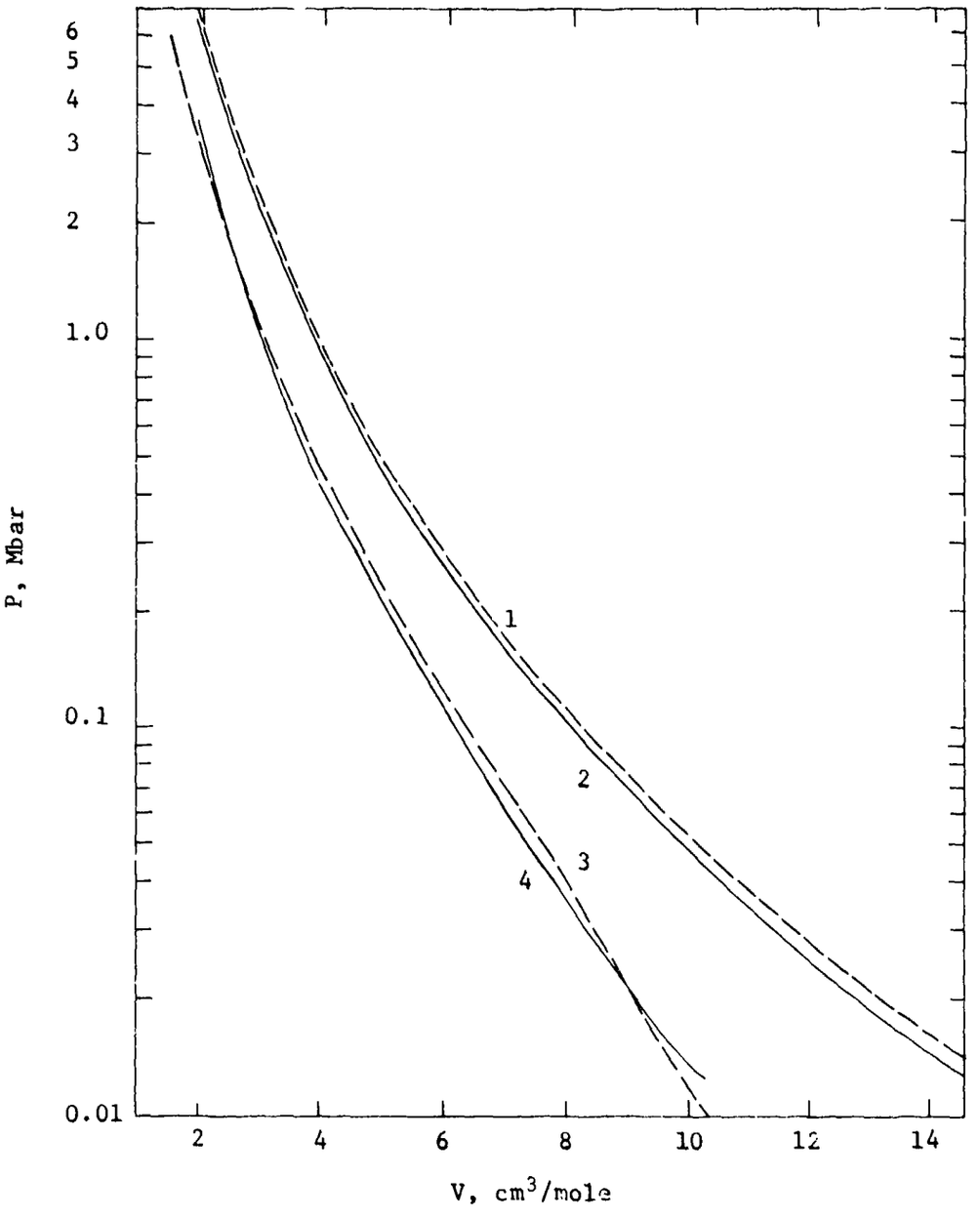

Fig. 9--Comparison of the 0 K isotherms (excluding vibrational pressure) calculated using HF, CI, and CI + ATT potentials given by Eqs. (4), (5), and (14), respectively, with that obtained by Liberman.

1 - calculated using HF potential
2 - calculated using CI potential
3 - Liberman's calculations
4 - calculated using CI + ATT potential

Since Liberman's calculations were made for a solid, they include many-body effects. Therefore, the good agreement between Liberman's calculations and those using CI + ATT pair potential, which was in good agreement with the shock and static data and was shown to include three-body effect, further substantiates the results of Ree and Bender on the importance of many-body effect.

An explanation of the observed energy lowering below that predicted by the CI pair potential and thus, possibly, indirect evidence for contribution of the many-body forces, is given in the recent theoretical work of Ramaker et al. [35] and Friedli [36], who have carried out calculations of the electronic structure of molecular hydrogen crystal. They found that, at very high pressures, the energy required to excite an electron from the valence to the conduction band decreases with decreasing lattice spacing, and eventually goes to zero. This leads to what might be a molecular insulator-to-molecular conductor transition at molecular hydrogen volumes between 5 and 2.5 cm^3/mole. These calculations will be discussed further in Section III in terms of their bearing on the metallic transition. However, it is clear that a decrease in the electronic excitation energy must cause an increase in the molecular polarizability and, hence, a lowering of the total energy. In other words, the increased polarizability leads to what might be observed as an additional effective attractive energy. This may be seen from the expression for the van der Waals attractive energy between two spherically symmetric molecules, a and b, separated by a distance, R, given by the following formula [37]:

$$E_{vw}(R) = -\frac{2}{3}\frac{e^4}{R^6}\sum_{m,n\neq 0}\frac{|R^a_{om}|^2|R^b_{on}|^2}{(\Delta E^a_{mo} + E^b_{no})}, \qquad (17)$$

where R^a_{mo} is the matrix element for an electronic transition in molecule a with an energy change ΔE^a_{mo} from the ground state 0 to an excited state, m. A decreasing energy gap of the type observed by Friedli, as shown in Fig. 10, would lead to enhanced attractive forces at high density, although the precise functional form valid at small R might

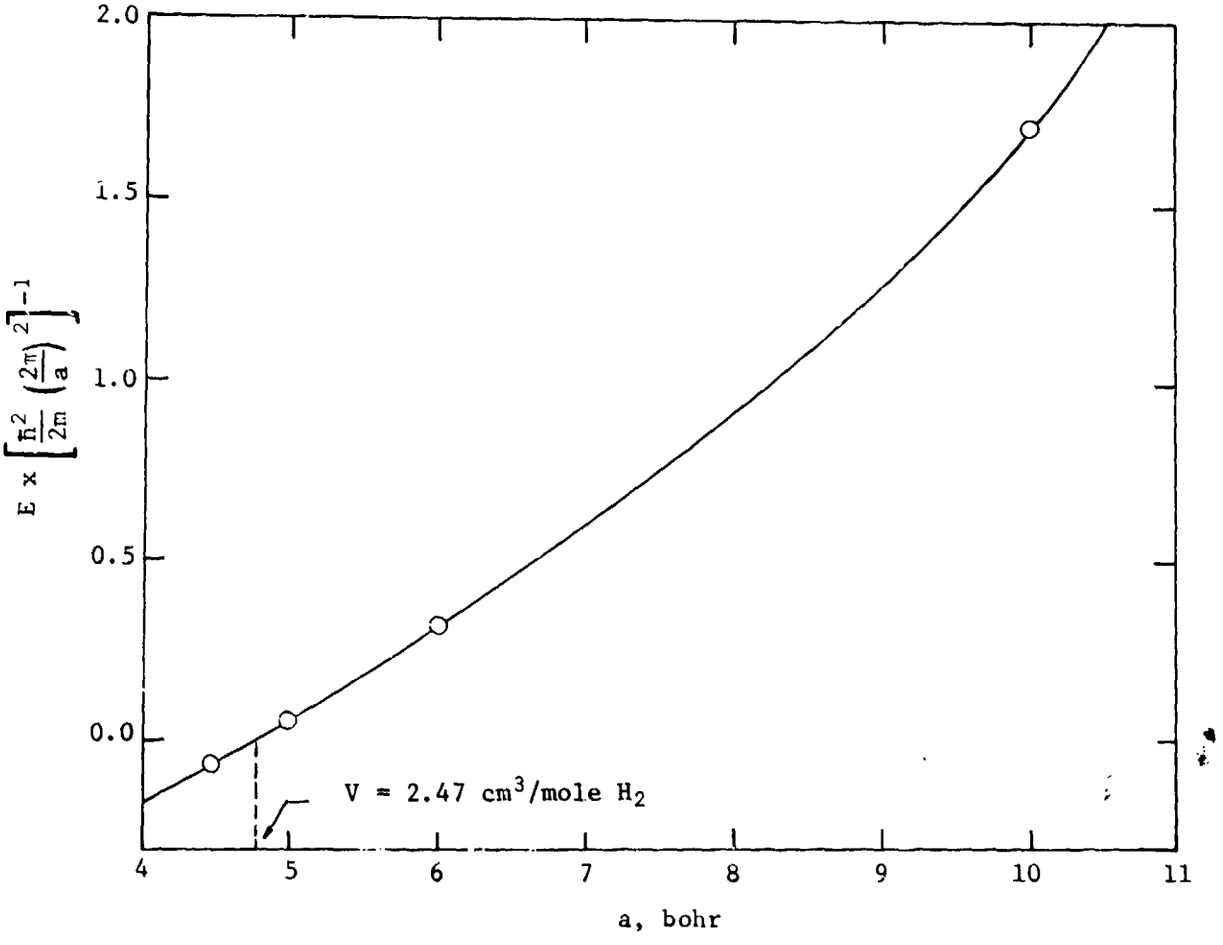

Fig. 10--Energy gap normalized to $(\hbar^2/2m)\cdot(2\pi/a)^2$ as a function of the lattice constant a. The solid line is an approximate interpolation between the calculated values, which are indicated by circles [36].

not be the expression given by Eq. (17), which is rigorous at large R. Since the increased polarizability results from the formation of conduction bands, which are electron states of the whole material, it is a many-body effect. These results emphasize the need for further work on the molecular solid to be carried out on the whole crystal.

In addition to the change in polarizability, which influences the effective pair potential, a decreasing optical band gap would require a reanalysis of the shock-wave data because this alone could result in a softening of the observed Hugoniot. A narrowing of the band gap allows enhanced electronic excitations, which, in turn, act as an energy sink absorbing energy that would otherwise be used in translation, thus keeping down the temperature and the observed pressure. In addition, it can be shown that a decreasing band gap ΔE will contribute a negative term to the total pressure proportional to $-\frac{\partial \Delta E}{\partial V}$. Such an anomalous softening has been observed in many shock-compressed materials, including xenon, where it was identified as resulting from the narrowing of the 5p to 5d band gap [38]. In the case of hydrogen, additional complexity arises from enhanced dissociation.

II. EQUATION OF STATE OF SOLID METALLIC HYDROGEN

A. GENERAL

In general, calculations of the equation of state and other thermodynamic parameters of metallic hydrogen have given more consistent results than those for the molecular hydrogen. For example, the results of the earliest calculation by Wigner and Huntington, using the approximate cellular method, do not differ significantly from the self-consistent Wigner-Seitz calculations of Neece et al. [39], who used the same method with an improved correlation potential energy function.

There are four general methods by which the equations of state of metals are commonly computed using current solid state theory. These are: (1) electron band methods, such as the augmented plane wave (APW); (2) free electron perturbation theory (PERT); (3) the linear combination of atomic orbitals (LCAO); and (4) the Wigner-Seitz (WS) method. Another widely used method--the KKR (Korringer-Kohn-Rostocker)--is formally equivalent to the APW. Although the earliest calculation of hydrogen by Wigner and Huntington [40] was based on the WS method, the most commonly used method has been PERT. Although metallic hydrogen calculations assume that the stable structure at 0 K is a solid, the possibility that it may be a quantum liquid cannot be ruled out and will be discussed in Section III.

In view of the fact that no experimental data on metallic hydrogen are available and all four methods are approximations, it is very difficult, if not impossible, to determine the accuracy of calculations, or even the best method to perform them. Nevertheless, it is possible to estimate the differences between the best results obtained by these four methods and, consequently, the extent to which predicted properties of the metal will be model-sensitive.

This section will first discuss the methods used in the calculations of thermodynamic parameters of metallic hydrogen and then compare and analyze the results obtained using the four techniques.

To be consistent, all calculations were performed for the fcc lattice. Therefore, the energy, pressure, and Gibbs free energy obtained by the APW, LCAO, PERT, and WS methods do not include contributions from zero-point motion or electron correlation. The latter two contributions to the energy, pressure, and Gibbs free energy were each calculated by the same method and tabulated separately. Whenever possible, as is the case in APW, PERT, and WS calculations, the Kohn-Sham free electron exchange potential was used in all calculations in order to retain as much as possible the same Hamiltonian, so that the study would be capable of systematically discerning differences among the models. The APW, LCAO, and WS were all carried out as self-consistent calculations.

B. CALCULATION METHODS

1. Augmented Plane Wave (APW)

The most sophisticated of the four methods used in this set of calculations is the APW technique. It is a modified Hartree-Fock procedure in which the exact exchange is replaced by a local free electron exchange. In this method, the boundary condition on the wave function of each electron state in the crystal is treated exactly.

The total energy, excluding zero point motion energy and electron correlation energy, is:

$$E = K + U, \tag{18}$$

where K is the total electron kinetic energy and U is the total potential energy, less correlation energy, given by the following expression:

$$U = \int dr\ \rho(\bar{r}) \left[V_{ne}(\bar{r}) + 1/2 V_{ee}(\bar{r}) + 3/4 V_{ex,\alpha}(\bar{r}) \right] + E_{nn}, \tag{19}$$

where $\rho(r)$ is the electron density, $V_{ne}(r)$ is the electron nuclear potential, $V_{ee}(r)$ is the electron-electron potential, $V_{ex,\alpha}=-(3\alpha/\pi)x[3\pi^2\rho(\bar{r})]^{1/3}$ is the local exchange potential, and α is a parameter that may be adjusted. (In calculations performed, it was taken to be 2/3--i.e., the Kohn-Sham value.) In order to satisfy the variational principle, making it possible to calculate pressure, the wave functions must satisfy the one-electron Schroedinger equation:

$$\epsilon_i\Psi_i = \left[-1/2\nabla^2 + V_{ne}(r) + V_{ee}(r) + V_{ex}(r)\right]\Psi_i. \quad (20)$$

The pressure is then computed from the virial theorem:

$$PV = \frac{2}{3}K + \frac{1}{3}U. \quad (21)$$

2. Linear Combination of Atomic Orbitals (LCAO)

The LCAO calculations were based on a method first proposed by Abrikosov [41] and, more recently, used by Harris et al. [42]. As first suggested by Abrikosov, the Block wave function for the k-th electron is written as:

$$\Psi_k(\bar{r}) = e^{i\bar{k}\cdot\bar{r}}\sum_n \phi(r-R_n), \quad (22)$$

where the sum is over all neighboring lattice sites located at R_n and $\phi(r)$ is a single Slater-type orbital (STO) of the form $e^{-\alpha r}$, where α is varied to minimize the total energy and satisfy the variational principle.

Another set of calculations taken from Ramaker et al. [35] are also used in this report. These authors wrote the wave function in the form:

$$\Psi_k(\bar{r}) = \sum_K \rho(\bar{k}+\bar{K})\exp[i(\bar{k}+\bar{K})\cdot\bar{r}]\sum_n \phi(\bar{r}-\bar{R}), \quad (23)$$

where $\bar{k}$ is restricted to the first Brillouin zone, $\bar{K}$ is a reciprocal lattice vector, and $\phi(r)$ is a single Slater-type orbital. Eq. (23) differs from Eq. (22) in that it contains a sum over $\bar{K}$.

It is interesting to note that correlation energy cannot be included in the LCAO calculations in any tractable fashion consistent with this method. It is a major reason why the correlation energy contribution to energy, pressure, and Gibbs free energy was calculated separately.

3. Wigner-Seitz (WS)

The results of WS calculations used in this report are taken from a paper by Neece et al. [39]. In the WS method, each atom is assumed to be in a spherical cell equal in size to the atomic volume. The energy of the spherical cell consists of the following contributions:

1. The Fermi energy of the electrons $E_F = 2.21\ \alpha'/r_s^2$ in Rydbergs, where α' represents a correction for the electron binding and is slightly less than unity and r_s is the radius of the spherical cell in units of the Bohr radius a_o.

2. The ground-state electron energy obtained by solving the Schroedinger equation subject to the boundary conditions that the wave function and its first derivative are continuous across the boundary.

3. Corrections for exchange and correlation between the electrons.

The equation of state for the pressure at 0 K is calculated from the following equation:

$$P = -\frac{nr_s}{3}\frac{dE}{dr_s}\ , \qquad (24)$$

where n is the number of electrons per cm^3. Neece et al. solved the Schroedinger equation for the k = 0 state so that the wave function is pure s. They assumed a free-electron density of solids, with an effective mass determined by the perturbation theory. Similarly to APW, LCAO, and PERT calculations, Neece et al. [39] used the value of 2/3 for the exchange parameter α (Kohn-Sham exchange potential). The calculations were done self-consistently and included correlation energy.

4. Perturbation Theory (PERT)

Since in the APW, LCAO, and WS methods it is assumed that the protons form an ideal lattice, the equations of state are valid only at or near 0 K temperature. On the other hand, the free electron perturbation theory (dielectric-constant method) is inherently more flexible and can be used to solve the problem for any ion configuration, so that equations of state may be obtained by this technique for a wide range of temperatures. In the PERT method, in the lowest approximation the free electrons are assumed to be free and the contributions to the free-electron density due to interactions are treated as first order perturbations. The self-consistent perturbation to the free electrons in plane wave states $|\bar{k}\rangle$ due to the proton potential and due to the induced electron density is calculated using the expression:

$$\delta n_e(\bar{k}) = (\varepsilon_k^{-1} - 1)\, n_p(\bar{k}), \qquad (25)$$

where $\delta n_e(\bar{k})$ is the Fourier transform of the perturbed electron density, $n_p(\bar{k})$ is the Fourier transform of the proton density distribution, and ε_k is the static dielectric function of a zero temperature electron gas. It is assumed that the electrons are in their ground state. Neglecting the exchange and correlation in deriving the static dielectric function results in the well-known Lindhard function. The energy per proton consists of the average kinetic energy per electron of the electron gas at zero temperature, the net electrostatic energy of interaction between protons and unperturbed electrons, and the energy change due to perturbed electron distribution. The pressure at 0 K is determined from Eq. (24).

The PERT calculations were performed using the version of the method described by Hammerberg and Ashcroft [43]. Since these authors have shown that the sum of the fourth order terms is negligible, calculations were made to third order only.

5. Zero-Point Energy Calculations

The contributions to the energy, pressure, and Gibbs free energy due to the zero point motion of protons were calculated from the

following expression:

$$E_{ZP} = \frac{9}{8} \Theta_D, \qquad (26)$$

where Θ_D is the Debye temperature. Below 2 Mbar, Θ_D was taken from the work of Neece et al. [39] and at higher pressures, from their unpublished results [44]. Neece et al. [39] used the well-known electrostatic model of Fuchs. This model suffices to approximate the magnitude of the zero-point properties of metallic hydrogen.

6. Correlation Energy Calculations

The free energy of a many-body system interacting via the Coulomb potential can be expressed in the form of a perturbation expansion whose leading term is the ring term. At near zero temperatures and high densities, it is the major contributor to the correlation energy of the electron gas. Graboske and de Witt [45] have numerically evaluated the generalized ring term for arbitrary density and temperature. In the low temperature limit and in the density range of interest, their numerical data were approximated by Neece et al. [39] by the following relationship:

$$E_{corr} = - 0.1303 + 0.0495 \ln(r_s), \qquad (27)$$

where r_s is the radius of the electron sphere. This expression used to calculate the electron correlation energies given in this report differs by less than 10 percent from the more common Nozieres-Pines [46] interpolation formula:

$$E_{corr} = - 0.115 + 0.031 \ln(r_s). \qquad (28)$$

A more recent and more rigorous expression for the correlation energy, as derived by Hedin and Lindqvist [47], lies between Eqs. (27) and (28), but is closer to the former.

C. RESULTS OF THE CALCULATIONS

The energy, pressure, and Gibbs free energy for the fcc lattice of metallic hydrogen calculated by the APW, LCAO, PERT, and WS methods described in Section B are listed in columns 2 through 5, respectively, in Tables 2, 3, and 4. The numbers in these columns do not include contributions from the zero-point motion or electron correlation. Column 6 in Table 2, labeled ΔE, is the difference between the highest and the lowest values of energy E calculated by all four methods (i.e., the highest and the lowest energy in columns 2 through 5) for each volume listed in column 1. In similar fashion, column 6 in Tables 3 and 4, labeled ΔP and ΔG, gives the difference between the highest and the lowest values of pressure P and Gibbs free energy G, respectively. Column 7 in each of these tables gives the contribution of the zero-point motion to E, P, and G as determined from Eq. (26). Although correlation energy was omitted from the APW results shown in column 2 of Tables 2, 3, and 4, another set of self-consistent APW calculations was made using Eq. (27) as a local correlation energy expression in which $\rho=\rho(r)$. In this approximation, the total correlation energy is written as:

$$\int E_{corr}(r)\rho(r)d\bar{r}. \qquad (29)$$

The problem was solved using the variational principle. The self-consistent results were found to differ by not more than one percent from the calculations in which the free-electron correlation had been added directly to the "uncorrelated" APW results obtained using the same free-electron expression but with a constant ρ, or $\rho=1/V$. Consequently, the contribution to the energy, pressure, and Gibbs free energy due to electron correlation could be based on the free-electron equation (Eq. (27)) using the constant charge density, $\rho=1/V$. These contributions are shown in column 8 in Tables 2, 3, and 4.

Excluding columns 3b and 5, all of the data in Tables 2, 3, and 4 are taken from a paper by Ross and McMahan [48]. The numbers in the LCAO column (3b) in Table 2 are taken or interpolated from the paper by Ramaker et al. [35].

Table 2 [48]

COMPUTER-CALCULATED ENERGY OF METALLIC HYDROGEN

Vol (cm^3/mole) (1)	Energy (Rydberg)							
	APW (2)	LCAO		PERT[c] (4)	WS (5)	ΔE (6)	E_{ZP} (7)	E_{corr} (8)
		(3)[a]	(3)[b]					
1.855	-0.968	-0.932	-0.950	-0.943 -(0.029)	-0.970	-0.038	0.015	-0.104
1.0	-0.926	-0.901	-0.902	-0.915 -(0.024)	-0.933	-0.031	0.020	-0.114
0.9	-0.910	-0.886	-0.886 (±0.001)	-0.901 -(0.0235)	-0.918	-0.032	0.021	-0.116
0.8	-0.887	-0.865	-0.865 (±0.001)	-0.881 -(0.023)	-0.898	-0.033	0.023	-0.118
0.7	-0.856	-0.836	-0.836 (±0.001)	-0.852 -(0.022)	-0.867	-0.031	0.024	-0.120
0.6	-0.810	-0.793	-0.793 (±0.001)	-0.809 -(0.021)	-0.823	-0.030	0.026	-0.123
0.5	-0.742	-0.729	-0.729 (±0.001)	-0.745 -(0.020)	-0.758	-0.029	0.029	-0.126

[a] Calculated by Ross and McMahan [48].

[b] Taken or interpolated from Ramaker, et al. [35].

[c] The terms in parentheses are the third order contributions to PERT energy values given in this column.

Table 3 [48]

COMPUTER-CALCULATED PRESSURE OF METALLIC HYDROGEN

Vol (cm^3/mole) (1)	Pressure (Mbar)						
	APW (2)	LCAO (3)	PERT[a] (4)	WS (5)	ΔP (6)	P_{ZP} (7)	P_{corr} (8)
1.855	+0.067	-0.068	-0.115 (.059)	+0.112	0.23	0.05	-0.12
1.0	1.85	1.63	1.58 (.094)	1.71	0.27	0.13	-0.22
0.9	2.52	2.27	2.22 (.10)	2.35	0.30	0.16	-0.24
0.8	3.49	3.21	3.16 (.11)	3.28	0.33	0.19	-0.27
0.7	4.93	4.61	4.56 (.12)	4.65	0.37	0.23	-0.31
0.6	7.20	6.81	6.76 (.14)	6.89	0.44	0.29	-0.36
0.5	11.02	10.54	10.49 (.16)	10.56	0.53	0.38	-0.43

[a]The terms in parentheses are the third order contributions to PERT energy values given in this column.

Table 4 [48]

COMPUTER-CALCULATED GIBBS FREE ENERGY OF METALLIC HYDROGEN

Vol (cm^3/mole) (1)	Gibbs free energy						
	APW (2)	LCAO (3)	PERT[a] (4)	WS (5)	ΔG (6)	G_{ZP} (7)	G_{corr} (8)
1.855	0.958	-0.942	-0.959 -(0.021)	-0.953	0.017	0.022	-0.120
1.0	0.785	-0.777	-0.795 -(0.017)	-0.803	0.026	0.030	-0.131
0.9	0.737	-0.730	-0.748 -(0.017)	-0.757	0.027	0.032	-0.132
0.8	0.675	-0.670	-0.689 -(0.016)	-0.698	0.028	0.034	-0.134
0.7	0.593	-0.595	-0.609 -(0.015)	-0.619	0.026	0.036	-0.137
0.6	0.481	-0.482	-0.499 -(0.0146)	-0.508	0.027	0.039	-0.139
0.5	0.322	-0.327	-0.356 -(0.014)	-0.356	0.034	0.043	-0.142

[a]The terms in parentheses are the third order contributions to PERT energy values given in this column.

The results of WS calculations, shown in column 5 of Tables 2, 3, and 4, are taken from the work of Neece et al. [39]. These authors used the Kohn-Sham $\alpha = 2/3$ exchange potential and also included correlation energy. For consistency, the correlation energy contribution to the energy, pressure, and Gibbs free energy calculated using Eq. (27) with a constant $\rho=1/V$ was subtracted from their results. Therefore, similarly to the data tabulated in columns 2 through 4 in Tables 2, 3, and 4, the numbers in column 5 also exclude contributions from zero-point motion and electron correlation.

The LCAO calculation is an exact minimal-basis Hartree-Fock procedure (a single STO), which treats the exchange energy exactly, rather than via the local electron approximation, as do APW, GRI, and WS methods. However, the results obtained, listed in the LCAO column in Tables 2, 3, and 4, show that the computed exchange is very close to that which could be obtained using a free-electron local exchange potential in which the adjustable parameter $\alpha = 2/3$. The calculations also show that high-pressure calculations made with the simpler wave function of Eq. (22) are equivalent to those made with Eq. (23), as in Ramaker et al. [35], which employ an additional sum over reciprocal lattice vectors.

The results of the third order PERT calculations of the energy, pressure, and Gibbs free energy (the upper numbers in column 4 in the tables) are in good agreement with similar calculations by Hammerberg and Ashcroft [43] and Brovman et al. [49,50], also made to third order. It should be noted that third order terms (numbers in parentheses in column 4), which have been omitted in most other PERT calculations of metallic hydrogen used to estimate the phase transition pressure into metallic state, are not negligible and should not be neglected. Hammerberg and Ashcroft [43] have also shown that the fourth order terms are negligible.

Tables 2, 3, and 4 show that, in the pressure range 0 to 10 Mbar, the maximum pressure differences for the same volume, computed by the APW, LCAO, PERT, and WS methods, are on the average 0.35 Mbar. This represents good agreement between the results of calculations using the four models. The average difference between the highest and the lowest values of the Gibbs free energy in the same pressure

range is 0.03 Ry. Hubbard and Smoluchowski [51] have compared the Wigner-Seitz, Thomas-Fermi-Dirac, and perturbation theory models at pressures near 20 Mbar ($r_s = 1.0$) and have concluded that the theoretical uncertainty in these models at these pressures is 10 percent. Thus, the APW, LCAO, PERT, and WS models appear to be more than adequate to calculate the energy, pressure, and Gibbs free energy of metallic hydrogen, less the zero-point energy and electron correlation contribution.

Column 8 in Tables 2, 3, and 4 shows that the free-energy contribution resulting from the inclusion of correlation energy is 0.13 Ry. Since this is four times larger than the differences between the results of the four different model calculations of Gibbs free energy, the accuracy of electron correlation calculations will have considerable effect on the calculations of the metallic transition of hydrogen. Local free-electron correlation potential energy expressions have been used in atomic calculations in the same spirit as local free-electron exchange. However, the correlation energy appears to be a much more sensitive function of the total wave function than is exchange. Therefore, the results obtained using the local free-electron approximation have not generally been as good as those estimated using the free-electron correlation energy. As an illustration, the correlation energies computed by Tong and Sham [52] using the free-electron approximation were twice as large as those estimated by Clementi [53] from experimental energies. Similar results have been obtained by Kim and Gordon [54], who have found the free-electron expression to overestimate the correlation by a factor of three in small molecules, such as He, Li, and LI+, and by a factor of two in molecules such as argon. Monkhorst and Oddershede [55] have used random phase approximation to calculate the correlation energy in metallic hydrogen using the Hartree-Fock-Block functions of Harris et al. [42]. They obtained correlation energy values approximately three-fourths as large as those calculated from the free-electron theory.

The calculations described in this section have shown that the correlation energy calculated using a local free-electron expression is approximately four times larger than the differences between the highest and the lowest values of energies at the same volume of

metallic hydrogen, determined by the four models. The theory of electron correlatio is a poorly understood quantum mechanical effect and, thus, the numerical results may be in error by a factor of two to three. Therefore, accurate determination of the correlation energy is the most important problem facing the *ab initio* calculations of the properties of metallic hydrogen.

D. STRUCTURE OF METALLIC HYDROGEN

All calculations described in the previous section were made for an fcc lattice. However, the actual structure of metallic hydrogen that could have an effect on the results of calculations is unknown. Therefore, this section will discuss the effect of the structure of metallic hydrogen on its calculated properties.

It is well known that calculations for bcc, fcc, and hcp lattice result in almost identical thermodynamic properties. However, recent calculations by Brovman et al. [49,50], using a third order PERT model have shown that the lowest energy structures for metallic hydrogen at zero pressure are not cubic, but a complicated anisotropic family of structures forming triangular two-dimensional proton lattices in an electron fluid. Along the c-axis, the atoms have a filamentary structure with no fixed periodicity in space. An interesting feature of this anisotropy is the almost complete absence of energy barriers between possible structures in the family. The next higher energy modification is made up of a quadratic family of similarly anisotropic structures. An energy barrier, or gap, exists between the triangular and quadratic families. Brovman et al. found that cubic structures that are characteristic of ordinary metals are absolutely unstable with respect to more anisotropic structures. The energy of the most stable anisotropic structure (triangular) is 0.018 Ry lower than that of fcc. This is less than the difference between the APW results and third order PERT calculations near zero pressure and, therefore, no significant changes are to be expected in the equations of state as a result of the anisotropy. Detailed calculations by Brovman et al. show that this tendency to anisotropy is unique to metallic hydrogen due to its electronic interactions being pure

Coulombic (metals such as sodium must be characterized by pseudopotentials and so do not have this tendency). It is shown that the larger the value of the Fourier component of the electron interaction for wave vectors on the order of the nearest reciprocal lattice vectors, the greater the tendency to this anisotropy. In hydrogen, the Coulombic interaction retains the same sign over all lattice vectors, while in the case of pseudopotentials, the signs change and the Fourier component passes through zero in the region of these vectors. Harrison [56] has also pointed out that multi-ion interactions are likely to be strongest when the ions form a straight line and are separated by nearest-neighbor distances. This work appears to confirm the tendency of metallic hydrogen to favor anisotropic structures. Brovman et al. [49,50] have also calculated the stabilities of the various structures under compression and conclude that the triangular lattice will be stable below 0.25 Mbar. The system then transforms into the quadratic structure and eventually, at extreme compressions, will stabilize in a cubic lattice.

These results of Brovman et al. appear to be corroborated at least qualitatively by the work of Beck and Straus [, and of Caron [58] who studied the dynamic structural instability of these lattices. These instabilities are manifested in the appearance of negative frequencies for some vectors in the Brillouin zone. These authors used the free-electron perturbation theory (Caron to second order and Beck and Straus to third) to compute the phonon spectra in the harmonic approximation. Beck and Straus determined the phonon frequencies from the dynamic matrix, while Caron used the self-consistent harmonic approximation (SCHA). According to calculations by Beck and Straus, the bcc lattice becomes unstable at $r_s > 0.6$ bohr and the fcc at $r_s > 1.0$ bohr, where r_s is the radius of the atomic sphere. Caron's calculations predict the fcc phase will become unstable at $r_s > 1.5$ bohr ($P < 0.7$ Mbar). The enhanced stability resulting from Caron's calculations is a direct consequence of the free energy minimization principle incorporated in the SCHA method used in determining the correct wave function. The SCHA technique has been successfully applied to the quantum solid helium isotopes for which application of the harmonic

approximation to the force constants is known to be inadequate. In helium, solution of the dynamic matrix (used by Beck and Straus) at low pressure leads to imaginary frequencies and an incorrect prediction of the solid instability. In the SCHA method, the use of a variational parameter to minimize the free energy and to compute the frequency leads to greater flexibility of the Gaussian wave function and to increased stability actually observed in the experiments.

Although the proper positioning of the instability may depend on the phonon model, Beck and Straus argue that the basic cause for the instability is the Kohn anomaly in the dielectric constant around $2\ k_f$, where k_f is the Fermi wave vector. Consequently, "the instability is not just a question of nearest neighbors, but involves the lattice structure as a whole." Clearly, both static and dynamic calculations based on free electron perturbation predict that cubic hydrogen lattices at low pressure are unstable to small displacements and presumably revert to a less symmetric arrangement.

The existence of highly anisotropic, stable structures and the instability of the cubic lattices was found using the free-electron perturbation theory. Since Caron points out that the phonon spectrum and, thus, the instability are considerably affected by the electron screening, it would be very interesting if similar calculations could be made using the LCAO method to determine whether the cubic lattice instability is a real effect or an artifact of the PERT method. The WS and APW methods as they are currently formulated are not suited for computations of highly anisotropic structures.

As noted, the difference between the energy of the most stable anisotropic structure and the least stable cubic structure computed by Brovman et al. [49,50] was 0.018 Ry. This is less than the difference between the highest and the lowest energy values at the same volume computed by the four different models. Therefore, the thermodynamic properties of metallic hydrogen will not change significantly as a result of structural changes. Consequently, it still appears that the most important theoretical problem in the path of an accurate quantitative calculation of the metallic phase of hydrogen is the correlation energy in real metals.

III. TRANSITION OF MOLECULAR HYDROGEN INTO A METALLIC PHASE

A. GENERAL

It has been almost universally accepted that molecular hydrogen will undergo a transition into a metallic phase at some elevated pressure and that this transition will occur directly from the insulating molecular phase to a conducting, or possibly, superconducting metallic phase. Calculations have indicated that such a transition should be first order and should occur at pressures above a megabar. Yet the possibility persists that the transition may in fact be similar to the gradual metallic transition observed in diatomic iodine in which, as the pressure is increased, the valence electrons gradually occupy states in the unfilled conduction band, leading to a higher order transition taking place at a lower than predicted pressure. Some preliminary theoretical calculations indicates that this may indeed be the case.

B. TRANSITION OF THE INSULATING MOLECULAR PHASE INTO A CONDUCTING MOLECULAR PHASE

Calculations of the energy and electronic structure of molecular hydrogen have been made by Ramaker et al. [35]. They used a Hartree-Fock method originally developed for calculations of the equation of state of metals and previously applied to cubic metallic hydrogen and lithium. This method as it applies to metallic hydrogen was used and is discussed in more detail in Section II, subsection B. In applying this technique to molecular hydrogen, each Block function $|\bar{k}\rangle$ is written as a sum over the atomic orbitals:

$$|k\rangle = \sum_{\bar{K}} C(\bar{k},\bar{K}) \exp[i(\bar{k}+\bar{K})\cdot\bar{r}]\, \phi(\bar{\mu}-\bar{R}_{\mu}+\bar{S}_{n}), \qquad (30)$$

where $\bar{k}$ is restricted to the first Brillouin zone, $\bar{K}$ is a reciprocal-lattice vector, ϕ is a Slater-type orbital, $\bar{R}_{\mu}$ is the origin of the cell μ where the sum over μ runs over all lattice cells, and $\bar{S}_{n}$ is the position of atom n relative to the cell origin. The coefficients

$C(\bar{k},\bar{K})$ are determined as functions of k, by the variational principle. Ramaker et al. use only a single ls-type Slater orbital. The molecular hydrogen crystal was constructed by placing one atomic nucleus at the origin of each cell. The other nucleus was moved to the position that yielded the minimum Hartree-Fock energy, thus optimizing the H-H intermolecular spacing at each density.

A very interesting prediction by Ramaker et al. [35] is that, at a volume of 5 cm^3/mole ($P \simeq 0.3$ Mbar), the electrons in the fully occupied first Brillouin zone will begin to occupy states in the second zone, and the molecular crystal will become a molecular metallic crystal. If this result is correct, then any attempt to locate the atomic-like metallic phase by measuring electrical conductivity alone is likely to be ambiguous. These results have been independently confirmed, at least qualitatively, by Friedli [36], who has determined that the valence-to-conduction band electron energy gap vanished at a density about 9.15 times the normal density, or at an approximate volume of 2.47 cm^3/mole and a pressure of about 1.8 Mbar. These recent results (1975) of Ramaker and of Friedli would represent upper bounds to the stability of the molecular insulating phase.

The work of Friedli was carried out using a combined plane wave localized orbital representation for the wave function. Unfortunately, this specific method has little prior history and is difficult to evaluate in terms of other better known methods. More serious are the approximate construction of the one electron potential using a dielectric formalism and the lack of self-consistency, which can cause large errors in the interband energy differences (band gap) even though accurate intraband relative energies may be obtained.

Despite these drawbacks (caused mainly by computational limitations), we would expect the results to be at least qualitatively correct. Friedli's results are summarized in Fig. 10 in Section I, subsection D-3, where they were used to suggest that the observed softening of the intermolecular potential obtained from the shock data might indeed be related to the closing of the band gap.

In contrast to these results, no suggestion of the onset of band overlap in molecular hydrogen appears to be present in the theoretical 0 K isotherm of Liberman [34], who used a KKR electron band method to calculate the solid molecular properties of hydrogen. His calculated isotherm was in very good agreement with the results from the shock wave experiments. Assuming that this transition is embedded in Liberman's work, the lack of any discernible discontinuity in the pressure may indicate that such a transition is higher than first order, as is observed in iodine.

For the sake of completeness, it may be useful to summarize some of the important features of the only experimentally observed metallic transition in a diatomic molecule, the metallic transition in iodine. This transition occurs gradually at pressures between 40 and 150 kbar [59] and has been identified as a continuous decrease in electrical resistivity of many orders of magnitude, from that typical of an insulator at 40 kbar to that of a metal at the highest pressure (metallic electrical conductivity). At atmospheric pressure, iodine is diatomic and its equation of state is well characterized by pair potentials and molecular lattice models, which, however, become increasingly inadequate under pressure. At low pressure ($P < 40$ kbar), the agreement between the experimental iodine Hugoniots and the results of calculations based on APW band theory used to compute the properties of monatomic metallic iodine [60] is poor. However, the agreement improves with increasing pressure and becomes good at $P > 150$ kbar. These results are consistent with the observed electrical resistivity measurements. No useful experimental determinations of the crystal structure of iodine are available at pressures above the onset of the transition. Therefore, only inferences may be made as to structural changes taking place in this material. The transition is not first order (the actual order is unknown) and it is reversible. The metallic phase is apparently not metastable, although no attempts have been made to determine whether unique conditions exist under which the metal may be prepared.

C. TRANSITION OF MOLECULAR HYDROGEN INTO A MONATOMIC METALLIC PHASE

If one neglects the possibility that molecular hydrogen may become unstable as a result of the conduction band overlap, then it is likely that the transition into a monatomic metallic phase

will occur at a pressure of at least 1 Mbar. Since such high pressures cannot presently be achieved in static presses having a sufficient working volume, one is forced to resort to theoretical calculations to determine the transition pressure and metastability.

The transition pressure at zero degree temperature is obtained either from the common tangent to the energy-volume curves for the molecular and metallic hydrogen phases or from the intersection of the Gibbs free energy vs pressure curves for the two solid phases. Because even a small difference in the equation of state of either phase results in a large change in the transition pressure, the methods require the knowledge of extremely accurate equations of state or other thermodynamic parameters of both the molecular and metallic hydrogen.

Extensive literature exists on the calculation of the transition pressure of metallic hydrogen. However, most authors use some variant of the models of molecular hydrogen discussed in this report. The usual approach is either to extrapolate some effective pair potential that is in agreement with low-density gas or solid data to yield a multimegabar equation of state for the molecular phase, or to use a pair potential obtained from first principles calculation. The equation of state of the metal phase is most commonly calculated by means of the approximate, free-electron gas perturbation (PERT) theory and, with a few exceptions, the calculations are made only to second order. The main objective in this report is not to perform another calculation of the transition pressure into metallic phase, but to systematically analyze the uncertainties that are introduced into the prediction of the metallic transition pressure as a result of uncertainties that are known to exist in the models of each of the two phases. From the previous discussion, it is to be expected that the largest uncertainties in such calculations should result from an incomplete understanding of the nonadditive forces in the molecular phase and correlation energy contribution to the metallic phase.

The Gibbs free energy vs pressure of molecular hydrogen used in determining the metallic transition pressure (P_T) was calculated in the harmonic approximation and includes the zero-point motion contribution. The static lattice energy term was calculated with the CI

pair potential, which obviously exclude many-body interactions, and with the effective CI + ATT potential that best fits the experimental data and is also in agreement with the theoretical estimates of nonadditive forces (many-body interaction contributions). The Gibbs free energy vs pressure of metallic hydrogen was calculated using the four methods discussed in Section II, subsection B, and includes zero-point-motion contribution calculated using Eq. (26). Two sets of phase-transition calculations were performed for each of the three models of metallic hydrogen. The results of the first set of calculations, which include the free-electron correlation contribution to the Gibbs free energy of metallic hydrogen computed from Eq. (27), are given in Table 5. The results of the second set of calculations, which do not include the free-electron correlation contribution, are given in Table 6. Results of the calculations, employing fractions of the free-electron correlation energy, scale linearly between these limits. The metallic transition pressures were determined by the intersection of the Gibbs free energy vs pressure curves for metallic and molecular phases.

Table 5

METALLIC HYDROGEN TRANSITION PRESSURES IN MBARS, WITH THE FREE-ELECTRON CORRELATION CONTRIBUTION TO THE GIBBS FREE ENERGY OF THE METALLIC HYDROGEN TAKEN INTO ACCOUNT

Comp Method	Transition Pressure - Mbars	
	CI	CI + ATT
WS	0.9	2.7
APW	0.9	3.1
PERT	1.1	3.7

It can be seen from Table 5 that the transition pressures calculated using the CI pair potential to compute the Gibbs free energy vs pressure variation of molecular hydrogen (P_T = 0.9 to 1.1 Mbar) depend very little on the model of metallic hydrogen used (WS, APW, PERT), all of which include the same correlation energy. However, transition pressures calculated using the CI + ATT potential to compute the Gibbs

Table 6

METALLIC HYDROGEN TRANSITION PRESSURES IN MBARS WITHOUT TAKING INTO ACCOUNT THE FREE-ELECTRON CORRELATION CONTRIBUTION TO THE GIBBS FREE ENERGY OF METALLIC HYDROGEN

Comp Method	Transition Pressure - Mbars	
	CI	CI + ATT
WS	3.3	~11
APW	3.7	~11
PERT	3.8	~11
LCAO	4.3	~11

free energy vs pressure variation are between 3.7 and 3.7 Mbar and are thus significantly higher (by ~2 Mbar) than the two previous cases. Physically, this means that the molecular hydrogen will be stable to higher pressures and densities, provided the potential energy of the molecular crystal is not a simple sum of pairwise-additive potentials, but includes many-body interactions that further lower the energy.

Referring to Table 6, it can be seen that exclusion of the correlation energy raises the free energy of the metallic hydrogen, allowing molecular hydrogen to be stable to higher pressures. Using the CI potential to compute the Gibbs free energy vs pressure variation for molecular hydrogen, the transition pressures calculated without the correlation energy for all-metal models average out to about 3.8 Mbar, an upward shift on the order of 3 Mbar when compared with the transition pressure calculated by including the correlation energy. Repeating the calculations in which the electron correlation is omitted, and using the CI + ATT potential to compute the Gibbs free energy vs pressure variation for the molecular phase, the predicted transition pressure goes up to approximately 11 Mbar, an increase of approximately 8 Mbar over the transition pressure calculated in the same manner, but with the correlation energy included in the computations. Thus, exclusion of the electron correlation and the use of either the purely theoretical potential (CI) or the empirical potential (CI + ATT) result in an upward shift in the metallic transition pressure of from

3 to 8 Mbar, respectively. Assuming that the free-electron correlation expression should be one-third the magnitude of the free-electron expression, as suggested by the results for small molecules, and the correlation energy is thus decreased by three, the metallic transition pressures then calculated using the CI and CI + ATT potentials to compute the molecular phase properties will be 3 Mbar and 10 Mbar, respectively. This is roughly a tripling of the pressure predicted by the commonly used free-electron expression.

A description of what is actually occurring may be seen from Fig. 11, which shows the variation of the Gibbs free energy vs pressure for the molecular and metallic hydrogen phases. The metallic transition pressure is determined from the intersection of the molecular and metallic solid curves. For simplicity, only a single molecular Gibbs free energy vs pressure curve calculated using the CI + ATT potential is plotted in this figure (curve 2). For the same reason, only the Gibbs free energy vs pressure variation for metallic hydrogen calculated in the third order PERT approximation is plotted in Fig. 11. It can be seen from this figure that the two curves for metallic hydrogen (curve 1, with electron correlation, and curve 3, without correlation) are parallel, that they are intersected by the molecular Gibbs free energy vs pressure curve at a small angle, and that the point of intersection of the two curves is extremely sensitive to small changes in Gibbs free energy (i.e., a small change in Gibbs free energy causes a large change in the transition pressure). It was pointed out earlier that most previous free-electron perturbation calculations included second order terms only. However, it can be shown that the omission of the third order energy terms results in an upward transition pressure shift of about 0.3 Mbar and is much smaller than the possible error in the uncertainty in the determination of the correlation energy. Since most previous calculations were made using one of the four metallic equations of state (WS, APW, PERT, LCAO) with full correlation energy and either a purely theoretical or empirical equation of state of molecular hydrogen, it is clear why most predictions range between 1.0 and 4 Mbar. However, serious inaccuracies in the correlation energy could change this estimate of the metallic hydrogen transition pressure considerably.

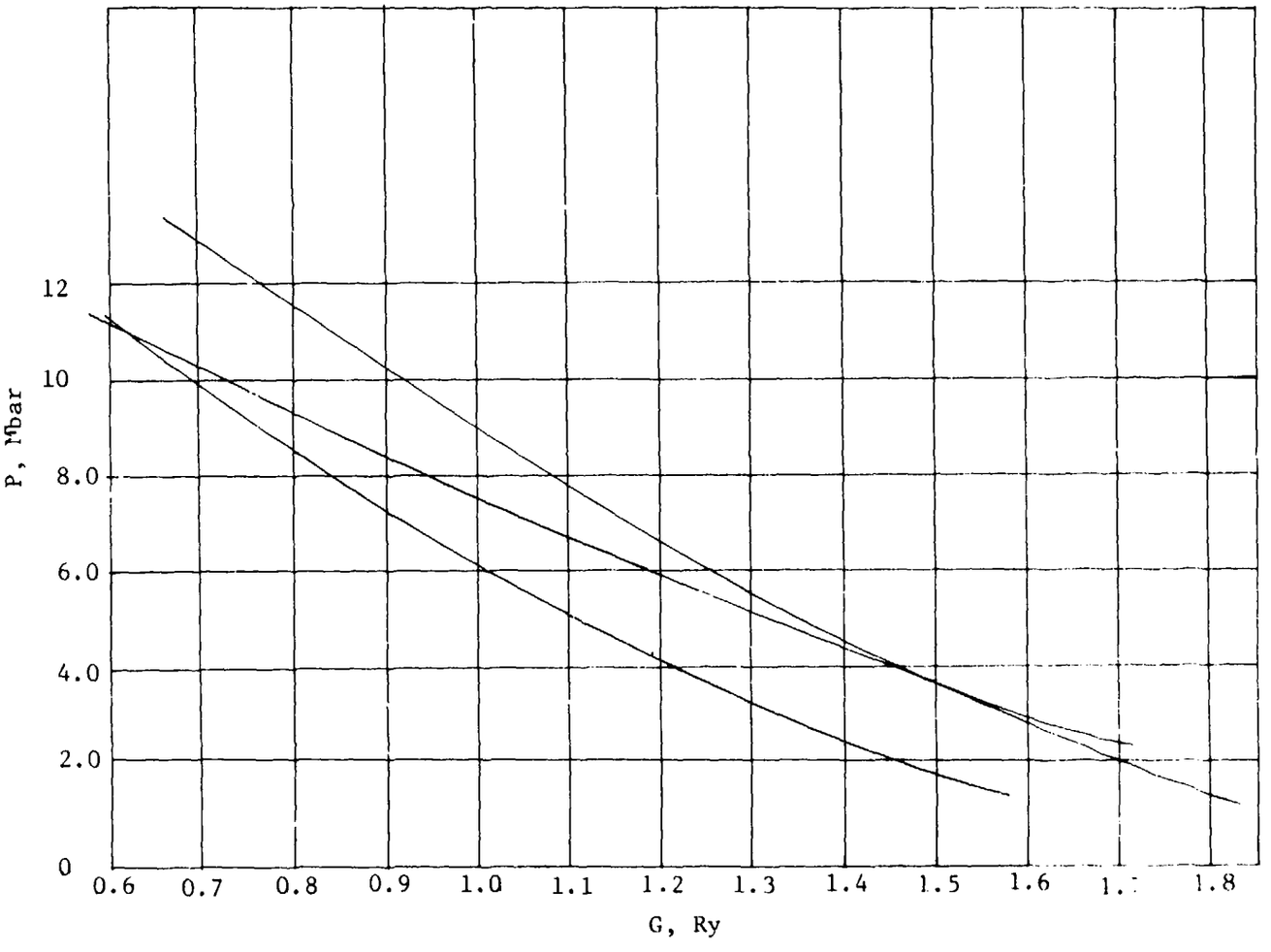

Fig. 11--A plot of pressure vs Gibbs free energy for molecular hydrogen (curve 2) calculated using the CI + ATT pair potential and for metallic hydrogen calculated in the third order PERT approximation with correlation taken into account (curve 1) without cor elation (curve 3).

Calculations made by Etters et al. [9,10], using their molecular hydrogen equation of state and a number of equations of state of metallic hydrogen taken from the literature, show that the transition into the metallic phase should occur at pressures between 1.4 and 3.3 Mbar. Since the stiffness of the EERD potential used in the calculations is intermediate between that of the CI and CI + ATT potential, these results are consistent with those given here.

The phase transition calculations were made on the assumption that the hydrogen molecule is spherical. Since this is not the case, Ross [6] has estimated the effect of nonsphericity on the transition pressure by approximating the molecule as a dumbbell in which the potential between two molecules is the sum of the potentials between the atoms on opposite molecules. An effective atom potential was determined from the sphericalized potential. He established that treating the atoms as diatomic results in a decrease in their Gibbs free energy and a rise in the metallic transition pressure by about 20 percent. Thus, assuming the validity of approximations used (including α structure for dense molecular hydrogen), the transition pressures given in Tables 9 and 10 should be less than 20 percent higher than the values given. These results are consistent with work of Raich and Etters [8], who have made similar calculations during the course of their work on the rotational transition in solid hydrogen at high pressure.

IV. STABILITY OF METALLIC HYDROGEN

A. GENERAL

To be technologically useful, metallic hydrogen has to be metastable at sufficiently low pressures and relatively "high" temperatures. Metallic hydrogen will be metastable if the decay rates from the less stable metal phase to the more stable molecular phase are small and, therefore, the lifetime of the metal is long. Traditionally, such calculations have been extremely difficult to perform and, as a result, the existence of metastable metallic hydrogen will probably remain unpredictable.

As is well known, metallic hydrogen has a very high Debye temperature (2000 to 3000 K) and could be a quantum liquid. Therefore, before discussing the possible existence of a metallic hydrogen phase that is metastable with respect to the molecular phase, one should consider whether the crystalline form at 0 K is even likely to be stable with respect to the liquid form. If the latter is the stable form at 0 K at the transition pressure, then it is unlikely to avoid rapid decay into the molecular form on decompression.

B. MELTING OF THE CRYSTALLINE METAL PHASE

It was pointed out by Yestrin [61] that, according to thermodynamics, the metling temperature of the metastable phase of any substance is always lower than that of its stable form. When both a stable and a metastable liquid phase exist, the melting temperature of the solid at which stable liquid is formed is always lower than that at which the metastable liquid is formed. In the general case of two solid and two liquid phases (stable and metastable), the lowest melting temperature is that for the metastable solid into a stable liquid. This implies that the lowest melting temperature at atmospheric pressure is the melting temperature of the metallic hydrogen accompanied by formation of a stable (molecular) liquid and that this temperature is lower than the melting temperature of molecular hydrogen forming molecular hydrogen liquid. However, it is not clear whether these arguments remain valid for quantum solids and quantum liquids, such as the solid and liquid molecular hydrogen.

Several attempts were made to calculate the melting curve of metallic hydrogen. Trubitsyn [62] used the Lindemann law, written in the following form:

$$T_m = C\Theta_d v_m^{2/3}, \qquad (31)$$

where T_m is the melting temperature, C is a constant, θ_d is the Debye temperature, and v_m is the atomic volume on melting. Trubitsyn assumes that the constant C, which applies to Li, Na, and K, can also be used for hydrogen. According to his estimate, $T_m \simeq 4000$ K for solid metallic hydrogen at atmospheric pressure. However, the use of this model implies that hydrogen is a classical solid. This may not be true since Hubbard and Smoluchowski [51] point out that, at sufficiently large θ_d, zero-point vibrations of the lattice will cause it to disintegrate even at zero pressure, so that the substance will be a quantum fluid such as helium. According to their argument, the work by deWette [63] and Carr [64] indicates that Lindemann law can be written as:

$$T_m \sim K\rho^{1/3}, \qquad (32)$$

where K is a constant and ρ is the density. This equation can be justified in that the lattice will presumably disintegrate when the root mean square of amplitude of proton vibrations exceeds a given fraction of the lattice spacing. Assuming that the protons are immersed in a uniform density electron fluid and the metal behaves as an ideal Coulomb lattice, the Debye temperature can be expressed as:

$$\Theta_d \sim 3400\ \rho^{1/2}K'. \qquad (33)$$

An inspection of the functional form of ρ in Eqs. (32) and (33) shows that θ_d increases more rapidly with density than T_m so that,

at some compression, the solid metal will eventually disintegrate into a liquid. However, unless the proportionality constants are known, it is impossible to determine the density at which this will occur.

An attempt at a quantitative theory may be made based on the work of Hansen [65], who has made extensive Monte Carlo calculations for a system of positive ions in a uniform background neutralizing the electron fluid. He calculated all of the thermodynamic properties, including the melting curve over a wide range of variables. All of these properties were expressed in terms of the reduced variable Γ, where

$$\Gamma = \frac{2}{r_s kT} , \tag{34}$$

r_s is radius of the electron sphere, T is the temperature, and kT is expressed in Rydbergs. Hansen showed that a bcc crystal of positive ions melts when $\Gamma = 155$. At larger Γ (smaller r_s or T), the crystal is stable. These calculations are purely classical, while we are interested in the analogous quantum melting problem at 0 K. The change from the classical to quantum system will be made on the assumption that the quantum system melts at 0 K, when its harmonic oscillator energy (zero point energy) is the same as that of the classical harmonic oscillator when it melts. The transformation from classical to quantum variables is made by equating the classical and 0 K quantum harmonic oscillator energies,

$$3kT = (9/8)\theta_D . \tag{35}$$

The reduced variable Γ, Eq. (34), written in terms of quantum variables, then becomes:

$$\Gamma = \frac{4}{3r_s\theta_D} . \tag{36}$$

Because $\Gamma = 155$ at the melting point, the variation of melting density with Debye temperature becomes:

$$155 = \frac{4}{3r_s^m\theta_D^m} . \qquad (37)$$

In Eq. (37), the superscripts denote the values of the variables at melting. Thus, the Lindemann law is generalized to 0 K by assuming that the same amount of harmonic oscillation energy is required to melt a crystal at any temperature.

Using Eq. (36) to compute θ_D as a function of r_s, it can be shown that when $r_s = 1.07$ bohr--i.e., at a density $\rho = 2.5$ g/cm^3 (0.4 cm^3/mole)--and at a pressure of 12.7 Mbar, $\Gamma = 155$. At larger volumes, the decrease in θ_D is more rapid than the increase in r_s. This indicates that above $\Gamma = 155$ the metal is a solid. Thus, according to these calculations, metallic hydrogen would be a solid at pressures below 12.7 Mbar and a liquid at pressures above 12.7 Mbar. However, these calculations assume a uniform background of electrons and do not include the electron screening--i.e. the piling up of electrons near the protons.

C. METASTABILITY OF THE METALLIC PHASE

The work of Brovman et al. [49,50], discussed in Section II, subsection D, indicates that the most stable hydrogen structure is highly anisotropic and similar to graphite. It has been suggested that, as a result, metallic hydrogen may be metastable in respect to molecular hydrogen in much the same manner as graphite is metastable in respect to diamond. This analogy drawn between carbon and hydrogen must be considered wishful thinking of physicists that could never be shared by organic chemists who are fully aware of the uniqueness of the carbon atom through its ability to hybridize its four outer shell electrons into a wide assortment of shapes and valences. The many complicated aromatic and aliphatic structures found in nature and synthesized are proof of the structural versatility of the carbon atom and its ability to form complicated bonding arrangements. On the other hand, the hydrogen atom generally appears in molecules

as an appendage forming a single simple bond. Thus, there appears to be no basis for drawing any such parallel between carbon and hydrogen.

Salpeter [66] has estimated the lifetime of metastable metallic hydrogen for the case when pairs of atoms evaporate and reform as molecules. Using known theoretical estimates of the cohesive energy and the Debye temperature of the metal, he obtains a binding energy curve for atoms in the metal in the outward direction from the crystal. The atoms are bound in a potential well near the surface with a barrier preventing their evaporation. The binding energy curve of two atoms in the molecule is well known, allowing Salpeter to construct a potential energy diagram connecting the two regions and to estimate the barrier height. Using WKB theory to evaluate the tunneling probability of an atom pair leaking away, it was estimated that the lifetime of metallic hydrogen at zero pressure is 100 sec. This estimate is claimed to be conservative, overestimating the lifetime. Salpeter points out that because at the same densities, the increase in energy of molecular hydrogen with pressure is more rigid than that for metallic hydrogen, the lifetime of the latter will increase with pressure.

One of the aspects ignored in these calculations is the thermal runaway, when the exothermic energy of formation of metallic hydrogen heats up the crystal, increasing the rate of evaporation and leading to a cascading disintegration.

An additional feature of crystalline metallic hydrogen likely to lead to an enhanced decay rate in the molecular form is the large zero-point motion that is equivalent to thermal temperatures of the order of 2000 to 3000 K. These large motions could allow neighboring protons to approach each other sufficiently close to permit the formation of dimers. Chapline [67] has calculated probable root mean square displacements of protons in a one-atmosphere crystal and, by examining the resultant energy change, had estimated that a given sample of metallic hydrogen would convert to the molecular form in about 10^{-3} sec.

One may summarize the calculations and arguments on the metastability question by noting they all have been heuristic and, while suggestive, lack the essential rigor to be convincing. This question is unlikely to be answered outside of the laboratory.

V. EXPERIMENTAL RESEARCH

A. GENERAL

Three experimental methods have been used to determine the high-density equations of state points of molecular hydrogen. These are the static isothermal (static high-pressure) experiments and shock compression and isentropic compression techniques. Isentropic compression and, possibly, static high-pressure experiments can be used to achieve compressions needed to convert molecular hydrogen into its metallic form. Laser and electron beam compression techniques have also been proposed for observing metallic hydrogen.

Assuming that Mbar static pressures can be achieved, static high-pressure experiments comprise the only technique potentially capable of manufacturing metallic hydrogen--i.e. producing it without destroying the sample, as is the case in shock, isentropic, and other types of experiments in which hydrogen can be compressed to metallic densities. While unproven and possibly unfeasible, condensation of spin-aligned hydrogen followed by static compression is the only other method proposed to date that can, in principle, be used to manufacture metallic hydrogen.

A comparison of the results that can be obtained from the static high-pressure and isentropic and shock compression methods is illustrated in Figs. 12 and 13, which show the variation of pressure and temperature of molecular hydrogen with molar volume. In these figures, the solid curves were computed using a molecular hydrogen equation of state determined from the CI + ATT potential, which is in agreement with the currently available experimental data. The temperatures in Fig. 13 were calculated theoretically. These figures demonstrate that each method is unique in its ability to study the thermodynamic properties of hydrogen over different ranges of temperature and density. As a result, each experimental method makes a unique contribution to the development and testing of theoretical models.

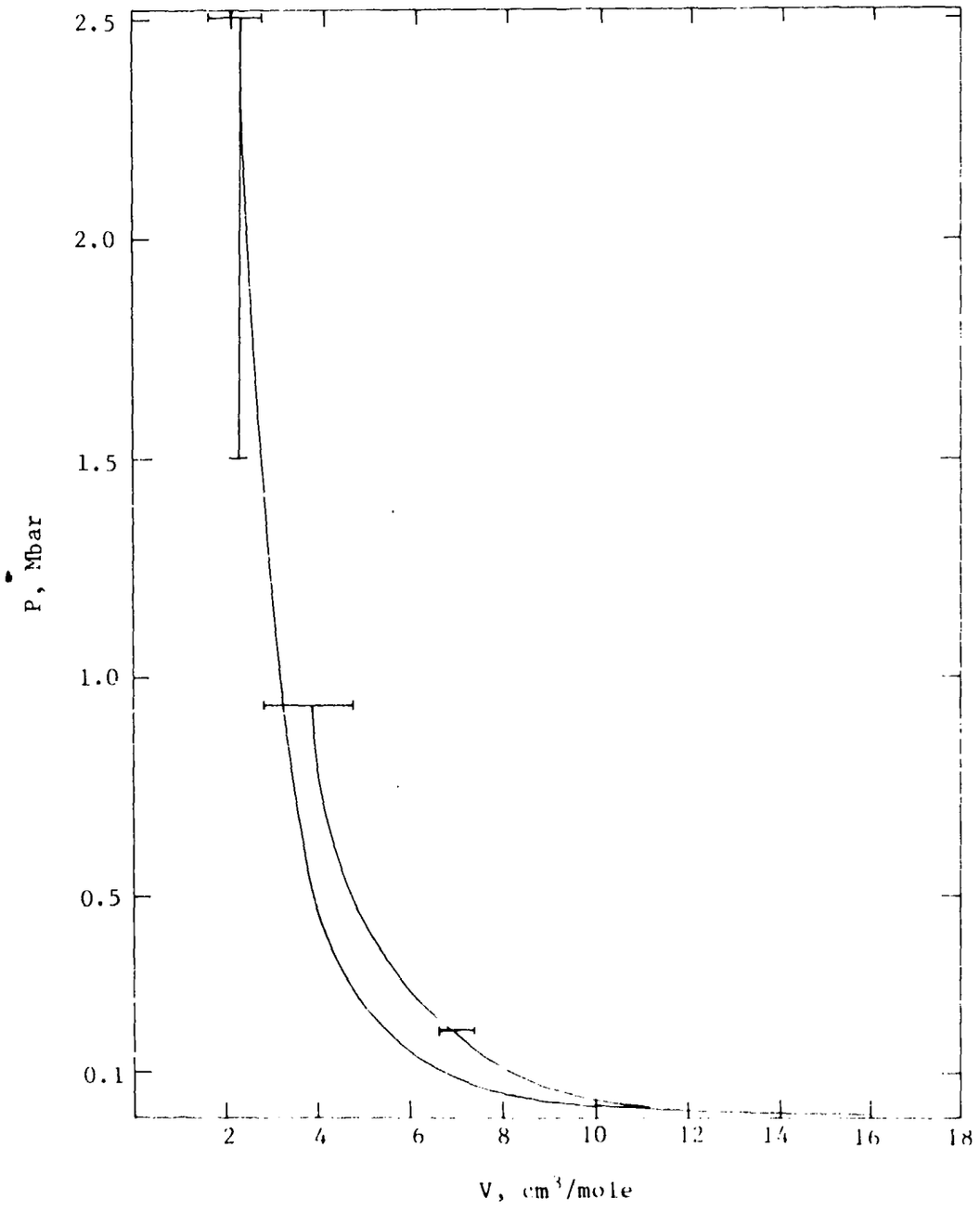

Fig. 12--A plot of pressure vs molar volume for molecular hydrogen, calculated using a hydrogen equation of state determined from the CI + ATT potential (Eq. (14)), which is in agreement with the available data.
1 - primary Hugoniot, 2 - reflected Hugoniot, 3 - isentrope.
The horizontal bars are estimates of the experimental errors in determining the pressure.

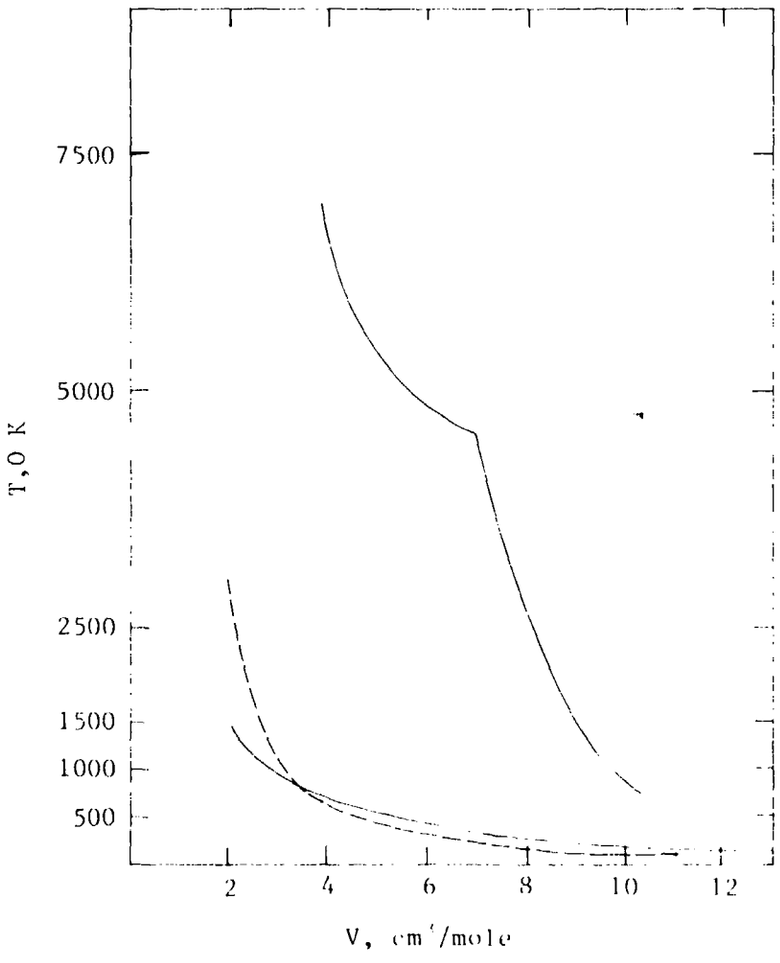

Fig. 13--A plot of temperature vs molar volume for molecular hydrogen, calculated using a hydrogen equation of state determined from the CI + ATT potential (Eq. (14)), which is in agreement with the available data. 1 - primary Hugoniot, 2 - reflected Hugoniot, 3 - isentrope, 4 - freezing curve.

B. ISOTHERMAL COMPRESSION

1. Experimental Molecular Hydrogen Equation of State Data

The best-known method of determining the equations of state of materials is static isothermal compression using high-pressure apparatus. Unfortunately, the only static isothermal data on solid hydrogen and deuterium are the low-pressure (up to 25 kbar), low-density (from 22.6 to 9.5 cm^3/mole) equation of state points measured by Stewart in 1956 [1] and Anderson and Swenson in 1974 [2].

Stewart [1] used a piston and a cylinder device to obtain eleven pressure vs volume equation of state points of molecular hydrogen at 4.2 K and at pressures up to 20 kbar. Until recently, his results were the only isothermal data available on molecular hydrogen and have been used extensively for testing its interaction potential and its cohesive energy. Anderson and Swenson [2] published the results of similar experiments on molecular hydrogen at 4.2 K, performed in an attempt to extend their range and accuracy. Their pressure vs volume points at pressures up to 25 kbar are in excellent agreement with Stewart's data. Table 7 summarizes the experimental data of Stewart, which are also plotted in Fig. 14 with the pressure vs volume curve of Anderson and Swenson.

Table 7 [1]

EXPERIMENTAL PRESSURE VS RELATIVE VOLUME DATA OF STEWART FOR MOLECULAR HYDROGEN

P (bar)	V/V_o	P (bar)	V/V_o
0	1000	3923	0.632
196.1	0.928	5884	0.583
392.2	0.883	7845	0.549
588.4	0.847	9806	0.523
980.7	0.794	11768	0.500
2003	0.711	15691	0.467
2942	0.667	19613	0.445

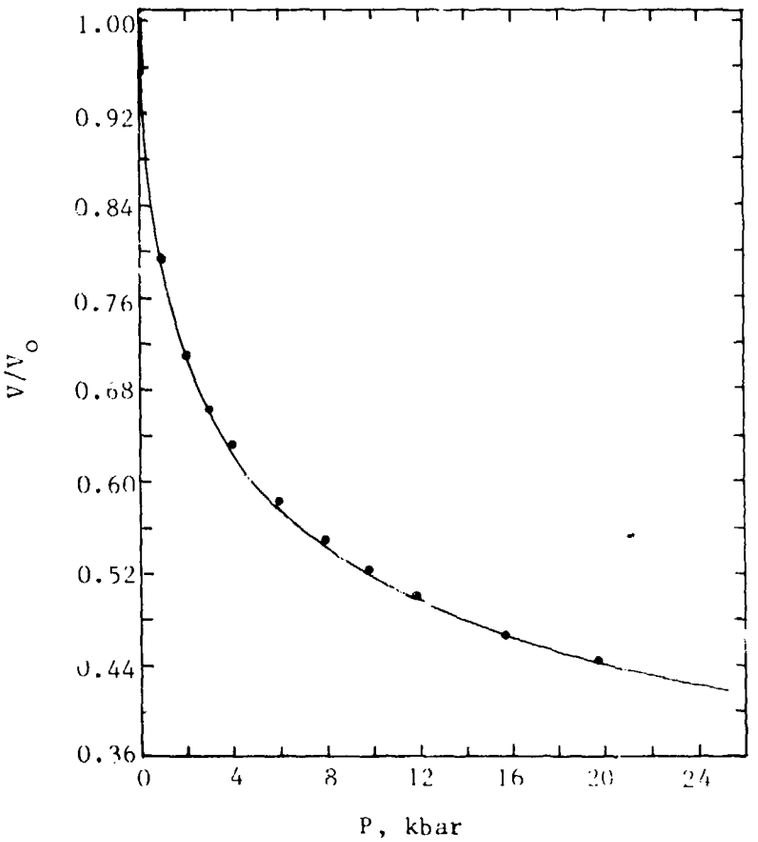

Fig. 14--A plot of relative volume vs pressure for molecular hydrogen acquired by Stewart (points) and Anderson and Swenson (solid curve) [2].

Comparison of Stewart's and Anderson and Swenson's data with the results of theoretical calculations should, in principle, provide a check on the quantum mechanical calculations for the intermolecular potential of hydrogen appropriate to these pressures and densities. However, accurate theoretical potential calculations at these intermolecular separations have not been made because such calculations require prohibitively large basis sets to compute the small quantum mechanical interaction energy. As a result of the importance of attractive forces at these separations, empirical intermolecular potentials fitted to low-pressure and low-density data would be likely to predict accurately the properties of molecular hydrogen at high density, where the behavior of the pair potential is governed by the steeply repulsive short-range forces. The latter is best studied by the use of high-pressure shock-wave data so that the two techniques, static and shock, are highly complementary.

Since hydrogen is a quantum solid with a large zero-point energy, the large compressions achieved in static isothermal experiments are actually deceptive. The molar volume of molecular hydrogen at 20 kbar is about 10 cm^3/mole--i.e. a compression of nearly 2.2. However, of the 20 kbar, only 13.5 kbar is static lattice pressure, the remaining 6.5 kbar being due to pressure from zero-point motion.

2. Experimental High-Pressure Research

A breakthrough in generation of Mbar static pressures was claimed to have been achieved by Kawai in 1970 [68,69] using a two-stage split (segmented) sphere, a modification of von Platen's apparatus developed in the 1950s. The simplest version of this device is the single-stage split sphere consisting of segments of a sphere with truncated inner faces, assembled together with small spaces between them. When the segments are pushed together, the truncated faces forming the anvils compress the sample. In the earlier version, the sphere is surrounded with a deformable membrane, whi n the later model, it fits into hemispherical cavities in a steel cylinder split into two equal parts. The whole assembly is immersed in a fluid

compressed by a hydraulic press. Assuming that the sample and the anvils are not deformed, the pressure P in the sample can be estimated from the approximate formula $P = P_{ext}\ (A_{ext}/A)$, where P_{ext} is the external hydrostatic pressure exerted on the outside of the sphere by the fluid, A_{ext} is the external area, and A is the internal area of the sphere. Since a sphere with $A_{ext}/A = 15{,}000$ can be readily constructed, in theory, pressure multiplication of ~15,000 can be achieved. In practice, this formula cannot be used due to the decrease in the applied forces resulting from the stiffness of the membrane, friction between the stages, compression of the stages, the opposing forces produced in the gasket material, etc. However, it can be modified by introducing the efficiency factor, a numerical parameter always less than one, which takes into account the drop in the applied forces due to various factors.

Since the mid-1960s Kawai has designed and used both a single-stage split sphere [70,71,72] and several versions of the two-stage split-sphere apparatus [69,72-75]. According to Spain [76], Kawai is also developing a three-stage split sphere. It is claimed that the use of several stages improves the efficiency of the device.

The simplest version of the press, called the single 8-anvil split sphere [70-72] is actually a two-stage sphere with each stage divided into eight equal sections by three perpendicular planes through the center of the sphere. The eight anvils are formed by gluing together with epoxy resin each of the eight sections of the inner stage with the corresponding section of the outer stage, which forms the backing block. The apex of each inner stage anvil is truncated to form an octahedral sample chamber at the center of the inner stage. The sample, surrounded by a machined sample-holder made of a pressure-transmitting medium such as pyrophyllite, is placed within the sample chamber. The anvils of the inner stage are made of tungsten carbide. The six corners between the four adjacent sections of the sphere from which the backing block is made are flat. Spherical shape of the outer stage subassembly is maintained by attaching six corner caps to the outer flat sides of the backing block. The corner caps prevent free rotation of the segmented sphere and shifting of the pistons during their advancement.

Sheets of soft insulating material, consisting of a combination of pyrophyllite and cardboard, are placed in the several millimeter-wide gaps between the anvils. As the pressure is increased, some of the material in the gaskets between the pistons and in the sample chamber is extruded. However, as the pistons move closer together, the filler becomes thinner, inhibiting further outflow of material and providing lateral support to the inner portion of the pistons. The whole spherical assembly is covered with a pair of thick hemispherical rubber shells and is placed in an oil reservoir consisting of a cylinder and two pistons. The cylinder is made from a section of a gun barrel sealed by rubber O-rings mounted in a groove cut into a nylon ring. The oil reservoir is set under a 2000-ton uniaxial hydraulic press. Fluid pressures up to 3000 kg/cm^2 were obtained using turbine oil. In one of the single 8-anvil split spheres, the outside diameter of the outer-stage sphere was 25 cm, the diameter of the sample chamber was 0.2 cm and, thus, the ratio of the two surface areas was 15,000. The sample could be heated to 2000°C by passing electric current through a graphite tube in the sample chamber. A thermocouple and a pressure calibration unit or other instrumentation could be placed in the sample space.

A later version of the segmented sphere is the 6-8 anvil split-sphere apparatus [69,72]. In this model, the outer anvils are formed by six identical sections of a hardened-steel sphere, with the inner tapered part of each section truncated to terminate in a square-shaped inner surface. Eight tungsten carbide cubes forming the inner anvils fit into the cubical cavity formed by the six outer-stage anvils. The innermost corner of each inner anvil is truncated so that, when placed together, the eight cubes form an octahedral sample chamber at the center of the apparatus. Insulation material is placed in the gaps between both the inner and the outer anvils. The inner anvils are also insulated from the outer anvils by sheets of mica. Slots at the joints of the outer anvils are sealed with Bakelite bars. The edges of the triangular faces of the inner stage anvils forming the sample chamber are 0.2 cm long. The edges of the pyrophyllite

octahedron sample chamber are 0.4 cm long. The dimensions of the samples are 0.03 to 0.07 x 0.3 x 1.5 mm. The electrical resistance of the sample is measured using a four-terminal DC technique. The rest of the 6-8 anvil apparatus is similar to that of the single 8-anvil split sphere.

The basic disadvantage of the earlier models of segmented-sphere static presses developed by Kawai is that they are cumbersome to use: the spheres have to be covered with a rubber shell, the attachment measuring the physical properties has to be replaced after each experiment, and handling of the spheres becomes more difficult with increasing diameter of the sphere. Therefore Kawai has simplified the design of the segmented sphere. His latest model [75], which will be referred to as the modified 6-8 split sphere, is similar to the 6-8 anvil apparatus. However, its outside surface is nearly spherical and is thus not equipped with either corner caps or hemispherical rubber shells. The sphere formed by the outer anvils made of sintered tungsten carbide fits into the upper and the lower hemispherical cavities in a hardened-steel cylinder that is split along its axis into two equal parts. One corner of each of the six outer anvils was cut off and replaced with a removable, hardened-steel, faceted block. The size of the corners replaced with the faceted blocks was determined by placing three of the outer anvils in the hemisphere in the upper part of the cylinder and removing the corner of each outer anvil protruding above the equator of the hemisphere.

Similar to the 6-8 anvil apparatus, the inner stage of the 6-8 split sphere is made of eight cubes with the octahedral sample cavity formed by truncating the innermost corner of each of the cubes forming the inner anvils. Of the eight inner anvils, two are made of tungsten carbide and used as electrodes and the remaining six are made of sintered alumina, which is an insulator. Cardboard spacers are placed between the equatorial contact planes and also between the inner anvils. According to Kawai, the load required to generate a given pressure in the specimen in the modified 6-8 split sphere is apparently only one-third of that necessary to produce the same hydrostatic pressure in the 6-8 split sphere.

Among the most interesting results obtained by Kawai using the older model (i.e. the 6-8 split sphere) was the observation of metallic-phase transition in Fe_2O_3, Cr_2O_3, TiO_2 [77], and NiO_2 [78] at room temperature under a load of up to 2000 tons and at oil pressures between 2000 and 3000 kg/cm^3. For the apparatus used, the magnifying ratio is 10^3. Assuming a 100 percent efficiency, the theoretical hydrostatic pressure in the chamber could be 2 to 3 Mbar. However, since no internal calibration was available and the efficiency is unknown, the actual pressure cannot be determined. Later experiments using the modified 6-8 split sphere indicate that the hydrostatic pressure achieved in the 6-8 apparatus was lower than originally estimated, but still claimed to be in excess of 1 Mbar.

Very significant phase transitions in several materials were observed by Kawai using his modified 6-8 split sphere. Unfortunately, the pressures at which these phase transitions occurred are unknown and the results are given in terms of the load. Metallic-phase transitions were observed in crystalline SiO_2 at a load pressure of approximately 700 tons [79], MgO at approximately 980 tons [80], and in pure water (ice) at approximately 950 tons [81]. Phase transition of molecular hydrogen into its metallic form claimed to have been observed in the latest experiments [82] is discussed in Section V, subsection C. For comparison, it is interesting to note that the transition of GaP into its metallic state, which is known to occur at 220 kbar, was attained in the modified 6-8 split sphere apparatus at a load of only 150 tons.

In 1959, Vereshchagin et al. [83], of the Soviet Institute of Physics of High Pressures, reported developing synthetic carbonado, a synthetic polycrystalline diamond compact containing less than one percent of transition metals. According to Vereshchagin et al. [84], the hardness of carbonado is approximately 1 Mbar, its Young's modulus is 9 Mbar, and its Poisson ratio is 1/4. Thus, carbonado is harder than, but otherwise appears to be similar to, natural diamond. The excellent properties of carbonado are claimed to be due to proper grain size (~1 mm), proper size distribution, absence of cleavage,

and low (less than 0.01) porosity (no reference is made as to whether diamond-to-diamond bonding was achieved). Although carbonado is fabricated at a pressure of approximately 90 kbar and a temperature of approximately 1200°C by direct conversion of graphite to diamond, the exact fabrication method is unknown. Carbonado can be formed to shape by machining diamond-grade graphite to the desired design and then converting it to carbonado in the press. The effect of conversion on the dimensions of items made of carbonado is readily taken into account. In 1972, the Soviets were able to fabricate finished precision industrial items of carbonado with linear dimensions of up to 1 cm.

In 1972, Vereshchagin et al. [84-86] reported contact pressures in excess of 5 Mbar using opposed carbonado anvils consisting of a conical indentor with a rounded tip pressed against a flat anvil. In most experiments, the angle defining the cone, β, was 6°. It was calculated that an estimated contact pressure of 1.6 Mbar was generated by a force of only 1 kg when the radius of the rounded conical tip, R, was 10 μm. Increasing the force to 30 kg and using an identor with R = 100 μm and R = 10 μm increased the estimated contact pressures to 1.1 and 5.1 Mbar, respectively.

In a number of subsequent papers, Vereshchagin et al. reported observing metallic transitions in diamond [87-89]; SiO_2 [90]; Al_2O_3, NaCl, and S [91]; H_2O (ice) [92], BN [93], and MgO [94] at pressures estimated to exceed 1 Mbar. Metallic-phase transition of molecular hydrogen [95] is discussed in Section V, subsection G. In these experiments, the metallic transitions were determined from the discontinuous changes in electrical resistivity of samples under pressure. Upon removal of pressure, the electrical resistivities of materials returned to their normal values. The insulator-metal transition pressure was observed to decrease with increasing temperature and vice versa. The discontinuous changes in electrical resistivity were occasionally caused by shorting of the anvils. However, in such cases, the sharp drop in electrical resistivity remained practically constant. A technique based on the existence

of metastable metal and insulator phases characteristic of the first order phase transitions in the insulator-metal system was developed by Vereshchagin et al. to ascertain that shorting of the anvils did not take place. After the sample was transformed into its metallic phase, the pressure was gradually decreased to a value just above the metal-insulator transition pressure. Heating the sample at this pressure caused transition of the metal into the insulator phase--i.e., a sharp increase in its electrical resistivity.

The most recent experiments were performed to set up a relative calibration scale based on the metallic-phase transitions of insulators observed at the very high pressures between opposed carbonado anvils. A thin film of a mixture of two insulators with the typical component ratio of 1 to 1 was deposited on the flat anvil and compressed until both components underwent transition into metallic phase at two different undetermined pressures. The concentration of one component was increased typically to a component ratio of 10 to 1. The increase in concentration of one component resulted in a larger drop in the electrical resistivity upon metallic-phase transition of that component, making it possible to determine whether it occurs at a lower or higher pressure than that of the other component. These experiments made it possible to establish the following sequence of insulator-metal transition pressure:

$$P_{GaP} < P_{NaCl} < P_{Al_2O_3} < P_{BN} < P_{C} < P_{SiO_2} < P_{MgO}$$

The transition pressures of SiO_2 and MgO are in the same sequence as those established by Kawai. According to the Japanese experiments, the transition of water into its metallic phase should occur at a higher pressure than that for MgO.

The contact pressures between carbonado anvils were calculated from equations derived by Hertz in 1881 for a paraboloidal indentor pressed against a flat plate. The contact area was determined from the area of the imprint left on a film of material deposited on the

flat anvil (cellulose nitrate varnish dissolved in acetone was frequently used). In a very recent paper, Ruoff and Chan [96] point out that since Hertz's equations are derived for a paraboloidal indentor, one limitation to its application to conical indentors with rounded tips used by Vereshchagin is that $a < xp$, where a is the contact radius and xp is the perpendicular distance from the piston axis to the point where the paraboloidal region joins the conical region. The authors then derive expressions for the maximum applied force and the maximum contact pressure which, for various indentor materials give the limiting values above which the Hertz theory does not apply due to the failure of the condition $a \leq xp$. It is shown that, in the case of a conical indentor with a rounded tip made of carbonado, Hertz's theory is invalid at contact pressures $P \geq 0.21$ Mbar. If the applied force is increased beyond its limiting value, the contact radius will increase much more rapidly and, as a result, the contact pressure will increase more slowly than indicated by Hertz's equations.

Ruoff and Chan developed a method for computing the contact pressure distribution under elastic conditions between an indentor, which is a body of revolution with profiles represented by $z(r)$, where $z(r)$ is a monotonically increasing function with $z(0) = 0$, and a flat anvil. It is shown that when the applied force exceeds its limiting value, the contact pressures obtained using a conical indentor with a rounded tip are much lower than pressures expected to be achieved with a paraboloidal tip for the same force. For example, for a conical indentor with a rounded tip with $\beta = 6°$ and $R = 100$ μm under a force of 200 kg (maximum load used by Vereshchagin and his colleagues), $a = 159$ μm and $P = 1$ Mbar. Thus, according to Ruoff and Chan, 1 Mbar is the maximum contact pressure that could have been achieved by Vereshchagin et al. in the opposed-anvil device made of carbonado. In the case of a paraboloidal indentor under the same conditions ($R = 100$ μm and applied force of 200 kg), $a = 67.9$ μm and $P = 2$ Mbar. In both examples, the condition $a \leq R$ was exceeded and the contact pressures determined are not very accurate, especially

in the first case. Because carbonado can be manufactured in different shapes, it would be interesting to see if paraboloidal indentors made of this material could reach the high pressures predicted by Ruoff and Chan without yielding.*

In the experiments performed by Kawai and Yakovlev described above, the pressures were determined using external calibration. The first internally calibrated experiments in which pressures of 1 Mbar were claimed to have been reached were reported in 1976 by Mao and Bell [97]. The diamond pressure cell used in the experiments consisted of two opposed anvils made of single-crystal diamonds with the work area of each anvil approximately equal to 1.5×10^{-3} cm^2. A scissors-shaped lever-block assembly was spring-loaded to apply a mechanical advantage of two. The diamonds were supported by two identical half-cylinder seats of tungsten carbide, with a 0.001-inch thick zirconium shim placed between the low-pressure-bearing surfaces. The half cylinders were adjusted to achieve and maintain alignment of the diamonds to better than one-half a Newton color fringe interference of the diamond faces. A 0.010-inch thick sheet of work-hardened steel was placed between the high-pressure diamond faces. A ruby crystal was placed on the steel and pressed into it as the diamond anvils were squeezed together.

The pressure was determined from the linear extension of the new NBS calibration scale based on the spectral shift of the R_1 ruby fluorescence line with pressure. Ruby fluorescence was excited with a cadmium-helium gas diffusion laser beam and its wavelength was monitored continuously with a spectrometer linked to the pressure cell by a fiber optic bundle. The pressure determination is believed to be accurate to within 10 percent and the data are reproducible. No mechanical failure was observed in the diamonds and Mao and Bell believe that with improved support it may be possible to increase the pressure to 1.5 Mbar.

---

*Diamond (and carbonado), at room temperature, fractures and cracks rather than yields. However, according to Ruoff, plastic flow should occur and should be followed by fracture, fragmentation, and pulverization of the tip during unloading.

The primary standard for calibration of the ruby fluorescence gauge used by Mao and Bell is the Decker equation of state for NaCl based on the central force model. This equation of state in conjunction with lattice parameter measurements was used to obtain the B1-B2 transition pressure in NaCl (P_T = 291 kbar). In a recent paper, Ruoff and Chhabaldas [98] show that the central force model is inadequate to describe NaCl, especially at high pressures where many-body forces become very important. Therefore, the central force equation of state for NaCl cannot be considered reliable. Using Keane's equation of state for NaCl, the authors calculate that the B1-B2 transition in NaCl occurs at a pressure of 260 kbar rather than 291 kbar, as was calculated from Decker's equation of state. Therefore, the pressures determined by Mao and Bell using linear extension of the NBS scale are too high. Mao and Bell also have failed to take into account the nonlinearity of the temperature dependence of the spectral shift of the R_1 ruby fluorescence line, which could be significant in materials such as ruby due to localized heating by the intense laser beam.

The basic advantages of carbonado are not its superior properties, as initially claimed by Soviet scientists, but the fact that it is inexpensive and can be made in various shapes of fairly large size. Thus, it would be advantageous to develop materials similar to carbonado for use in the very high-pressure research.

In 1970, Hall [99], of Brigham Young University, reported preparation of carbonado by sintering diamond powder. The compressive strength of the carbonado fabricated from diamond powder ranges up to 58 kbar and its density ranges up to 3.48 g/cm^3. However, according to Asada [100], materials obtained by sintering microcrystals of diamond available in early 1972 did not prove useful as anvils.

In 1974, Hibbs and Wentorf [101] reported developing Man-Made diamond® * compact with diamond-to-diamond bonding. While its properties have not been described, according to Wentorf [102], it

---

* ® Trademark of General Electric Company.

is superior to carbonado. The diamond compact is made by sintering, under conditions similar to those used for the synthesis of diamond from graphite, and is expensive. For application in high-pressure research, a film of up to 1 mm of diamond compact is deposited on materials such as tungsten carbide. A disadvantage of diamond compact is the difficulty of depositing a film of compact on materials of different geometrical shapes. Diamond compact, which is available commercially, has been used in an opposed-anvil device designed for Bundy [103], in which he achieved estimated pressures of about 0.6 Mbar. Higher pressures were not attempted due to possible failure of this unique device. General Electric also has available thick-walled carbide cylinders with diamond compact in the center, which are sold as wire drawings die blanks and could find an application in an opposed-anvil device.

NASA Lewis Research Center in Cleveland has an operational 6-inch-diameter, room-temperature segmented-sphere apparatus. A 12-inch-diameter, cryogenic segmented sphere is in the planning stages and is expected to be constructed in a few years. However, material procurement difficulties may result in cancellation of its construction [104]. A 22-inch-diameter, room-temperature, four-stage, segmented sphere constructed for the Materials Center at Cornell University is undergoing calibration tests [105]. According to an earlier design, the hydrostatic pressure was to increase from 5.5 kbar at the outside of the outer shell to several Mbar in the sample chamber. The sample diameter was expected to be about 2 mm. The pressure calibration scale was to be based on the increase in the decay rate of radioactive ^{7}Be in ^{7}BeO with pressure. Ruoff's design is very unusual in that the fourth stage, made of boron nitride, was to be in a plastic state.

A large static press for the generation of pressures in the Mbar range in a volume of at least a few cm^3 has been constructed by the Institute of High Pressure Physics [106]. The press weighs 4.5×10^3 tons and consists of a 50,000-ton ram in a 30-m high steel frame. It is located in a building that was specially

constructed for the press. Very few details pertaining to the press have been published; however, one of its major applications will be the conversion of molecular hydrogen into its metallic phase. According to newspaper and science journal accounts [106-109], the press will operate on the cascade principle and will involve five stages. Proceeding from the outer to the inner stage, the stages will be made of stainless steel, hardened steel, tungsten carbide, diamond alloy (as described in Reference 110), and carbonado.

The finite-difference HEMP computer program in two or three space dimensions and with time-dependence, recently developed by Wilkins et al. [111] at the Lawrence Livermore Laboratory, can be used to solve problems in solid mechanics involving plasticity and material behavior. It includes a graphics program that monitors the computer input and displays its output in the form of pictures of three-dimensional objects and is interactively capable of rotating, translating, and scaling the object in the field of view. Three-dimensional, finite-element meshes can be displayed either as line drawings or half-tone pictures shaded from a light source. The program can also generate pictures with shading or with surface contours determined by an arbitrary variable, such as temperature, stress, etc. The program could be modified to design extremely high-pressure static presses.

3. Theoretical Considerations

It has been generally accepted that the basic limitation to generation of static high pressures is the strength of materials used in the high-pressure apparatus. It is also accepted that the use of different types of apparatus (different configurations) cannot remove this limitation. At present, the segmented sphere and the opposed-anvil apparatus appear to be the most promising configurations for reaching the highest attainable pressures. However, there are two schools of thought on the subject of the highest pressures that can be achieved using the strongest available materials, such as carbonado and diamond compact, without yielding or fracturing. One group of material scientists and high-pressure researchers is convinced that the highest pressures that can be achieved in elastic case are

somewhere between 0.6 and < 1 Mbar. Another group believes that multi-Mbar pressures can be generated using these materials without the onset of plastic flow. Because theoretical calculations appear to be uncertain and only approximate, the generation of maximum pressures will have to be resolved experimentally. However, the absence of a reliable calibration scale makes this task very difficult.

The limitation on the maximum pressures that can be achieved in a static apparatus is clearly illustrated by the following example. The highest pressures that can be generated in a spherical pressure vessel can be determined by considering a completely plastic sphere. The equation for the radial equilibrium, expressed in spherical coordinates r, ψ, and θ, is:

$$\frac{\partial \sigma_{rr}}{\partial r} + \frac{2(\sigma_{rr}-\sigma_{\psi\psi})}{r} = 0, \qquad (38)$$

with $\sigma_{\theta\theta} = \sigma_{\psi\psi}$, $\tau_{r\psi} = \tau_{\psi\theta} = \tau_{\theta r}$. For von Mieses' criterion, the condition for the onset of yielding is:

$$\sigma_{\theta\theta} - \sigma_{rr} = \sigma_{\psi\psi} - \sigma_{rr} = \sigma_0, \qquad (39)$$

where σ_0 is the tensile yield stress. Assuming that no strain hardening occurs, Eq. (39) holds throughout the deformation and Eq. (38) can be written in the form:

$$d\sigma_{rr} = 2\sigma_0 dr/r. \qquad (40)$$

Integrating Eq. (40), assuming that σ_0 = const, leads to the expression for the internal pressure in a plastic sphere:

$$P = P_{ext} + \sigma_0 \ln \frac{r_0}{r} \qquad (41)$$

where r is the radius of the spherical pressure vessel, and P_{ext} is the hydrostatic pressure at the surface of the sphere.

From this formula, it can be seen that as $r \to 0$, $P \to \infty$. However, the increase in pressure is very slow and the pressures that can be reached in a laboratory-size vessel are not very high.

Ruoff [112] recognized that the basic deficiency in the derivation of Eq. (41) is the fact that σ_0 is assumed to be constant. He pointed out that the large external pressures that can be exerted on a sphere in a multistage system can drastically increase the yield stress of material and, thus, can have a significant effect on the pressures that can be attained in a static pressure vessel. In a 1973 paper, Ruoff [112] assumes that the yield strength is proportional to the average dislocation line energy of material. Assuming that the pressure dependence of the elastic constant, C, is linear, it can be expanded in Taylor series, where only the first term is retained:

$$C = C_0 + C_0'P, \tag{42}$$

where C_0 is the value of C at $P = 0$ and C_0' is the pressure derivative of C at zero pressure. Because σ_0 is proportional to C, it can be written in the form:

$$\sigma_0 = \sigma_{00} + \sigma_0'P, \tag{43}$$

where

$$\sigma_0' = \sigma_{00}C_0'/C_0. \tag{44}$$

Using Eq. (38), subject to conditions given by Eq. (39), and the fact that at large external hydrostatic pressures, $P \simeq -\sigma_n \simeq \sigma_{rr}$, where σ_n is the mean normal stress, Eq. (43) takes the form:

$$d\sigma_{rr} = 2\,\sigma_{00}\,[1-(C_0'\sigma_{rr}/C_0)]dr/r. \tag{45}$$

Assuming that the boundary conditions are:

$$\sigma_{rr} = - P_{ext} \text{ at } r = b_0 > a,$$
$$\sigma_{rr} = - P \text{ at } r = a_0, \qquad (46)$$

Eq. (45) is easily integrated. The resulting expression for the internal pressure inside a plastic sphere subjected to a large external hydrostatic pressure, P_{ext}, is:

$$P = (C_0/C_0') \left| [1 + (C_0' P_{ext}/C_0)] K^{2\sigma_{00} C_0'/C_0} - 1 \right| , \qquad (47)$$

where K is the ratio of the outer radius to the inner radius. Approximate calculations made by Ruoff for the inner stage of a spherical pressure vessel exposed to external hydrostatic pressure, P_{ext} = 500 Mbar, show that the internal pressures for K = 100 and K = 1000 are P = 1.6 Mbar and P = 2.6 Mbar, respectively. Using tungsten carbide instead of steel increases the pressure to P = 3.7 Mbar for K = 100. Strain-hardening and the use of materials with very high values of C_0 could make it possible to contain pressures exceeding 10 Mbar.

Eq. (47) involves a ratio of two effective constants that can only be estimated. A different solution of the problem of determining the internal pressure that can be attained in a plastic sphere exposed to large external hydrostatic pressure was recently obtained by Fadeyenko [113]. His solution contains no unknown constants, but is based on the use of a generalized equation of state of materials at high pressures.

Fadeyenko assumes that the tensile yield strength is a linear function of pressure and can be expressed in the form given by Eq. (43). Using the expression:

$$\sigma_{rr} = \sigma_n - \frac{2}{3} \sigma_0 , \qquad (48)$$

where σ_n is the mean normal stress and, assuming that in the presence of a large external hydrostatic pressure $\sigma_n \simeq P$, Eq. (52) can be written in the form:

$$\frac{d(-3P-2\sigma_0)}{6\sigma_0} = \frac{dr}{r} . \qquad (49)$$

Using Eq. (43), the solution of Eq. (49) is:

$$\frac{\sigma_{00} + \sigma_0' P}{\sigma_{00} + \sigma_0' P_{ext}} = \left(\frac{r_0}{r}\right)^{\mu} , \qquad (50)$$

$$\text{where } \mu = \frac{6\sigma_0'}{3 + 2\sigma_0'} . \qquad (51)$$

At very high pressures ($P >> \sigma_{00}/\sigma_0'$):

$$P \simeq \left(P_{ext} + \frac{\sigma_{00}}{\sigma_0'}\right)\left(\frac{r_0}{r}\right)^{\mu} . \qquad (52)$$

An estimate of σ_0' for typical solids under very high pressures can be obtained using the following generally valid expression:

$$\sigma_{00} = G/k = \frac{E}{2k(1 + \nu)} , \qquad (53)$$

where G is the shear modulus, E is Young's modulus, ν is the Poisson ratio, and k is a proportionality constant. For materials with 0 K isotherm,

$$P = A\left[\left(\frac{\rho}{\rho_0}\right)^{n} - 1\right] , \qquad (54)$$

Young's modulus and σ_{00} are given by the following relationships:

$$E = 3n(1 - 2\nu)\ (P+A), \qquad (55)$$

$$\sigma_{00} = \frac{3n}{2k}\,\frac{1 - 2\nu}{1 + \nu}\ (P+A), \qquad (56)$$

and

$$\sigma_0' = \frac{3n}{2k}\left(\frac{1-2\nu}{1+\nu}\right). \qquad (57)$$

In the range of Mbar pressure, $n \approx 3$ to 5. Using Eq. (57) with $n = 3$ to 5, k = 10 to 30, and $\nu = 0.25$ to 0.33, σ_0' is found to be 0.04 to 0.3 and μ is 0.14 to 0.77. A numerical example shows that an internal pressure of 4.5 Mbar can be achieved in a plastic sphere with K = 100.

C. SHOCK-COMPRESSION EXPERIMENTS

Shock compression has provided virtually all the reliable pressure density measurements of solids and liquids above 0.025 Mbar. A Hugoniot (shock-compression curve) represents the locus of all thermodynamic points that can be reached in a material when a shock wave is passed through it. By varying the initial density through compression or solidification, one can also obtain a set of different Hugoniots. However, unless the initial state can be varied considerably, the final Hugoniots will not differ sufficiently to justify the extra work. Considerable variation in the path of the Hugoniot can be achieved by means of reflected experiments (see Figs. 12 and 13). In a reflected shock experiment, the primary shock is passed through the material and then reflected from an anvil, such as a brass plate. The reflected wave then compresses the already compressed material to a much higher pressure. The reflected Hugoniot curve is very sensitive to the density reached by the first shock. Thus, by varying the intensity of the first shock, it is possible to cover a wide range of the thermodynamic space.

The shock process is adiabatic, but highly irreversible. As a result of this, very high temperatures are achieved in shock compression experiments. As can be seen from Fig. 13, the temperatures along the Hugoniot are generally an order of magnitude greater than those along the isentropes. Since the reflected Hugoniot is a two-step compression, the final temperature at the same final density as that for the unreflected one-step Hugonoit is lower. The limiting case of compression by a shock wave reflected an infinite number of times is equivalent to isentropic compression.

While very high pressures (>10 Mbar) have been achieved in the past in stiff materials using high explosives (pressure >40 Mbar have been obtained by Soviet scientists, apparently by means of shock waves from nuclear explosions), the maximum pressure that can be generated by shock waves is much lower in highly compressible low-density materials. Thus, the highest pressure that can be achieved in liquid hydrogen and liquid deuterium by means of an unreflected, one-step shock wave is ~150 kbar and ~220 kbar, respectively. The use of a reflected shock wave makes it possible to increase the pressure generated in liquid deuterium to approximately 0.9 Mbar. However, except for multiple reflected shock waves, as it is commonly used at present, this technique cannot generate the compressions required for the metallic-phase transition of molecular hydrogen. (The high material compressibility of hydrogen converts too much energy into thermal heating, limiting the degree of compression.)

The high temperatures generated during shock compression tend to greatly complicate any theoretical analysis. However, they also allow molecules to penetrate their neighbors' repulsive cores to a much greater extent than is possible in material compressed to the same density at low temperature. This makes it possible to perform theoretical analysis of the data to determine the intermolecular pair potentials to very small internuclear distances. This point is illustrated in Section I, where it is shown that the high temperatures generated in shock compression experiments make it possible to determine the intermolecular potential at about the density required to reliably predict the metallic transition.

The shock compression data obtained by workers at the Lawrence Livermore Laboratory consists of a Hugoniot point of hydrogen at P = 40.5 kbar, determined in 1966 using high explosives [26], and 8 Hugoniot points at P = 0.82 to 0.94 Mbar, obtained in 1974 with the two stage-gun at the Santa Barbara facility of General Motors [32]. The experimental methods used in determining the Hugoniot points by means of high explosives and the general data analysis techniques are widely used and well known, and will not be discussed

in this report. The two-stage gun is described in detail in Reference [32]. Therefore, the discussion below will summarize the results of shock-compression experiments on molecular hydrogen used in deriving its equation of state.

Table 8 summarizes the Hugoniot data on hydrogen and deuterium determined from the shock-wave data acquired in unreflected one-step compression experiments (P, V points) and in reflected two-step compression experiments (the temperatures are computed). The Hugoniot points obtained by Van Thiel and Alder [26] and Van Thiel et al. [32] are also plotted in Figs. 5 and 6 (solid bars with circles at their centers), together with theoretical Hugoniots calculated for a number of intermolecular potentials. The single point in Fig. 5 at 40 kbar was reached by shocking liquid hydrogen at P_0 = 1 bar, T_0 = 20.7 K, and V_0 = 28.6 cm^3/mole, while the points in Fig. 6 were reached by shocking liquid deuterium at P_0 = 1 kbar, T_0 = 20.7 K, and V_0 = 23.79 cm^3/mole. The lower points at 210 kbar in Fig. 6 were obtained by a single shock. The points near 900 kbar were reached by first shocking to 210 kbars and then reflecting the shock wave off a brass anvil.

Because the parameters measured in shock-compression experiments are pressure and change in volume, the error is in terms of change in volume or compression. In the case of D_2, the change in volume in the first shock wave, from 22 to 7 cm^3/mole, is 15 cm^3/mole. Because the error is ±3 percent, the error in absolute terms is ±0.5 cm^3/mole. Unfortunately, in the case of reflected shocks, the errors roughly double. Therefore, in the case of deuterium further compressed from 7 cm^3/mole to 3.6 cm^3/mole by the reflected shock wave, the total absolute error is ±1 cm^3/mole.

The Hugoniot temperatures listed in Table 8 were calculated by van Thiel et al. [33] on the assumption that the heat capacity of the liquid hydrogen and deuterium along the Hugoniot can be approximated by that of a Debye solid with a superposed free-rotor heat capacity. Recent calculations by Grigor'yev et al. [114] indicate that the temperatures are one-half of their values given in Table 8. The Russian authors attribute the discrepancy to the fact that van Thiel

Table 8 [26,32]

EXPERIMENTAL HUGONIOT POINTS OF MOLECULAR HYDROGEN AND DEUTERIUM

Material	P_o bar	V_o cm^3/g	P_1 Mbar	V_1 cm^3/mole	T_1 K	P_2 Mbar	V_2 cm^3/mole	T_2 K
H_2 (single shock)	1.8	28.43	0.0395	10.4	~1100	-	-	-
D_2 (single shock)	1.07	-	0.215	6.65	~4500	-	-	-
	0.65	-	0.213	6.53	" "	-	-	-
D_2 (double shock)	1.6	23.732	0.212	6.85	~4500	0.944	3.621	~7000
	1.8	23.744	0.211	6.9[illegible]	" "	0.892	3.500	" "
	1.8	23.857	0.208	[illegible].10	" "	0.869	3.568	" "
	1.2	23.817	0.208	6.98	" "	0.820	3.060	" "
	1.6	23.801	0.192	6.53	" "	0.827	3.012	"
	1.6	23.761	0.217	6.98	" "	0.889	3.290	"

and Alder [26] and van Thiel et al. [33] used the specific heat at constant volume of a solid (C_v = 3R), rather than that of a liquid (C_v = 3/2R), used by Grigor'yev. However, calculations by Ross [6, 7], using liquid perturbation theory and liquid cell models are in good agreement with those of van Thiel et al. [33] (see Section I). The Hugoniot temperature has an important bearing on the theoretical calculations of the intermolecular pair potential of molecular hydrogen and on its equation of state calculated using experimental Hugoniot data. In particular, higher dissociation, complete excitation of vibration states, and greater deviation from sphericity of the H_2 molecule (asymmetry of molecular forces) due to smaller effective volume of molecules will occur at the higher temperatures of 7000 to 14,000 K.

A two-stage gun recently put into operation [115] at the Lawrence Livermore Laboratory is capable of achieving pressures slightly greater than those achieved for hydrogen on the two-stage gun at the Santa Barbara facility (just under 1 Mbar). Improvements in technology will make it possible to repeat these experiments with a threefold increase in accuracy over the previous work. Such experiments will supply the data making it possible to determine the high-density equation of state of molecular hydrogen to within ±5 percent in pressure at 1 Mbar and test the theoretical models of the pair potential. Recent advances in technology will also make it possible to simultaneously measure the electrical resistivity of materials undergoing shock compression. However, it should be emphasized that shock experiments will not achieve metallic-like densities despite possible Mbar pressures because, as the result of shock heating, much of the pressure is thermal and is not due to compression.

D. ISENTROPIC COMPRESSION

The least known and least advanced of the three experimental methods is the isentropic-compression technique. It is a constant entropy, reversible process. Figs. 12 and 13 show that the increase in temperature along the isentrope is quite small in comparison with

that along the Hugoniot and that the pressures generated are closer to the isotherms than to the Hugoniots. Potentially, the final pressures that can be achieved by isentropic compression are in the multimegabar range. Thus, the attractive features of the isentropic experiments are that the compression that can be attained is much higher than in the static experiments, although the temperatures are not nearly as high as in the shock compression method. However, one of the drawbacks of this method as it was applied to hydrogen is its failure to measure pressure directly. The density of the sample can be determined from x-ray shadowgraphs or gamma radiography, but the pressure has to be obtained from hydrodynamic or magnetohydrodynamic calculations. In addition, only a single point can be measured in each experiment. While all of the work done so far has not provided any useful (accurate) high-density equation-of-state measurements, considerable progress was made by Grigor'yev et al. [114,116] and Hawke [117] in their attempts to achieve metallic-phase transition in isentropically compressed hydrogen.

In the experiments performed by Grigor'yev [114,116] a cylindrical high-explosive charge compressed a cylindrical metal shell containing hydrogen gas at a temperature of 300 K. The density of hydrogen was determined directly by measuring the diameter of the shell during isentropic compression by means of gamma radiography, using a device with a short exposure time. The pressure was calculated from a hydrodynamic computer code. Six different pressure vs density points were obtained at densities between 0.45 and 1.95 g/cm^3 (4.48 to 1.03 cm^3/mole) and at calculated pressures between 0.37 and 8.0 Mbar, by varying the initial gas pressure and parameters of the enclosure. Unfortunately, no other experimental details are given by the Soviet authors.

Hawke et al. [117] developed a magnetic flux compression technique for isentropic compression of soft materials. In the device used by Hawke, a capacitor bank is discharged through a pair of coils that generate a magnetic field that diffuses through the stainless steel liner surrounded by a high-explosive charge. When the diffused magnetic field reaches a peak, the charge is detonated, imploding the

cylindrical liner. The implosion compresses the magnetic flux, increasing the magnetic field intensity. (In the hydrogen compression experiments, the magnetic-field intensity increased from ~60 kG to ~10 MG in about 10 μs.) Eddy currents generated in the sample tube and the liner interact with the magnetic field and exert an outward pressure on the liner and an inward pressure on the sample tube. The sample volume compression is determined from the ratio of the sample tube diameters measured during and before the experiment by means of a flash x-ray device. A one-dimensional magnetohydrodynamic code is used to calculate the pressure from the compression of the sample. A wire is placed axially in the sample and the resistance between the wire and the sample tube is monitored to detect metallic-phase transition.

Liquid hydrogen at T = 20 K was used by Hawke et al. [117] in the experiments. Unfortunately, they obtained only a single point for hydrogen at an estimated pressure between 2 and 5 Mbar and at an apparently metallic conductivity. Since Hawke has not had the opportunity to repeat the experiment, the data obtained should be considered preliminary.

Table 9 summarizes the results of isentropic compression experiments performed by Grigor'yev et al. [114,116] and Hawke et al. [117]. This table lists the density of hydrogen measured during the experiments and the pressure and temperature computed from a hydrodynamic code by Grigor'yev and a magnetohydrodynamic code by Hawke. The three lower pressure points ($P \leq 2.63$ Mbar) determined by Grigor'yev are in excellent agreement with the theoretical isentrope for liquid molecular hydrogen calculated by the authors. The remaining three higher pressure points ($P \geq 3.24$ Mbar) obtained by Grigor'yev are shifted in respect to the isentrope and the lower pressure points. This shift is interpreted to be a transition occurring at 2.8 Mbar at 0 K. It is estimated that the temperature at this pressure is close to 6000 K, while the melting temperature of molecular hydrogen is estimated to be 700 K at P = 2.44 Mbar and 910 K at P = 4.66 Mbar.

Therefore, the transition observed is interpreted as the phase transition into metallic state accompanied by a change in density

Table 9

RESULTS OF THE ISENTROPIC-COMPRESSION EXPERIMENTS ON HYDROGEN

No	ρ_{exp} g/cm^3	P_{cal} Mbar	T_{cal} °K	Ref
1	0.45±0.03	0.37	3100	[116]
2	0.67±0.03	1.00	4200	[114]
3	0.98±0.08	2.63	5600	[116]
4	1	2	~1500	[117]
5	1.15±0.1	3.24	6000	[116]
6	1.4 ±0.14	4.40	6500	[116]
7	1.95±0.39	8	9100	[116]

from 1.08 to 1.3 g/cm (from 1.87 to 1.55 cm^3/mole). As a result of a very large uncertainty in both density and pressure, the pressure vs density point determined by Hawke in magnetic flux experiments does not contradict the data obtained by Grigor'yev.

In an isentropic experiment, the final temperature is proportional to the initial temperature multiplied by the compression. Therefore, the much higher temperature achieved in Grigor'yev's experiments near metallic density (6000 K) in comparison with that of Hawke (~1500 K) is not a discrepancy, but the result of different initial temperatures (Grigor'yev used gaseous hydrogen at T_i = 300 K, and Hawke used liquid hydrogen at T_i = 20 K). Also, because these temperatures are computed and not measured, they likewise reflect differences in the equation-of-state models.

As can be seen from Table 9, the error in measuring the density of molecular hydrogen claimed by Grigor'yev is about 8 percent. No details or error estimates are given concerning the pressure calculations

using the hydrodynamic code. However, such calculations are rather difficult and insufficiently accurate. Also, it is most likely that a one-dimensional, rather than two-dimensional, hydrodynamic code was used in pressure computations. Since the experimental geometry is two-dimensional axisymmetric, the isentropic compression experiments by Grigor'yev are not considered definitive and the data obtained are insufficiently accurate to be used in theoretical calculations of the equations of state of hydrogen [6,7]. Partly as a result of this criticism, Grigor'yev et al. published their second paper [114], which includes a detailed discussion of the agreement between the available experimental data and the Hugoniots, isotherms, and isentropes calculated from the Mie Gruneisen equation of state for solid molecular hydrogen and an equation of state for liquid molecular hydrogen based on that for the solid phase, using their isentropic compression data. This later paper also includes an additional pressure vs density point at P = 1 Mbar (point No. 2 in Table 9). Although no error estimate in determining the pressure is given and the hydrodynamic code used in the calculations is not described, the results of their theoretical calculations are in good agreement with the available experimental data.

Alt'shuler et al. [118] have proposed a modification of the technique used by Grigor'yev, in which quasi-isentropic compression is obtained by means of multiply reflected shock waves. The major change in the experimental set up is that a concentric layer of solid molecular hydrogen is deposited on a cylindrical rod made of high-impedance material, such as copper, cooled to liquid helium temperature. The copper rod is located at the center of the cylindrical charge system. An extra cylindrical layer of low-stiffness material is added on the inner side of the imploding copper liner. During the initial stage, isentropic compression is achieved by the gaseous products of the low-stiffness material vaporized by the converging shock wave. During the later stages, compression is by means of the imploding liner. Compression by multiply reflected shock waves makes it possible to generate much higher pressures in hydrogen with a much smaller increase in entropy. For example, assuming that the ratio of acoustic impedances of material comprising the rod with hydrogen is m, the increase in entropy of the system

under consideration is $4/(3m^2+1)$ times lower than that of the system shock compressed to the same pressure. The problem considered is actually similar to compression of a soft target impacted from opposite directions by two heavy flyers. Numerical calculations by the authors for two copper flyers impacting a layer of solid hydrogen at a velocity of 2 km/sec show that the final pressure in hydrogen is 1.18 Mbar. The amplitude of the first shock wave was 8 kbar; that of the second, third, and fourth was 32, 64, and 125 kbar, respectively. Further increase in pressure to its maximum value was generated by reflected shock waves with rapidly decreasing amplitudes. The fraction of the thermal pressure does not exceed 5 percent.

Yampol'skiy [119] discussed various techniques of isentropically compressing materials by shock waves. Among the methods that could be applied to hydrogen is the use of a charge consisting of layers of explosives with different detonation velocities. The thickness of each layer can be chosen so that the pressure exerted by the detonation products would increase monotonically with time. Cylindrical layers of charge could be used in an implosion system. In a similar fashion, the use of several layers of molecular hydrogen deposited on the cylindrical copper rod in the implosion scheme proposed by Alt'shuler et al. [118] would enhance compression.

A significant contribution to magnetic implosion experiments was recently reported by Scudder [120], who has developed a magneto-optic technique employing Faraday rotation for measuring multi-megabar magnetic pressures generated by magnetic flux under compression. This technique, together with a sample field probe, is capable of providing sufficiently accurate pressure vs. density data of magnetically imploded hydrogen as well as other soft materials over a wide dynamic range.

E. LASER COMPRESSION

According to Nuckolls et al. [121], achievement of laser fusion will require symmetric spherical compression of heavy-hydrogen isotopes

to densities of $\sim 10^3$ g/cm^3,* or 10^4 times the density of liquid hydrogen. Intensive research in this area led to the development of 1 to 1.3 kJ lasers both in the United States and the Soviet Union. Several laboratories in both countries have designed (and are planning to construct in the near future) 10 to 20 kJ laser systems. Compared to laser fusion, an approximately tenfold compression required for metallic-phase transition of hydrogen is a relatively simple problem. Thus, it is somewhat surprising that only a few papers have been published on the possibility of attaining laser-generated transition of molecular hydrogen into a metallic phase.

Anisimov [123] has considered the problem and obtained numerical results on the assumption that the laser-induced compression due to the subsonic thermal wave is equivalent to compression by the accelerating motion of a piston in an ideal gas. The piston path and the energy flow are determined on the assumption that the process is adiabatic and the approximate adiabatic equation of molecular hydrogen is given by the 0 K isotherm derived by Trubitsyn [25], written in the following form:

$$P = a\rho^{\gamma}, \qquad (58)$$

where $\gamma = 3$ and $a = 3.3 \times 10^6$ (the pressure is given in bars and the density in g/cm^3). Inhomogeneous, one-dimensional adiabatic compression by a piston has a self-similar solution.** Assuming that the shock wave is not formed before the piston travels a distance x_o, the piston position is given by the equation:

$$x = x_o\,(1 + r - 2\sqrt{r}), \qquad (59)$$

---

*Basov's scheme [122] calls for an order-of-magnitude lower compression (to density of $\sim 10^2$ g/cm^3), requiring about the same amount of laser energy to initiate laser fusion in a 100-fold larger hydrogen isotope mass.

**The solution is not discussed by Anisimov. However, its main features are summarized by Lengyel [124].

where $r = 1 - \frac{c_o t_m}{x_o}$ * and c_o is the initial sonic velocity. The shape of the laser pulse is given by the equation:

$$q(t) = \rho_o c_o^3 \, r^{-2} \, (1-2\sqrt{r}), \qquad (60)$$

and the total energy per unit area expended in compression up to the time t_m is:

$$Q \approx \frac{1}{3} \rho_o c_o^2 x_o r_m^{-1}, \qquad (61)$$

$$\text{where } r_m = 1 - \frac{c_o t_m}{x_o} . \qquad (62)$$

Assuming that at the end of compression, the pressure in a layer of thickness δ exceeds transition pressure P_t, and determining x_o by maximizing Q, then $r_m \approx 0.5a^{-2}$, $x_o \approx 2.5a\delta$, and $Q \approx 5\delta P_t$, where a is the compression ratio. The thickness δ is determined from the experimental conditions. Assuming that $\delta = 0.1$ mm and $P_t = 5$ Mbar, then $q_{max} = 3.10^{13}$ W/cm^2 and $Q \approx 2.5.10^4$ J/cm^2. In order for the problem to be one-dimensional, the area irradiated by the laser should be on the order of x_o. Disregarding reflection and other losses, the laser energy required for the metallic-phase transition of molecular hydrogen is about 2 kJ. Because the transition pressure is believed to be 3 Mbar, laser-induced metallic-phase transition of hydrogen may be within the reach of present-day technology.

Van Kessel and Siegel [125] observed the spatial development of laser-driven shock waves in a plane solid hydrogen target using high-speed photography. The peak pressure achieved in these experiments, as determined from the shock velocities generated by a 10 J 5 nsec pulse from a Nd glass laser, was 2 Mbar. The authors suggest that a programmed laser pulse may be used to observe metallic transition of hydrogen.

---

*According to Anisimov, in the case of spherical compression, $r \sim r^{1/\gamma}$.

F. ELECTRON-BEAM COMPRESSION

In a 1971 paper, Bogdankevich and Rukhadze [126] discussed the possibility of obtaining metallic hydrogen by means of a beam of relativistic electrons. The Fermi energy of an electron gas is proportional to $n^{2/3}$, where n is the number of electrons. Multiple ionization of atoms of a target bombarded by a beam of relativistic electrons can result in the gas becoming degenerate with the pressure determined by the electron pressure. These authors determine the parameters of a beam of relativisitic electrons necessary to achieve pressure of ~1 Mbar in a degenerate gas, requiring an electron concentration of 1.5×10^{23} cm^{-3}, corresponding to quintuple ionization of material. Assuming a volume $V = a^3$ of material, where a is on the order of the length of the mean-free path of an electron in the electron beam (several millimeters for 3-5 MeV electrons), quintuple ionization requires energy of about $4 \times 10^5 a^3$ J. Setting a equal to 0.5 cm, the total beam energy required is 50 kJ, and for ~5 MeV electrons, the number of electrons in the pulse has to be $\sim 10^{17}$. Assuming that the pulse duration is 10^{-6} sec, the electron beam power is estimated to be $\sim 5 \times 10^5$ W and the current, ~10 kA. Under such conditions, the electrons will interact with the target layer having a thickness of 0.3 cm. Therefore, in order to obtain metallic hydrogen, small granules of an easily ionized substance should be placed near the surface of liquid hydrogen and irradiated by a focused electron beam of relativistic electrons. If the temperature of the electron gas during multiple ionization of the target by relativistic electrons is small compared with the mean ionization energy, the method described above may be used to induce metallic-phase transition of molecular hydrogen.

Similar to compression by laser radiation, metallic-phase transition of molecular hydrogen by means of a relativistic beam is a much simpler problem than achievement of electron-beam induced fusion. According to unclassified sources [127], the most intense source of electron beams at the present is the Aurora facility at Harry Diamond Laboratories in White Oak, Maryland. The Aurora facility generates a 3 MJ electron beam of 1.25×10^{-7} sec duration, which is much more

than is required to obtain metallic-phase transition of hydrogen. However, it is not well suited for pellet-compression work. According to Velikhov [127], a 5 to 6 MJ electron-beam facility intended for electron-beam-induced fusion and, thus, ideally suited for compression work is being designed in the Soviet Union and should be constructed in about five years.

However, according to Keldysh [128], Soviet scientists have already succeeded in generating electron beams with densities of 5×10^{12} W/cm^2, which is close to the electron density required to initiate electron-beam-induced fusion.

G. RECENT REPORTED OBSERVATIONS OF METALLIC HYDROGEN

The isothermal compression experiments described below and the isentropic compression experiments discussed in Section V, subsection D, in which metallic-phase transition of molecular hydrogen may have been detected, were made before the possibility of the insulating molecular-conducting molecular hydrogen transition was discussed in the scientific literature. If, indeed, such a transition does occur in molecular hydrogen, it should take place at pressures below the transition pressure to a monatomic metal. Because, in all experiments, the transition was inferred from abrupt changes in electrical resistivity, it is impossible to determine which transition may have been detected. However, it is not at all certain that a phase transition has occurred in isentropic experiments performed by Grigor'yev [114, 116] and Hawke [117] and whether the pressures generated were sufficiently high for the metallic-phase transition to have taken place. The pressure generated in isothermal experiments was much lower and the first discontinuous decrease in electrical resistivity observed would more likely than not indicate insulating molecular-to-conducting molecular phase transition.

In a paper published in 1975, Yakovlev et al. [95] reported achieving transition of molecular hydrogen into its metallic form using the opposed-anvil apparatus made of carbonado. In the experiments

performed, a thin film of solid molecular hydrogen, deposited on the surface of the flat carbonado anvil cooled to 4.2 K, was compressed by a conical anvil with a rounded tip. As the force applied to the anvils reached 20 kg, the electrical resistivity (ρ) was observed to decrease abruptly from 10^8 ohm to ~10^2 ohm. The six order of magnitude drop in the electrical resistivity of hydrogen was attributed to the metallic-phase transition of hydrogen at contact pressures estimated in excess of 1 Mbar.

The fact that the decrease in ρ was actually caused by a phase transition was verified by initially compressing a sample of molecular hydrogen to the point where ρ decreased to ~10^2 ohm. The force on the anvil was then decreased until ρ began to increase slightly, indicating the appearance of the insulating phase. The temperature was then slowly raised, keeping the force constant. Under these conditions, a rise in the temperature from 4.2 K to ~18 K resulted in a sudden increase of electrical resistivity of the hydrogen sample to its normal value for the solid molecular hydrogen (~10^8 ohm).

Experiments were also performed using thick films of hydrogen. However, the electrical resistivity of the samples did not change with the applied pressure. Failure to achieve phase transition in thick films of hydrogen can possibly be attributed to the fact that the high pressure achieved by means of opposed carbonado anvils is the pressure acting at the surface, which decreases sharply with depth, rather than hydrostatic pressure. Another possibility is that the increase in conductivity in thin films is due to shorting of the anvils.

In his latest series of experiments, Kawai [82] has also reported achieving metallic hydrogen by compressing hydrogen gas at room temperature until it became electrically conducting. Kawai used the modified 6-8 anvil segmented-sphere apparatus described in Section V, subsection B. In the experiments performed, the sample chamber was surrounded by semi-sintered MgO and cardboard spacers. The spherical outer-stage shell of the apparatus was enclosed between the upper and lower holders, with a rubber ring placed between them to prevent

gas leakage. Gas was injected and evacuated and the oxygen that may have remained was removed by injecting and evacuating nitrogen. Nitrogen was then removed by twice-injecting and evacuating hydrogen. The hydrogen gas used in the experiments was injected and compressed to 100 bar by a bomb, with the sample chamber volume at this pressure $\simeq$ 1 mm^3. The pressure in the oil reservoir was gradually increased by an external load. The voids in the MgO were closed at a pressure of 200 kbar, with some of the hydrogen gas expelled into the sample chamber. As the external load was increased above 855 tons, the electrical resistivity of the sample dropped abruptly from 126.3 Mohm to 100 ohm and then to zero. In the absence of calibration, the pressure at which the inferred metallic transition occurs is unknown.

In another series of experiments in which hydrogen gas was replaced with MgO, no such drastic change in the electrical resistivity of the sample was observed even when the external load was increased to 1100 tons. Earlier experiments by Kawai [80] have demonstrated that MgO becomes metallic at pressures below those used to compress hydrogen. Also, extremely high pressures could have reduced MgO by hydrogen to a mixture of Mg and H_2O. Therefore, in yet another series of experiments on hydrogen, MgO was replaced with diamond powder. Once again, the electrical resistivity was observed to decrease to almost zero under the same load. Unfortunately, the experiments were made using six inner anvils made of Al_2O_3, which were determined by Yakovlev et al. [91] to undergo metallic-phase transition--thus providing a possible alternate explanation for the observed decrease in electrical conductivity under high pressure.

REFERENCES

1. Stewart, J. W., "Compression of Solidified Gases to 20,000 kg/cm^2 at Low Temperatures," *Journal of Physical Chemistry of Solids*, Vol. 1, No. 2, 1956, pp. 146-158.

2. Anderson, M. S., and C. A. Swenson, "Experimental Compressions for Normal Hydrogen and Normal Deuterium to 25 kbar at 4.2 K," *Physical Review B*, Vol. 10, No. 12, 1974, pp. 5184-5191.

3. Krumhansl, J. A., and S. Y. Wu, "Quantum Theory of the Equation of State for Solid Hydrogen," *Physical Review B*, Vol. 5, No. 10, 1972, pp. 4155-4170.

4. Bruce, T. A., "Equation of State for Solid Hydrogen," *Physical Review B*, Vol. 5, No. 10, 1972, pp. 4170-4179.

5. Pollock, E. L., T. A. Bruce, G. V. Chester, and J. A. Krumhansl, "High-Pressure Behavior of Solid H_2, D_2, He^3, He^4, and Ne^{20}," *Physical Review B*, Vol. 5, No. 10, 1972, pp. 4180-4190.

6. Ross, M., "A Theoretical Analysis of the Shock Compression Experiments of the Liquid Hydrogen Isotopes and a Prediction of Their Metallic Transition," *Journal of Chemical Physics*, Vol. 60, No. 9, 1974, pp. 3634-3644.

7. Ross, M., F. H. Ree, and R. N. Keeler, "A Summary of the Recent Lawrence Livermore Laboratory (LLL) Work on the Equation of State of Dense Molecular Hydrogen," *Lawrence Livermore Laboratory Report*, UCRL 75761, February 1975.

8. Raich, J. C., and R. D. Etters, "Rotational Molecular Motion in Solid H_2 and D_2 Under Pressure," *Journal of Low Temperature Physics*, Vol. 6, No. 3-4, 1972, pp. 229-240.

9. Etters, R. D., R. Danilowicz, and W. England, "Properties of Solid and Gaseous Hydrogen, Based upon Anisotropic Pair Interactions," *Physical Review A*, Vol. 12, No. 5, 1975, pp. 2199-2212.

10. Anderson, A. B., J. C. Raich, and R. D. Etters, "Self-Consistent Phonon Calculations and Equations and State of Solid Hydrogen and Deuterium," *Physical Review B*, Vol. 14, No. 2, 1976, pp. 814-822.

11. Margenau, H., and N. R. Kestner, *Theory of Intermolecular Forces*, 2nd ed., Pergamon Press, Oxford, 1971.

12. McMahan, A. K., H. Beck, and J. A. Krumhansl, "Short-Range Interaction Between Hydrogen Molecules," *Physical Review A*, Vol. 9, No. 5, 1974, pp. 1852-1864.

13. Ree, F. H., and C. F. Bender, "Nonadditive Interaction in Molecular Hydrogen at High Pressure," *Physical Review Letters*, Vol. 32, No. 3, 1974, pp. 85-88.

14. Bender, C. F., and E. R. Davidson, "A Natural Orbital-Based Energy Calculation for Helium Hydride and Lithium Hydride," *Journal of Physical Chemistry*, Vol. 70, No. 8, 1966, pp. 2675-2685.

15. de Boer, J., and B. S. Blaisse, "Quantum Theory of Condensed Permanent Gases. II. The Solid State and Melting Line," *Physica*, Vol. 14, No. 2-3, 1948, pp. 149-164.

16. Saunders, E. M., "Ground State of Solid He^3," *Physical Review*, Vol. 126, No. 5, 1962, pp. 1724-1736.

17. Bernardes, N., "Theory of the Compressibility of Solid He^4 and He^3 at 0 K," *Physical Review*, Vol. 120, No. 6, 1960, pp. 1927-1932.

18. Hurst, R. P., and J. M. H. Levelt, "Quantum Mechanical Cell Model of the Liquid State. II. Application to the Zero Point Properties of Close-Packed Crystals," *Journal of Chemical Physics*, Vol. 34, No. 1, 1961, pp. 54-63.

19. Nosanow, L. H., and G. L. Shaw, "Hartree Calculations for the Ground State of Solid He and Other Noble Gas Crystals," *Physical Review*, Vol. 128, No. 2, 1962, pp. 546-550.

20. Mullin, W. J., "Theory of Solid Neon at 0 K," *Physical Review*, Vol. 134, No. 5A, 1962, pp. A1249-A1254.

21. Etters, R. D., and R. L. Danilowicz, "Dynamic-Local Field Approximation for the Quantum Solids," *Physical Review A*, Vol. 9, No. 4, 1974, pp. 1698-1710.

22. Metropolis, N., A. W. Rosenbluth, M. N. Rosenbluth, A. H. Telly, and E. Teller, "Equation of State Calculations by Fast Computing Machines," *Journal of Chemical Physics*, Vol. 29, No. 21, 1953, pp. 1087-1092.

23. Hansen, J. P., and D. Levesque, "Ground State of Solid Helium-4 and -3," *Physical Review*, Vol. 165, No. 1, 1968, pp. 293-299.

24. Ross, M., "Equation of State of H_2 and D_2," *Lawrence Livermore Laboratory Report*, UCRL 50911, July 1970.

25. Trubitsyn, V. P., "Phase Transition in a Hydrogen Crystal," *Fizika tverdogo tela*, Vol. 8, No. 3, 1966, pp. 862-865.

26. Van Thiel, M., and B. J. Alder, "Shock Compression of Liquid Hydrogen," *Molecular Physics*, Vol. 19, 1966, pp. 427-435.

27. Barker, J. A., and D. Henderson, "Perturbation Theory and Equation of State for Fluids: The Square Well Potential," *Journal of Chemical Physics*, Vol. 47, No. 8, 1967, pp. 2856-2861.

28. Barker, J. A., and D. Henderson, "Perturbation Theory and Equation of State for Fluids. II. A Successful Theory of Liquids," *Journal of Chemical Physics*, Vol. 47, No. 11, 1967, pp. 4714-4721.

29. Mansoori, G. A., and F. B. Canfield, "Variational Approach to the Equilibrium Thermodynamic Properties of Simple Liquids," *Journal of Chemical Physics*, Vol. 51, No. 11, 1969, pp. 4958-4967.

30. Ross, M., and D. Seale, "Perturbation Approximation to the Screened Coulomb Gas," *Physical Review A*, Vol. 9, No. 1, 1974, pp. 396-399.

31. Ross, M., "Shock Compression and the Melting Curve for Argon," *Physical Review A*, Vol. 8, No. 3, 1973, pp. 1466-1474.

32. Van Thiel, M., L. B. Hord, W. H. Gust, A. C. Mitchell, M. D'Addario, K. Boutwell, E. Wilbarger, and B. Barrett, "Shock Compression of Deuterium to 900 kbar," *Physics of the Earth and Planetary Interiors*, Vol. 9, No. 1, 1974, pp. 57-77.

33. Dick, R., unpublished, Los Alamos Scientific Laboratories.

34. Liberman, D. A., "Equation of State of Molecular Hydrogen at High Pressure," *Los Alamos Scientific Laboratory Report*, LA-4727-MS, July 1971.

35. Ramaker, D. E., L. Kumar, and F. E. Harris, "Exact-Exchange Crystal Hartree-Fock Calculations of Molecular and Metallic Hydrogen and Their Transitions," *Physical Review Letters*, Vol. 34, No. 13, 1975, pp. 812-814.

36. Friedli, C., "Band Structure of Highly Compressed Hydrogen," Ph.D. thesis, Materials Science Center, Cornell University.

37. Kauzmann, W., *Quantum Chemistry*: Academic Press, Inc., New York, 1957, pp. 512-516.

38. Ross, M., "Shock Compression of Argon and Xenon. IV. Conversion of Xenon to a Metal-Like State," *Physical Review*, Vol. 171, No. 3, 1968, pp. 777-784.

39. Neece, G. A., F. J. Rogers, and W. G. Hoover, "Thermodynamic Properties of Compressed Solid Hydrogen," *Journal of Computational Physics*, Vol. 7, No. 3, 1971, pp. 621-636.

40. Wigner, E., and H. B. Huntington, "On the Possibility of a Metallic Modification of Hydrogen," *Journal of Chemical Physics*, Vol. 3, No. 12, 1935, pp. 764-770.

41. Abrikosov, A. A., "Equation of State of Hydrogen at High Pressures," *Astronomicheskiy zhurnal*, Vol. 31, No. 2, 1954, pp. 112-123.

42. Harris, F. E., L. Kumar, and H. J. Monkhorst, "Electronic-Structure Studies of Solids. II. 'Exact' Hartree-Fock Calculations for Cubic Atomic Hydrogen Crystals," *Physical Review B*, Vol. 7, No. 6, 1973, pp. 2850-2866.

43. Hammerberg, J., and N. W. Ashcroft, "Ground State Energies of Simple Metals," *Physical Review B*, Vol. 9, No. 2, 1974, pp. 409-424.

44. Rogers, F. J., Personal communication.

45. Graboske, H., Jr., and H. de Witt, unpublished.

46. Nozieres, P., and D. Pines, "A Dielectric Formulation of the Many Body Problem Application to the Free-Electron Gas," *Nuovo Cimento*, Vol. 9, No. 3, 1958, pp. 470-490.

47. Hedin, L., and B. L. Lindqvist, "Explicit Local Exchange-Correlation Potentials," *Journal of Physics C*, Vol. 4, No. 14, 1971, pp. 2064-2083.

48. Ross, M., and A. K. McMahan, "Comparison of Theoretical Models for Metallic Hydrogen," *Physical Review B*, Vol. 13, No. 12, 1976, pp. 5154-5157.

49. Brovman, Ye. G., Yu. Kagan, and A. Kholas, "Structure of Metallic Hydrogen at Zero Pressure," *Zhurnal eksperimental'noy i teoreticheskoy fiziki*, Vol. 61, No. 6(12), 1971, pp. 2429-2458.

50. Brovman, Ye. G., Yu. Kagan, and A. Kholas, "Properties of Metallic Hydrogen Under Pressure," *Zhurnal eksperimental'noy i teoreticheskoy fiziki*, Vol. 62, No. 4, 1972, pp. 1492-1501.

51. Hubbard, W. B., and R. Smoluchowski, "Structure of Jupiter and Saturn," *Space Science Reviews*, Vol. 14, 1973, pp. 599-662.

52. Tong, B. Y., and L. J. Sham, "Application of a Self-Consistent Scheme Including Exchange and Correlation Effects to Atoms," *Physical Review*, Vol. 144, No. 1, 1966, pp. 1-7.

53. Clementi, E., "Correlation Energy in Atomic Systems. III. Configurations with 3d and 4s Electrons," *Journal of Chemical Physics*, Vol. 42, No. 8, 1965, pp. 2783-2787 (and earlier references cited in the paper).

54. Kim, Y. S., and R. G. Gordon, "Study of the Electron Gas Approximation," *Journal of Chemical Physics*, Vol. 60, No. 5, 1974, pp. 1842-1850.

55. Monkhorst, H. J., and J. Oddershede, "Random-Phase-Approximation Correlation Energy in Metallic Hydrogen Using Hartree-Fock Block Functions," *Physical Review Letters*, Vol. 30, No. 17, 1973, pp. 797-800.

56. Harrison, W. A., "Multi-Ion Interactions and Structures in Simple Metals," *Physical Review B*, Vol. 7, No. 6, 1973, pp. 2408-2415.

57. Beck, H., and D. Straus, "On the Lattice Dynamics of Metallic Hydrogen and Other Coulomb Systems," *Helvetica Physica Acta*, Vol. 48, No. 5-6, 1975, pp. 655-659.

58. Caron, L. G., "Low-Temperature Thermostatics of Face-Centered-Cubic Metallic Hydrogen," *Physical Review B*, Vol. 9, No. 12, 1974, pp. 5025-5038.

59. Drickamer, H. C., and C. W. Frank, *Electronic Transitions and the High Pressure Chemistry and Physics of Solids*, Chapman and Hall, London, 1973.

60. McMahan, A. K., B. L. Hord, and M. Ross, "An Experimental and Theoretical Study on Metallic Iodine," *Physical Review B*, Vol. 14, No. 12, 1976 (to be published).

61. Yestrin, Ye. I., "Temperature Instability of the Metallic Hydrogen Phase," *Zhurnal eskperimental'noy i teoreticheskoy fiziki, pis'ma*, Vol. 13, No. 12, 1971, pp. 719-720.

62. Trubitsyn, V. P., "Phase Diagrams of Hydrogen and Helium," *Astronomicheskiy zhurnal*, Vol. 48, No. 2, 1971, pp. 390-398.

63. de Wette, F. W., "Note on the Electron Lattice," *Physical Review A*, Vol. 135, No. 2A, 1964, pp. A287-A294.

64. Carr, W. J., Jr., "Energy, Specific Heat, and Magnetic Properties of the Low-Density Electron Gas," *Physical Review*, Vol. 122, No. 5, 1961, pp. 1437-1446.

65. Hansen, J. P., "Statistical Mechanics of Dense Ionized Matter. I. Equilibrium Properties of the Classical One-Component Plasma," *Physical Review B*, Vol. 8, No. 6, 1973, pp. 3096-3109.

66. Salpeter, E. E., "Evaporation of Cold Metallic Hydrogen," *Physical Review Letters*, Vol. 28, No. 9, 1972, pp. 560-562.

67. Chapline, G. F., Jr., "Metal-Insulator Transition in Solid Hydrogen," *Physical Review B*, Vol. 6, No. 5, pp. 2067-2070.

68. Kawai, N., S. Mochizuki, and H. Fujita, "Densification of Vitreous Silica under Static High Pressures Higher than 2 Mb," *Physics Letters*, Vol. 34, No. 2, 1971, pp. 107-108.

69. Kawai, N., "2-Mbar High-Pressure Experiment at Osaka University," *Technology of Japan*, Vol. 3, No. 2, 1971, pp. 68-70.

70. Kawai, N., "Equipment for Generating Pressures up to 800 Kilobars," Proceedings of the Symposium on Accurate Characterization of the High Pressure Environment, held at the National Bureau of Standards at Gaithersburg, Md., on October 14-18, 1968, *NBS Special Publication 326*, March 1971, pp. 45-48.

71. Kawai, N., "Pistons of Fluid Pressurized Superhigh Pressure Generator," Japanese Patent, Class 73B0 (B30 b 11/32), No. 48-42911, submitted on 10 March 1970, published on 15 December 1973.

72. Kawai, N., and S. Endo, "The Generation of Ultrahigh Hydrostatic Pressures by a Split Sphere Apparatus," *The Review of Scientific Instruments*, Vol. 41, No. 8, 1970, pp. 1178-1181.

73. Kawai, N., "A Device for Generating Superhigh Pressures," Japanese Patent, Class 73B0 (B30b), No. 18430, submitted on 13 November 1967, published on 22 May 1971.

74. Kawai, N., "A Device for Generating Superhigh Pressures," Japanese Patent, Class 73B0 (B30b) No. 18431, submitted on 13 November 1967, published on 22 May 1971.

75. Kawai, N., M. Togaya, and A. Onodera, "A New Device for Pressure Vessels," *Proceedings of the Japan Academy*, Vol. 49, No. 8, 1973, pp. 623-626.

76. Spain, I. L., K. Ishizaki, J. M. Marchello, "Prospects for Obtaining Metallic Hydrogen with Spherical Presses," *Advances in Cryogenic Engineering*, Vol. 18, 1973, pp. 441-446.

77. Kawai, N., and S. Mochizuki, "Metallic States in the Three 3d Transition Metal Oxides, Fe_2O_3, Cr_2O_3, and TiO_2 Under Static High Pressures," *Physics Letters*, Vol. 36A, No. 1, pp. 54-55.

78. Kawai, N., and S. Mochizuki, "Insulator-Metal Transition in NiO," *Solid State Communications*, Vol. 9, No. 16, 1971, pp. 1393-1395.

79. Kawai, N., and A. Nishiyama, "Conductive SiO_2 Under High Pressure," *Proceedings of the Japan Academy*, Vol. 50, No. 1, 1974, pp. 72-75.

80. Kawai, N., and A. Nishiyama, "Conductive MgO Under High Pressure," *Proceedings of the Japan Academy*, Vol. 50, No. 8, 1974, pp. 634-635.

81. Kawai, N., O. Mishima, M. Togaya, and B. le Neindre, "H_2O Rendered Metallic Under High Pressure," *Proceedings of the Japan Academy*, Vol. 51, No. 7, 1975, pp. 627-629.

82. Kawai, N., M. Togaya, and O. Mishima, "A Study of the Metallic Hydrogen," *Proceedings of the Japan Academy*, Vol. 51, No. 7, 1975, pp. 630-633.

83. Vereshchagin, L. F., Ye. N. Yakovlev, T. D. Varfolomeyeva, V. N. Slesarev, and L. Ye. Shterenberg, "Synthesis of Carbonado Type Diamonds," *AN SSSR, Doklady*, Vol. 185, No. 3, 1969, pp. 555-556.

84. Vereshchagin, L. F., Ye. N. Yakovlev, B. V. Vinogradov, G. N. Stepanov, K. Kh. Bibayev, T. I. Alayeva, and V. P. Sakun, "Megabar Pressure Between Anvils," *High Temperatures--High Pressures*, Vol. 6, No. 5, 1974, pp. 499-504.

85. Vereshchagin, L. F., Ye. N. Yakovlev, G. N. Stepanov, K. Kh. Bibayev, and B. V. Vinogradov, "2.5 Mbar Pressure Between Anvils of Carbonado Type Diamonds," *Zhurnal eksperimental'noy i teoreticheskoy fiziki, pis'ma*, Vol. 16, No. 4, 1972, pp. 240-242.

86. Vereshchagin, L. F., Ye. N. Yakovlev, G. N. Stepanov, K. Kh. Bibayev, and B. V. Vinogradov, "2.5 Mbar Pressure Between Anvils of Carbonado Type Diamonds," *Zhurnal tekhnicheskoy fiziki*, Vol. 42, No. 12, 1972, pp. 2621-2622.

87. Vereshchagin, L. F., Ye. N. Yakovlev, G. N. Stepanov, and B. V. Vinogradov, "Possibility of Transition of Diamonds into Metallic State," *Zhurnal eksperimental'noy i teoreticheskoy fiziki, pis'ma*, Vol. 16, No. 7, 1972, pp. 382-383.

88. Vereshchagin, L. F., Ye. N. Yakovlev, B. V. Vinogradov, V. P. Sakun, and G. N. Stepanov, "Transition of Diamonds into Metallic State," *Zhurnal eksperimental'noy i teoreticheskoy fiziki, pis'ma*, Vol. 17, No. 8, 1973, pp. 422-424.

89. Vereshchagin, L. F., Ye. N. Yakovlev, B. V. Vinogradov, V. P. Sakun, and G. N. Stepanov, "Transition of Diamonds into the Metallic State," *High Temperatures--High Pressures*, Vol. 6, No. 5, 1974, pp. 505-508.

90. Vereshchagin, L. F., Ye. N. Yakovlev, B. V. Vinogradov, and V. P. Sakun, "Transition of SiO_2 into a Conducting State," *Zhurnal eksperimental'noy i teoreticheskoy fiziki, pis'ma*, Vol. 20, No. 7, 1974, pp. 472-474.

91. Vereshchagin, L. F., Ye. N. Yakovlev, B. V. Vinogradov, and V. P. Sakun, "Transition of Al_2O_3, NaCl, and S into a Conducting State," *Zhurnal eksperimental'noy i teoreticheskoy fiziki, pis'ma*, Vol. 20, No. 8, 1974, pp. 540-544.

92. Vereshchagin, L. F., Ye. N. Yakovlev, and Yu. A. Timofeyev, "Transition of H_2O into a Conducting State at Static Pressures P ≈ 1 Mbar," *Zhurnal eksperimental'noy i teoreticheskoy fiziki, pis'ma*, Vol. 21, No. 11, 1975, pp. 643-645.

93. Vereshchagin, L. F., Ye. N. Yakovlev, B. V. Vinogradov, and Yu. A. Timofeyev, "Transition of BN into Conducting State," *Fizika tverdogo tela*, Vol. 18, No. 1, 1976, pp. 113-114.

94. Yakovlev, Ye. N., L. F. Vereshchagin, B. V. Vinogradov, and Yu. A. Timofeyev, "The Sequence of Dielectric-Metal Transitions in the Megabar Static Pressure Range," *Zhurnal tekhnicheskoy fiziki*, Vol. 2, No. 12, 1976, pp. 570-574.

95. Vereshchagin, L. F., Ye. N. Yakovlev, and Yu. A. Timofeyev, "Possibility of Transition of Metallic Hydrogen into a Metallic State," *Zhurnal eksperimental'noy i teoreticheskoy fiziki, pis'ma*, Vol. 21, No. 3, 1975, pp. 190-193.

96. Ruoff, A. L., and K. S. Chan, "Contact Pressures and Ultrapressures," *Cornell University Report*, 2667, May 1976.

97. Mao, H. K., and P. M. Bell, "High-Pressure Physics: The 1-Megabar Mark on the Ruby R_1 Static Pressure Scale," *Science*, Vol. 191, No. 4229, 1976, pp. 851-852.

98. Ruoff, A. L., and L. C. Chhabildas, "The Sodium Chloride Primary Pressure Gauge," *Cornell University Report*, 2669, May 1976.

99. Hall, H. T., "Sintered Diamond: A Synthetic Carbonado," *Science*, Vol. 169, No. 3946, 1970, pp. 868-869.

100. Asada, T. quoted by Spain et al. in reference [76].

101. Hibbs, L. E., and R. H. Wentorf, Jr., "Borazon and Diamond Compact Tools," *High Temperatures--High Pressures*, Vol. 6, No. 4, 1974, pp. 409-413.

102. Wentorf, R. H., Personal communication.

103. Bundy, F. P., Personal communication.

104. Aron, P. R., Personal communication.

105. Ruoff, A. L., Personal communication.

106. Vereshchagin, L. F., and R. G. Arkhipov, "Obtaining Metallic Hydrogen," *Priroda*, No. 3, 1972, pp. 9-12.

107. Vereshchagin, L. F., "Metallic Hydrogen and Superconductivity," *Tekhnia i nauka*, No. 8, 1975, pp. 22-23.

108. Vereshchagin, L. F, "Metallic Hydrogen--Truth or Fable," *Sotsialisticheskaya industriya*, January 13, 1974, p. 3.

109. Repetskiy, L. (correspondent), "A Giant!," *Izvestiya*, November 28, 1974, p. 6.

110. Vereshchagin, L. F., A. A. Semerchan, V. P. Modenov, T. T. Bocharova, and M. Ye. Dmitriyev, "Synthetic Diamond--Material for High Pressure Chambers on the Order of a Megabar," *AN SSSR, Doklady*, Vol. 195, No. 3, pp. 593-594.

111. Wilkins, M. L., R. E. Blum, E. Cronshagen, and P. Grantham, "A Method for Computer Simulation of Problems in Solid Mechanics and Gas Dynamics in Three Dimensions and Time," Lawrence Livermore Laboratory Report, UCRL-51574, Rev. 1, May 1975.

112. Ruoff, A. L., "Penultimate Static Pressure Containment Considerations and Possible Applications to Metallic Hydrogen Preparation," *Advances in Cryogenic Engineering*, Vol. 18, 1973, pp. 435-440.

113. Fadeyenko, Yu. I., "Super-high Pressure Press," *Zhurnal prikladnoy matematiki i tekhicheskoy fiziki*, Vol. 5, 1975, pp. 159-162.

114. Grigor'yev, F. V., S. B. Kormer, O. L. Mikhaylova, A. P. Tolochko, and V. D. Urlin, "Equation of State of Liquid and Solid Molecular Hydrogen at High Pressure," *Zhurnal eksperimental'noy i teoreticheskoy fiziki*, Vol. 69, No. 2(8), 1975, pp. 743-749.

115. Shaner, J., Lawrence Livermore Laboratory, Personal communication.

116. Grigor'yev, F. V., S. B. Kormer, O. L. Mikhaylova, A. P. Tolochko, and V. D. Urlin, "Experimental Determination of the Compressibility of Hydrogen at Densities of 1.5-2 g/cm^3. Metallic Phase Transition of Hydrogen," *Zhurnal eksperimental'noy i teoreticheskoy fiziki, pis'ma*, Vol. 16, No. 5, 1972, pp. 286-290.

117. Hawke, R. S., D. E. Duerre, J. G. Huebel, R. N. Keeler, and H. Klapper, "Isentropic Compression of Fused Quartz and Liquid Hydrogen to Several Mbar," *Physics of Earth and Planetary Interiors*, Vol. 6, Nos. 1-3, 1972, pp. 44-47.

118. Alt'shuler, L. V., Ye. A. Dynin, and V. A. Svidinskiy, "Gasdynamic Methods of Low-Temperature Compression of Solid Hydrogen," *Zhurnal eksperimental'noy i teoreticheskoy fiziki, pis'ma*, Vol. 17, No. 1, 1973, pp. 20-22.

119. Yampol'skiy, P. A., "Isentropic Compression by Means of Shock Waves," *AN SSSR. Vestnik*, No. 4, 1975; pp. 42-49.

120. Scudder, J. K., "Diagnostic Development for Magnetic Flux Compression Experiments," Lawrence Livermore Laboratory Report, UCRL 51767, March 1975.

121. Nucholls, J., L. Wood, A. Thiessen, and G. Zimmerman, "Laser Compression of Matter to Super-High Densities: Thermonuclear (CTR) Applications," *Nature*, Vol. 239, No. 5368, 1972, pp. 139-142.

122. Afanas'yev, Yu. V., N. G. Basov, P. P. Volosevich et al., "Laser Initiation of a Thermonuclear Reaction in Inhomogeneous Spherical Targets," *Zhurnal eksperimental'noy i teoreticheskoy fiziki, pis'ma*, Vol. 21, No. 2, 1975, pp. 150-155.

123. Anisimov, S. I., "Transition of Hydrogen into Metallic State in a Laser-Pulse Generated Compression Wave," *Zhurnal eksperimental'noy i teoreticheskoy fiziki, pis'ma*, Vol. 16, No. 10, 1972, pp. 570-572.

124. Lengyel, L. L., "Exact Steady-State Analogy of Transient Gas Compression by Coalescent Waves," *AIAA Journal*, Vol. 11, No. 9, 1973, pp. 1347-1349.

125. Van Kessel, G. G. M., and R. Siegel, "Observation of Laser-Driven Shock Waves in Solid Hydrogen," *Physical Review Letters*, Vol. 33, No. 17, 1974, pp. 1020-1023.

126. Bogdankevich, O. V., and A. A. Rukhadze, "Possibility of Generating High Pressure in a Solid by Means of a High-Current Electron Beam," *Zhurnal eksperimental'noy i teoreticheskoy fiziki, pis'ma*, Vol. 13, No. 9, 1971, pp. 517-519.

127. Sullivan, W., "Fusion Research in U.S. and Soviet Turning to New Techniques," *New York Times*, January 19, 1976, pp. 22.

128. Keldysh, M. V., "Foreword. Annual Meeting of the Soviet Academy of Sciences," *AN SSSR, Vestnik*, No. 5, 1976, pp. 7-12.

SUPPLEMENTARY

INFORMATION

For: Dr. R. D. Turner

AD-A040578

7-18-77

PUBLICATIONS DEPARTMENT

ERRATUM

R-2056-ARPA MOLECULAR AND METALLIC HYDROGEN, Marvin Ross and Charles Shishkevish, May 1977, UNCLASSIFIED

Please correct the fourth sentence in the first new paragraph on p. xv to read as follows:

However, another group of materials scientists and high pressure specialists, which includes such prominent researchers as Ruoff, Bundy, and Wentorf, is firmly convinced that static pressures above 1 Mbar have not yet been achieved.

Rand
SANTA MONICA, CA. 90406